

# Tensor Networks for Big Data Analytics and Large-Scale Optimization Problems

Andrzej CICHOCKI

RIKEN Brain Science Institute, Japan

and Systems Research Institute of the Polish Academy of Science, Poland

Part of this work was presented on the Second International Conference on Engineering and Computational Mathematics (ECM2013), Hong Kong December 16-18, 2013 (invited talk)

arXiv:1407.3124v2 [cs.NA] 22 Aug 2014

**Abstract**—Tensor decompositions and tensor networks are emerging and promising tools for data analysis and data mining. In this paper we review basic and emerging models and associated algorithms for large-scale tensor networks, especially Tensor Train (TT) decompositions using novel mathematical and graphical representations. We discuss the concept of tensorization (i.e., creating very high-order tensors from lower-order original data) and super compression of data achieved via quantized tensor train (QTT) networks. The main objective of this paper is to show how tensor networks can be used to solve a wide class of big data optimization problems (that are far from tractable by classical numerical methods) by applying tensorization and performing all operations using relatively small size matrices and tensors and applying iteratively optimized and approximative tensor contractions.

**Keywords:** Tensor networks, tensor train (TT) decompositions, matrix product states (MPS), matrix product operators (MPO), basic tensor operations, optimization problems for very large-scale problems: generalized eigenvalue decomposition (GEVD), PCA/SVD, canonical correlation analysis (CCA).

## I. Introduction and Motivations

Big Data can have a such huge volume and high complexity that existing standard methods and algorithms become inadequate for the processing and optimization of such data. Big data is characterized not only by big Volume but also by other specific “V” features/challenges: Veracity, Variety, Velocity, Value. Fig. 1 illuminates the big data characteristics for brain research related problems. High Volume implies the need for algorithms that are scalable; high Velocity is related to the processing of stream of data in near real-time; high Veracity calls for robust and predictive algorithms for noisy, incomplete and/or inconsistent data, high Variety require

integration across different types of data, e.g., binary, continuous data, images, time series, etc., and finally Value refers to extracting high quality and consistent data which could lend themselves to meaningful and interpretable results.

Multidimensional data is becoming ubiquitous across the sciences and engineering because they are increasingly being gathered by information-sensing devices and remote sensing. Big data such as multimedia data (speech, video), and medical/biological data, the analysis of which critically requires a paradigm shift in order to efficiently process massive datasets within tolerable time. Tensors – multi-dimensional generalizations of matrices, provide often a natural sparse and distributed representation for such data.

Tensors have been adopted in diverse branches of data analysis, such as in signal and image processing, Psychometric, Chemometrics, Biometric, Quantum Physics/Information, Quantum Chemistry and Brain Science [1]–[8]. Tensors are particularly attractive for data which exhibit not only huge volumes but also very high variety, for example, they are suited for problems in bio- and neuro-informatics or computational neuroscience where data are collected in various forms of big, sparse tabular, graphs or networks with multiple aspects and high dimensionality.

Tensor decompositions (TDs) provide some extensions of blind source separation (BSS) and 2-way (matrix) Component Analysis (2-way CA) to multi-way component analysis (MWCA) methods [1]. Furthermore, TNs/TDs are suitable for dimensionality reduction, they can handle missing values, and noisy data [9]. They are also potentially useful for analysis of linked (coupled) block of big tensors with millions and even billions of non-zero entries, using the map-reduce paradigm, as well as out-

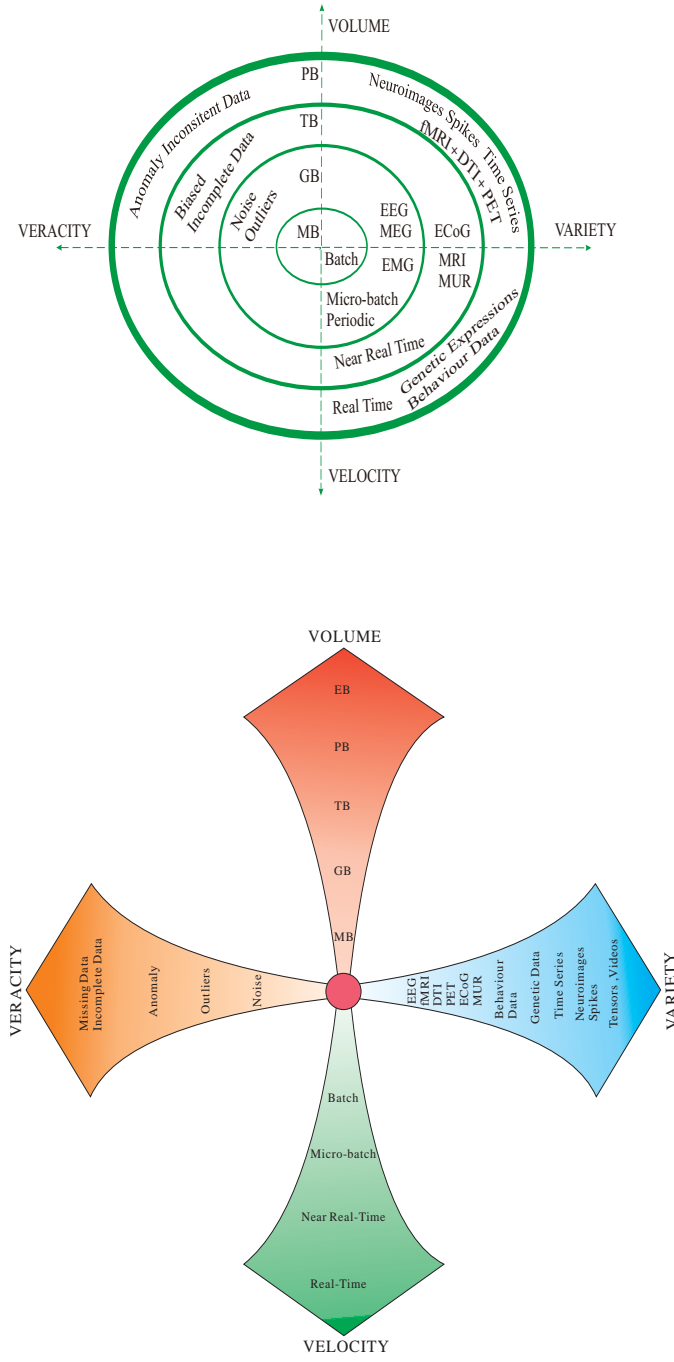


**Figure 1:** Four “V”s of big (brain) data: Volume - scale of data, Variety - different forms (types) of data, Veracity - uncertainty of data, and Velocity - speed at which stream of data is generated and processed. Illustration of challenges for human brain data, which involves analysis of multi-modal, multi-subjects neuroimages, spectrograms, time series, spikes trains, genetic and behavior data. One of the challenges in computational and system neuroscience is to perform fusion or assimilation for various kinds of data and to understand the relationship and links between them. Brain data can be recorded by electroencephalography (EEG), electrocorticography (ECoG), magnetoencephalography (MEG), fMRI, DTI, PET, Multi Unit Recording (MUR), to name a few.

of-core approaches [2], [10]–[13]. Moreover, multi-block tensors which arise in numerous important applications (that require the analysis of diverse and partially related data) can be decomposed to common (or correlated) and uncorrelated or statistically independent components. The effective analysis of coupled tensors requires the development of new models and associated algorithms and software that can identify the core relations that may exist among the different tensors, and scale to extremely large datasets.

Complex interactions and operations between tensors can be visualized by tensor network diagrams in which tensors are represented graphically by nodes or any shapes (e.g., circles, spheres, triangular, squares, ellipses) and each outgoing edge (line) emerging from a node represents a mode (a way, a dimension, indices) (see Fig. 2). In contrast to classical graphs, in tensor network diagrams an edge does not need connect two nodes, but may be connected to only one node. Each such free (dangling) edge corresponds to a (physical) mode that is not contracted and, hence, the order of the entire tensor network is given by the number of free (dangling) edges (see Fig. 3). Tensor network diagrams are very helpful not only in visualizing tensor decompositions but also to express complex mathematical (multilinear) operations of contractions of tensors. Tensor networks are connected to quantum physics, quantum chemistry and quantum information, which studies the ways to possibly build a quantum computer and to program it [14], [15].

To summarize, the benefits of multiway (tensor) analysis methods for big data include:

- “Super” - compression of huge multidimensional data via tensorization and decompositions of a high-order tensor into factor matrices and/or core tensors of low-rank and low-order;
- By performing all mathematical operations in feasible tensor formats [16];
- Very flexible distributed representations of structurally rich data;
- Possibility to operate with noisy and missing data by using powerful low-rank tensor/matrix approximations and by exploiting robustness and stability of tensor network decomposition algorithms;
- A framework to incorporate various diversities or constraints in different modes or different factors (core tensors) and thus naturally extend

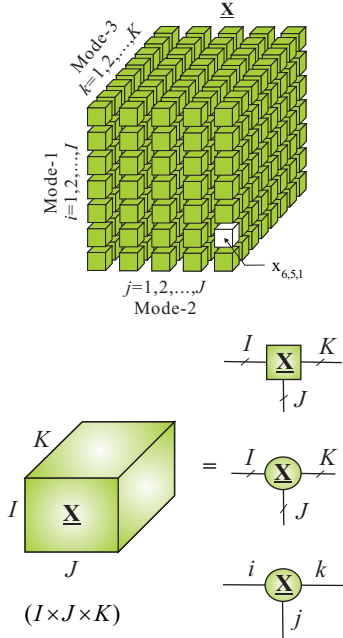


**Figure 2:** A 3rd-order tensor  $\underline{\mathbf{X}} \in \mathbb{R}^{I \times J \times K}$  with entries  $x_{ijk} = \underline{\mathbf{X}}(i, j, k)$  and exemplary symbols used in tensor network diagrams. Each node in the diagram represents a tensor and each edge represents a mode or dimension. We indicate maximum size in each mode by  $I, J, K$  or running indices:  $i = 1, 2, \dots, I$ ;  $j = 1, 2, \dots, J$  and  $k = 1, 2, \dots, K$ .

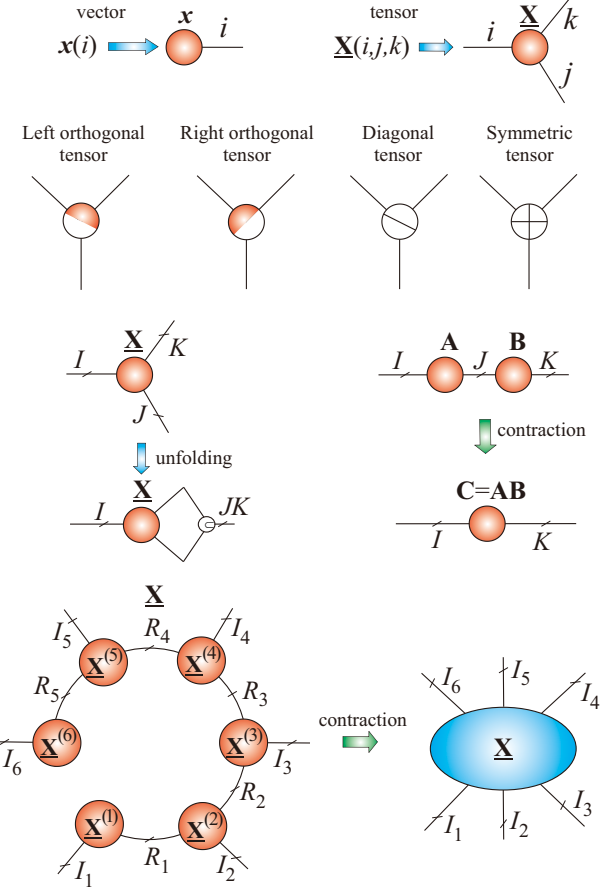


**Figure 3:** Basic symbols and operations for tensor network diagrams. Modes (dimensions) are indicated by running indices  $(i, j, k, \dots)$  where  $i = 1, 2, \dots, I$ ;  $j = 1, 2, \dots, J$ ;  $k = 1, 2, \dots, K$ ;  $r = 1, 2, \dots, R$  in each mode or size of the modes  $(I, J, K, R, \dots)$ . For higher order tensors we will use the symbol  $i_n = 1, 2, \dots, I_n$  for  $n = 1, 2, \dots, N$ , where  $N$  is the order of a tensor. The minimum set of internal indices  $\{R_1, R_2, R_3, \dots\}$  is called the multilinear rank of a specific tensor network [14].

the standard (2-way) CA and BSS methods to large-scale multidimensional data;

- Tensor networks not only provide graphically illustrative large distributed networks but also perform complex tensor operations (i.e., tensor contractions and reshaping) in an intuitive way and without using explicitly mathematical expressions.

Review and tutorial papers [1], [4], [17]–[20] and books [3], [6]–[8] dealing with TDs and TNs already exist, however, they typically focus on standard models and/or do not provide explicit links to big data processing topics and/or do not explore connections to wide class of optimization problems. This paper extends beyond the standard tensor decomposition models such as the Tucker and CPD models, and aims to demonstrate flexibilities of TNs in the optimization problems of multi-dimensional, multi-modal data, together with their role as a mathematical backbone for the discovery of hidden structures in large-scale data [3], [4].

Our objective is to both review tensor models for big data, and to systematically introduce emerging models and associated algorithms for large-scale TNs/TDs, together with illustrating the many

potential applications. Apart from the optimization framework considered many other challenging problems for big data related to anomaly detection, visualization, clustering, feature extraction and classification can also be solved using tensor network decompositions and low-rank tensor approximations.

## II. Basic Tensor Operations

A higher-order tensor can be interpreted as a multiway array of numbers, as illustrated in Figs. 2 and 3. Tensors are denoted by bold underlined capital letters, e.g.,  $\underline{\mathbf{X}} \in \mathbb{R}^{I_1 \times I_2 \times \dots \times I_N}$  (we assume we shall assume that all entries of a tensor are real-valued). The order of a tensor is the number

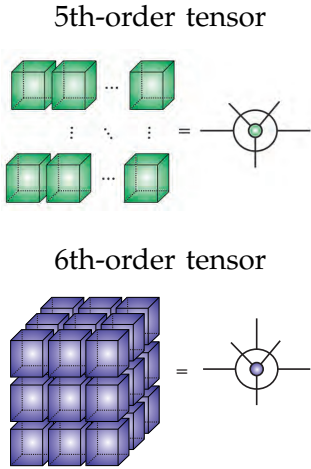


**Figure 4:** Symbols and graphical representations of higher-order block tensors. Outer circle indicates global structure of a block tensor (e.g., matrix, a 3rd-order tensor), while inner circle indicate the structure of each element or block of the tensor.

of its “modes”, “ways” or “dimensions”, which include e.g., space, time, frequency, trials, classes, and dictionaries. Matrices (2nd-order tensors) are denoted by boldface capital letters, e.g.,  $\mathbf{X}$ , and vectors (1st-order tensors) by boldface lowercase letters; for instance the columns of the matrix  $\mathbf{A} = [a_1, a_2, \dots, a_R] \in \mathbb{R}^{I \times R}$  are denoted by  $a_r$  and elements of a matrix (scalars) are denoted by lowercase letters, e.g.,  $a_{ir}$ . Basic tensor and TN notations are given in Table I and illustrated in Figs. 2 – 4. It should be noted that hierarchical block matrices can be represented by tensors and vice versa. For example, 3rd- and 4th-order tensors can be represented by block matrices and all algebraic operations can be equally performed on block matrices [2].

The most common tensor multiplications are denoted by:  $\otimes$  for the Kronecker,  $\odot$  for the Khatri-Rao,  $\circledast$  for the Hadamard (componentwise),  $\circ$  for the outer and  $\times_n$  for the mode- $n$  products (see also Table I). General basic operations, e.g.,  $\text{vec}(\cdot)$ ,  $\text{diag}\{\cdot\}$ , are defined as in MATLAB. We refer to [2]–[4] for more detail regarding the basic notations and tensor operations.

Subtensors are formed when a subset of indices is fixed. Of particular interest are *fibers* (vectors), defined by fixing every index but one, and *slices* which are two-dimensional sections (matrices) of a tensor, obtained by fixing all the indices but two. A matrix has two modes: rows and columns, while an  $N$ th-order tensor has  $N$  modes.

The process of unfolding (see Fig. 5) flattens a tensor into a matrix [4]. In the simplest scenario, mode- $n$  unfolding (matricization, flattening) of the tensor  $\mathbf{A} \in \mathbb{R}^{I_1 \times I_2 \times \cdots \times I_N}$  yields a matrix  $\mathbf{A}_{(n)} \in \mathbb{R}^{I_n \times (I_1 \cdots I_{n-1} I_{n+1} \cdots I_N)}$ , with entries  $a_{i_1, i_2, \dots, i_{n-1}, i_n, i_{n+1}, \dots, i_N}$  such that grouped indices  $(i_1, \dots, i_{n-1}, i_n, i_{n+1}, \dots, i_N)$  are arranged in a specific order, (in this paper rows and columns are ordered colexicographically). In tensor networks we use, typically a generalized mode- $([n])$  unfolding as illustrated in Fig. 5.

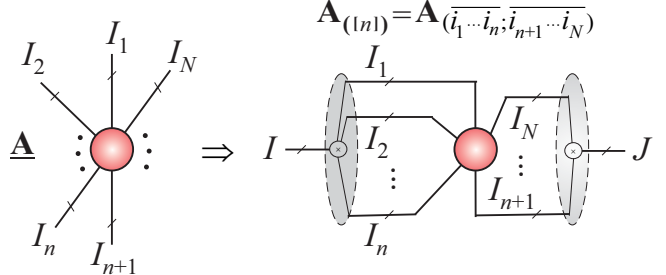


**Figure 5:** Unfolding the  $N$ th-order tensor  $\mathbf{A} \in \mathbb{R}^{I_1 \times I_2 \times \cdots \times I_N}$  into a matrix  $\mathbf{A}_{([n])} = \mathbf{A}_{(\overline{i_1 \cdots i_n}; \overline{i_{n+1} \cdots i_N})} \in \mathbb{R}^{I_1 I_2 \cdots I_n \times I_{n+1} \cdots I_N}$ . All entries of an unfolded tensor are arranged in a specific order. In a more general case, let  $\mathbf{r} = \{m_1, m_2, \dots, m_R\} \subset \{1, 2, \dots, N\}$  be the row indices and  $\mathbf{c} = \{n_1, n_2, \dots, n_C\} \subset \{1, 2, \dots, N\} - \mathbf{r}$  be the column indices, then the mode- $(\mathbf{r}, \mathbf{c})$  unfolding of  $\mathbf{A}$  is denoted as  $\mathbf{A}_{(\mathbf{r}, \mathbf{c})} \in \mathbb{R}^{I_{m_1} I_{m_2} \cdots I_{m_R} \times I_{n_1} I_{n_2} \cdots I_{n_C}}$ .

By a multi-index  $i = \overline{i_1, i_2, \dots, i_N}$  we denote an index which takes all possible combination of values of  $i_1, i_2, \dots, i_n$ , for  $i_n = 1, 2, \dots, I_n$ , in a specific order.

**Remark.** The entries of tensors in matricized and/or vectorized form can be ordered in different forms. In fact, the multi-index can be defined using two different conventions [21]:

## 1) Little-endian convention

$$\begin{aligned} \overline{i_1, i_2, \dots, i_N} &= i_1 + (i_2 - 1)I_1 + (i_3 - 1)I_1 I_2 \\ &\quad \dots + (i_N - 1)I_1 \dots I_{N-1}, \end{aligned} \quad (1)$$

## 2) Big-endian

$$\begin{aligned} \overline{i_1, i_2, \dots, i_N} &= i_N + (i_{N-1} - 1)I_N + \\ &+ (i_{N-2} - 1)I_N I_{N-1} + \dots + (i_1 - 1)I_2 \dots I_N. \end{aligned} \tag{2}$$

The little-endian notation is consistent with the Fortran style of indexing, while the big-endian notation is similar to numbers written in the positional system and corresponds to reverse lexicographic order [21], [22]. The definition of unfolding and the

**TABLE I:** Basic tensor notation and matrix/tensor products.

$\underline{\mathbf{X}} \in \mathbb{R}^{I_1 \times I_2 \times \dots \times I_N}$	Nth-order tensor of size $I_1 \times I_2 \times \dots \times I_N$
$\underline{\mathbf{G}}^{(n)}, \underline{\mathbf{X}}^{(n)}, \underline{\mathbf{S}}$	core tensors
$\underline{\mathbf{\Lambda}} \in \mathbb{R}^{R \times R \times \dots \times R}$	diagonal core tensor with nonzero $\lambda_r$ entries on diagonal
$\underline{\mathbf{A}} = [\underline{\mathbf{a}}_1, \underline{\mathbf{a}}_2, \dots, \underline{\mathbf{a}}_R] \in \mathbb{R}^{I \times R}$	matrix with column vectors $\underline{\mathbf{a}}_r \in \mathbb{R}^I$ and entries $a_{ir}$
$\underline{\mathbf{A}}, \underline{\mathbf{B}}, \underline{\mathbf{C}}, \underline{\mathbf{B}}^{(n)}, \underline{\mathbf{U}}_n$	component matrices
$\underline{\mathbf{X}}_{(n)} \in \mathbb{R}^{I_n \times I_1 \dots I_{n-1} I_{n+1} \dots I_N}$	mode- $n$ unfolding of $\underline{\mathbf{X}}$
$\text{vec}(\underline{\mathbf{A}})$	vectorization of $\underline{\mathbf{A}}$
$\underline{\mathbf{C}} = \underline{\mathbf{A}} \times_n \underline{\mathbf{B}}$	mode- $n$ product of $\underline{\mathbf{A}} \in \mathbb{R}^{I_1 \times I_2 \times \dots \times I_N}$ and $\underline{\mathbf{B}} \in \mathbb{R}^{J_n \times I_n}$ yields $\underline{\mathbf{C}} \in \mathbb{R}^{I_1 \times \dots \times I_{n-1} \times J_n \times I_{n+1} \dots \times I_N}$ with entries $c_{i_1 \dots i_{n-1} j_n i_{n+1} \dots i_N} = \sum_{i_n=1}^{I_n} a_{i_1 \dots i_{n-1} i_n} b_{j_n i_n}$ , and $\underline{\mathbf{C}}_{(n)} = \underline{\mathbf{B}} \underline{\mathbf{A}}_{(n)}$
$\underline{\mathbf{C}} = [\underline{\mathbf{A}}; \underline{\mathbf{B}}^{(1)}, \dots, \underline{\mathbf{B}}^{(N)}] = \underline{\mathbf{A}} \times_1 \underline{\mathbf{B}}^{(1)} \times_2 \underline{\mathbf{B}}^{(2)} \dots \times_N \underline{\mathbf{B}}^{(N)}$	
$\underline{\mathbf{C}} = \underline{\mathbf{A}} \circ \underline{\mathbf{B}}$	tensor or outer product of $\underline{\mathbf{A}} \in \mathbb{R}^{I_1 \times I_2 \times \dots \times I_N}$ and $\underline{\mathbf{B}} \in \mathbb{R}^{J_1 \times J_2 \times \dots \times J_M}$ yields $(N+M)$ -th-order tensor $\underline{\mathbf{C}}$ with entries $c_{i_1 \dots i_N j_1 \dots j_M} = a_{i_1 \dots i_N} b_{j_1 \dots j_M}$
$\underline{\mathbf{X}} = \underline{\mathbf{a}} \circ \underline{\mathbf{b}} \circ \underline{\mathbf{c}} \in \mathbb{R}^{I \times J \times K}$	tensor or outer product of vectors forms a rank-1 tensor with entries $x_{ijk} = a_i b_j c_k$
$\underline{\mathbf{C}} = \underline{\mathbf{A}} \otimes \underline{\mathbf{B}}$	Kronecker product of $\underline{\mathbf{A}} \in \mathbb{R}^{I_1 \times I_2 \times \dots \times I_N}$ and $\underline{\mathbf{B}} \in \mathbb{R}^{J_1 \times J_2 \times \dots \times J_M}$ yields $\underline{\mathbf{C}} \in \mathbb{R}^{I_1 J_1 \times \dots \times I_N J_N}$ with entries $c_{\overline{i_1, j_1}, \dots, \overline{i_N, j_N}} = a_{i_1 \dots i_N} b_{j_1 \dots j_N}$ , where $i_n, j_n = j_n + (i_n - 1) J_n$
$\underline{\mathbf{C}} = \underline{\mathbf{A}} \odot \underline{\mathbf{B}}$	Khatri-Rao product of $\underline{\mathbf{A}} \in \mathbb{R}^{I \times J}$ and $\underline{\mathbf{B}} \in \mathbb{R}^{K \times J}$ yield $\underline{\mathbf{C}} \in \mathbb{R}^{IK \times J}$ , with columns $c_j = \underline{\mathbf{a}}_j \otimes \underline{\mathbf{b}}_j$

Kronecker (tensor) product  $\otimes$  should be also consistent with the chosen convention<sup>1</sup>. In this paper we will use the big-endian notation, however to follow this work it is sufficient to remember that  $c = \underline{\mathbf{a}} \otimes \underline{\mathbf{b}}$  means that  $c_{\overline{i_j}} = a_i b_j$ .

The Kronecker product of two tensors  $\underline{\mathbf{A}} \in \mathbb{R}^{I_1 \times I_2 \times \dots \times I_N}$  and  $\underline{\mathbf{B}} \in \mathbb{R}^{J_1 \times J_2 \times \dots \times J_N}$  yields  $\underline{\mathbf{C}} = \underline{\mathbf{A}} \otimes \underline{\mathbf{B}} \in \mathbb{R}^{I_1 J_1 \times \dots \times I_N J_N}$  with entries  $c_{\overline{i_1, j_1}, \dots, \overline{i_N, j_N}} = a_{i_1 \dots i_N} b_{j_1 \dots j_N}$ , where  $\overline{i_n, j_n} = j_n + (i_n - 1) J_n$  [23].

The outer or tensor product  $\underline{\mathbf{C}} = \underline{\mathbf{A}} \circ \underline{\mathbf{B}}$  of the tensors  $\underline{\mathbf{A}} \in \mathbb{R}^{I_1 \times \dots \times I_N}$  and  $\underline{\mathbf{B}} \in \mathbb{R}^{J_1 \times \dots \times J_M}$  is the tensor  $\underline{\mathbf{C}} \in \mathbb{R}^{I_1 \times \dots \times I_N \times J_1 \times \dots \times J_M}$  with entries  $c_{i_1 \dots i_N, j_1 \dots j_M} = a_{i_1 \dots i_N} b_{j_1 \dots j_M}$ . Specifically, the outer product of two nonzero vectors  $\underline{\mathbf{a}} \in \mathbb{R}^I$ ,  $\underline{\mathbf{b}} \in \mathbb{R}^J$  produces a rank-1 matrix  $\underline{\mathbf{X}} = \underline{\mathbf{a}} \circ \underline{\mathbf{b}} = \underline{\mathbf{a}} \underline{\mathbf{b}}^T \in \mathbb{R}^{I \times J}$  and the outer product of three nonzero vectors:  $\underline{\mathbf{a}} \in \mathbb{R}^I$ ,  $\underline{\mathbf{b}} \in \mathbb{R}^J$  and  $\underline{\mathbf{c}} \in \mathbb{R}^K$  produces a 3rd-order rank-1 tensor:  $\underline{\mathbf{X}} = \underline{\mathbf{a}} \circ \underline{\mathbf{b}} \circ \underline{\mathbf{c}} \in \mathbb{R}^{I \times J \times K}$ , whose entries are  $x_{ijk} = a_i b_j c_k$ . A tensor  $\underline{\mathbf{X}} \in \mathbb{R}^{I_1 \times I_2 \times \dots \times I_N}$  is said to be rank-1 if it can be expressed exactly as  $\underline{\mathbf{X}} = \underline{\mathbf{b}}^{(1)} \circ \underline{\mathbf{b}}^{(2)} \circ \dots \circ \underline{\mathbf{b}}^{(N)}$  with entries  $x_{i_1, i_2, \dots, i_N} = b_{i_1}^{(1)} b_{i_2}^{(2)} \dots b_{i_N}^{(N)}$ , where  $\underline{\mathbf{b}}^{(n)} \in \mathbb{R}^{I_n}$  are nonzero vectors.

The mode- $n$  product of the tensor  $\underline{\mathbf{A}} \in \mathbb{R}^{I_1 \times \dots \times I_N}$  and vector  $\underline{\mathbf{b}} \in \mathbb{R}^{I_n}$  is defined as a tensor  $\underline{\mathbf{C}} = \underline{\mathbf{A}} \bar{\times}_n \underline{\mathbf{b}} \in \mathbb{R}^{I_1 \times \dots \times I_{n-1} \times I_{n+1} \times \dots \times I_N}$ , with entries  $c_{i_1 \dots i_{n-1}, i_n, i_{n+1} \dots i_N} = \sum_{i_n=1}^{I_n} (a_{i_1, i_2, \dots, i_N})(b_{i_n})$ , while a mode- $n$  product of the tensor  $\underline{\mathbf{A}} \in \mathbb{R}^{I_1 \times \dots \times I_N}$  and a matrix  $\underline{\mathbf{B}} \in \mathbb{R}^{J \times I_n}$  is the tensor  $\underline{\mathbf{C}} = \underline{\mathbf{A}} \times_n \underline{\mathbf{B}} \in \mathbb{R}^{I_1 \times \dots \times I_{n-1} \times J \times I_{n+1} \times \dots \times I_N}$  with entries  $c_{i_1, i_2, \dots, i_{n-1}, j, i_{n+1}, \dots, i_N} = \sum_{i_n=1}^{I_n} a_{i_1, i_2, \dots, i_N} b_{j, i_n}$ . This can be also expressed in a matrix form as  $\underline{\mathbf{C}}_{(n)} = \underline{\mathbf{B}} \underline{\mathbf{A}}_{(n)}$ .

A full multilinear product of a tensor and a set of matrices takes into account all the modes, and can be compactly written as (see Fig 6 (a)):

$$\begin{aligned} \underline{\mathbf{C}} &= \underline{\mathbf{A}} \times_1 \underline{\mathbf{B}}^{(1)} \times_2 \underline{\mathbf{B}}^{(2)} \dots \times_N \underline{\mathbf{B}}^{(N)} \\ &= [\underline{\mathbf{A}}; \underline{\mathbf{B}}^{(1)}, \underline{\mathbf{B}}^{(2)}, \dots, \underline{\mathbf{B}}^{(N)}]. \end{aligned} \quad (3)$$

In a similar way, we can define the mode- $\binom{m}{n}$  product of two tensors  $\underline{\mathbf{A}} \in \mathbb{R}^{I_1 \times I_2 \times \dots \times I_N}$  and  $\underline{\mathbf{B}} \in \mathbb{R}^{J_1 \times J_2 \times \dots \times J_M}$  with common modes  $I_n = J_m$  that produces a  $(N+M-2)$ -order tensor  $\underline{\mathbf{C}} \in \mathbb{R}^{I_1 \times \dots \times I_{n-1} \times I_{n+1} \dots \times I_N \times J_1 \times \dots \times J_{m-1} \times J_{m+1} \dots \times J_M}$ :

$$\underline{\mathbf{C}} = \underline{\mathbf{A}} \times_n^m \underline{\mathbf{B}}, \quad (4)$$

<sup>1</sup>The standard and more popular definition in multilinear algebra assumes the big-endian convention, which corresponds to colexicographic order, while for the development of the efficient program code, usually, the little-endian convention seems to be more convenient (See more detail the paper of Dolgov and Savostyanov [21]).

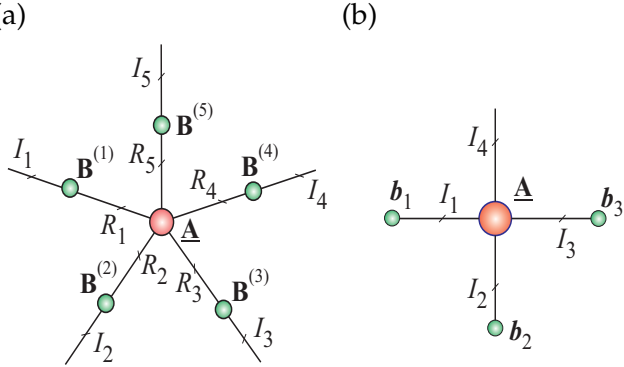


**Figure 6:** (a) Multilinear product of tensor  $\underline{A} \in \mathbb{R}^{I_1 \times R_2 \times \dots \times R_5}$  and 5 factor (component) matrices  $\underline{B}^{(n)} \in \mathbb{R}^{I_n \times R_n}$  ( $n = 1, 2, \dots, 5$ ) yields  $\underline{C} = \underline{A} \times_1 \underline{B}^{(1)} \times_2 \underline{B}^{(2)} \times_3 \underline{B}^{(3)} \times_4 \underline{B}^{(4)} \times_5 \underline{B}^{(5)} \in \mathbb{R}^{I_1 \times I_2 \times \dots \times I_5}$  and (b) Multilinear product of tensor  $\underline{A} \in \mathbb{R}^{I_1 \times I_2 \times I_3 \times I_4}$  and vectors  $\underline{b}_n \in \mathbb{R}^{I_n}$  ( $n = 1, 2, 3$ ) yields a vector  $\underline{c} = \underline{A} \bar{\times}_1 \underline{b}_1 \bar{\times}_2 \underline{b}_2 \bar{\times}_3 \underline{b}_3 \in \mathbb{R}^{I_4}$ .

with entries  $c_{i_1 \dots i_{n-1} i_{n+1} \dots i_N, j_1 \dots j_{m-1} j_{m+1} \dots j_M} = \sum_{i=1}^{I_n} a_{i_1 \dots i_{n-1} i_{n+1} \dots i_N} b_{j_1 \dots j_{m-1} i_{j_{m+1} \dots j_M}}$  (see Fig. 7(a)).

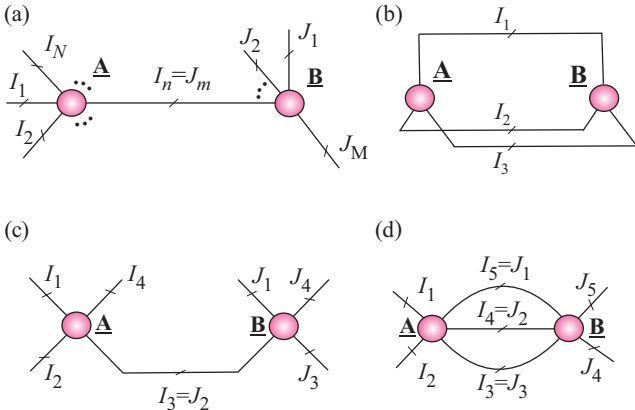


**Figure 7:** Examples of contraction of two tensors: (a) Multilinear product of two tensors is denoted by  $\underline{C} = \underline{A} \times_n^m \underline{B}$ . (b) Inner product of two 3rd-order tensors yields  $c = \langle \underline{A}, \underline{B} \rangle = \underline{A} \times_{1,2,3}^{1,2,3} \underline{B} = \underline{A} \times \underline{B} = \sum_{i_1, i_2, i_3} a_{i_1, i_2, i_3} b_{i_1, i_2, i_3}$ . (c) Tensor contraction of two 4th-order tensors yields the 6th-order tensor  $\underline{C} = \underline{A} \times_3^2 \underline{B} \in \mathbb{R}^{I_1 \times I_2 \times I_4 \times J_1 \times J_3 \times I_4}$ , with entries  $c_{i_1, i_2, i_4, j_1, j_3, j_4} = \sum_{i_3} a_{i_1, i_2, i_3, i_4} b_{j_1, i_3, j_3, j_4}$ . (d) Tensor contraction of two 5th-order tensors yields the 4th-order tensor  $\underline{C} = \underline{A} \times_{3,4,5}^{1,2,3} \underline{B} \in \mathbb{R}^{I_1 \times I_2 \times J_4 \times J_5}$ , with entries  $c_{i_1, i_2, i_4, i_5} = \sum_{i_3, i_4, i_5} a_{i_1, i_2, i_3, i_4, i_5} b_{i_5, i_4, i_3, j_4, j_5}$ .

When not confusing, the super-index  $m$  can be neglected. For example, the mode-1 product of the tensors  $\underline{A} \in \mathbb{R}^{I_1 \times I_2 \times \dots \times I_N}$  and  $\underline{B} \in \mathbb{R}^{J_1 \times J_2 \times \dots \times J_M}$ , with a common first mode  $I_1 = J_1$  can be written as

$$\underline{C} = \underline{A} \times_1^1 \underline{B} = \underline{A} \times_1 \underline{B} \in \mathbb{R}^{I_2 \times \dots \times I_N \times J_2 \times \dots \times J_M}, \quad (5)$$

with entries  $c_{i_{2:N}, j_{2:M}} = \sum_{i=1}^{I_1} a_{i, i_{2:N}} b_{i, j_{2:M}}$ , when using MATLAB notation,  $i_{p:q} = \{i_p, i_{p+1}, \dots, i_{q-1}, i_q\}$ . This operation can be considered as a tensor contraction of two modes. Tensors can be contracted in several modes or even in all modes (see Fig. 7).

Tensor contraction is a fundamental operation, which can be considered as a higher dimensional analogue of inner product, outer product and matrix multiplications, and comprises computationally dominant operations in most numerical algorithms. However, unlike the matrix by matrix multiplications for which many efficient distributed-memory parallel schemes have been developed, for a tensor contraction we have a rather limited number of available optimized algorithms [24]–[26]. In practice, we usually implement approximate tensors contractions with reduced ranks [27]. A significant help in developing effective distributed tensor contraction algorithms is that the tensors used in computational models often exhibit symmetry over all or multiple modes; exploitation of the symmetry is essential, both in order to save on storage as well as to avoid unnecessary arithmetic operations [25], [26].

Tensors often need to be converted to traces, scalars, vectors, matrices or tensors with reshaped modes and reduced orders, as illustrated in Fig. 8 and Fig. 9.

### III. Low-Rank Tensor Approximations via Tensor Networks

#### A. Basic Tensor Network Models

Tensor networks can be considered as a new “language” for big data tensor decompositions in simulation of large complex systems (e.g., in condensed matter physics and quantum physics) even with using standard computers [2], [15], [28], [29]. In other words, tensor networks, can be considered as a diagrammatic language for capturing the internal structure of high-order tensor decompositions.

In contrast to the CPD or Tucker decompositions, that have only one single core tensor, TNs decompose a high-order tensor into several lower-order core tensors. The branches (leads, lines, edges) connecting core tensors between each other correspond to contracted modes (and represent a TN rank), whereas lines that do not go from one tensor to another correspond to physical modes in the TN. A tensor network is a set of weakly connected core tensors, where some or all indices are contracted according to some rules.

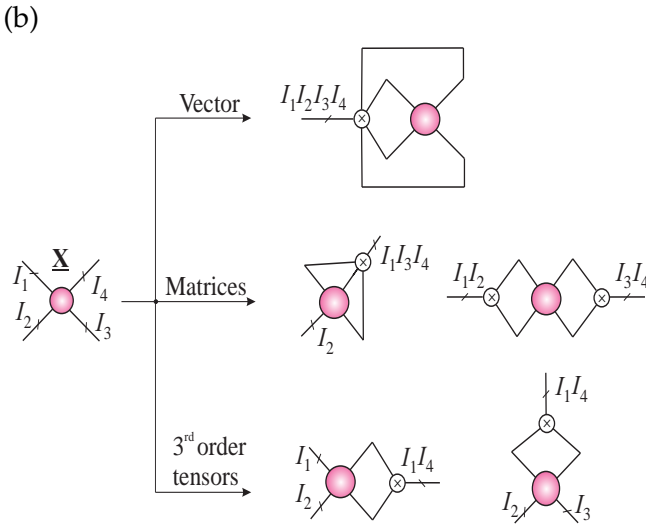
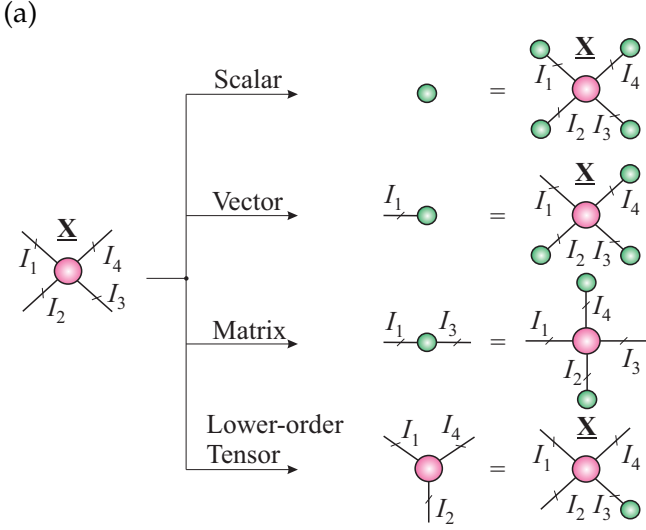


**Figure 8:** (a) Transforming or compressing a 4th-order tensor into scalar, vector, matrix and 3rd-order tensor by multilinear product of the tensor and vectors. (b) Reshaping of a tensor by its vectorization, unfolding and reducing the order by merging the modes.

Some examples of basic tensor network diagrams are given in Figs. 10, 11, 12, and 13 [2], [14]. A tensor network may not contain any loops, i.e., any edges connecting a node with itself. If a tensor network is a binary tree, i.e., if it does not contain any cycles (loops), each of its edges splits the modes of the data tensor into two or more groups, which is related to the suitable matricization of the tensor [30], [31]. A tree tensor network, whose all nodes have degree 3 or 4, corresponds to a Hierarchical Tucker (HT) decomposition of the tensor illustrated in Fig. 13 (a). The HT decompositions in the numerical analysis community have been introduced by Hackbusch and Kühn [32] and Grasedyck [33] (see also [30], [34]–[37] and references therein).

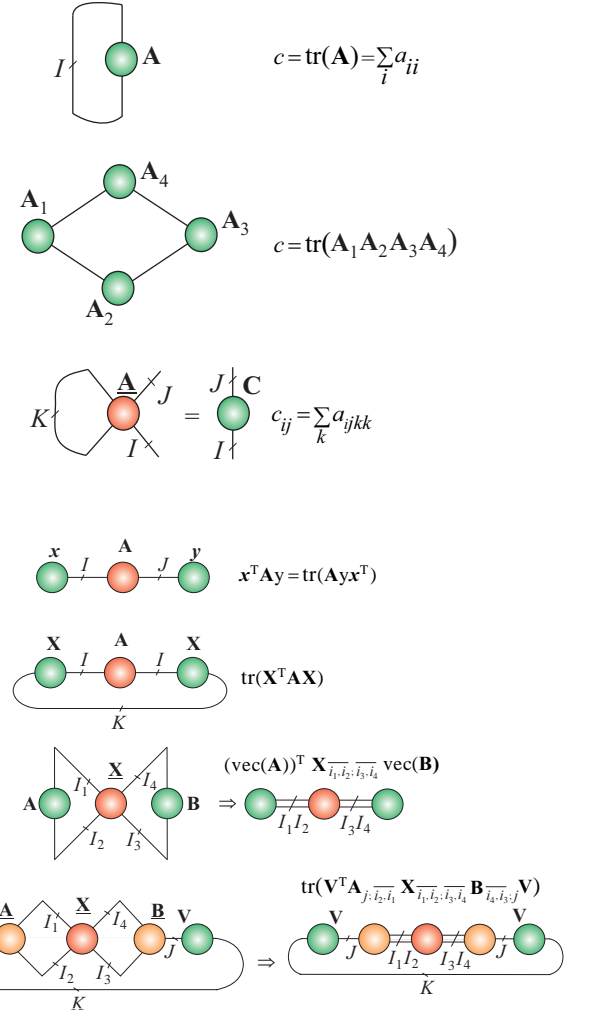


**Figure 9:** Tensor network notation and operations for traces of matrices and higher-order tensors.

The general construction of the HT decomposition requires a hierarchical splitting of the modes (with sizes  $I_1, I_2, \dots, I_N$ ). The construction of Hierarchical Tucker format relies on the notion of a dimension tree, chosen *a priori*, which specifies the topology of the HT decomposition. Intuitively, the dimension tree specifies which groups of modes are “separated” from other groups of modes, where sequential HT decomposition can be performed via (truncated) SVD applied to unfolded matrices [30].

The Tensor Train (TT) format proposed in the numerical analysis community by Oseledets and Tyrtyshnikow [38] (see also [13], [39]–[43]) can be interpreted as a special case of the HT, where all nodes of the underlying tensor network are aligned and where, moreover, the leaf matrices are assumed to be identities (and thus need not be stored). An advantage of the TT format is its simpler practical implementation, as no binary tree need be involved.

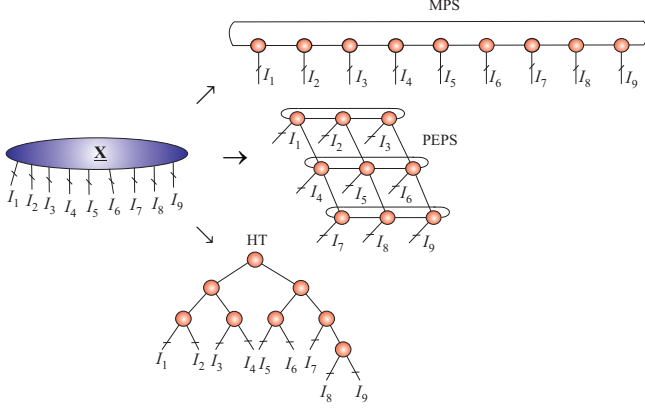


**Figure 10:** Illustration of decomposition of 9th-order tensor  $\underline{X} \in \mathbb{R}^{I_1 \times I_2 \times \dots \times I_9}$  into different forms of tensor networks (TNs): The Matrix Product State (MPS) with periodic boundary conditions (PBC), called also the Tensor Chain (TC), the Projected Entangled-Pair States (PEPS) with PBC and Hierarchical Tucker (HT) decomposition, which is equivalent to the Tree Tensor Network State (TTNS). In general, the objective is to decompose very high-order tensor into sparsely (weakly) connected low-order and low-rank tensors, typically 3rd-order and 4th-order tensors, called cores.

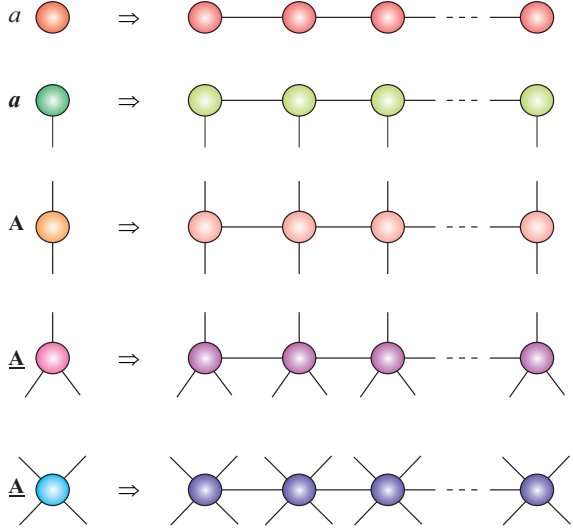


**Figure 11:** Different forms of tensor train decompositions depending on input data: For scalar functions  $a$ , vectors  $\underline{a}$ , matrices  $\mathbf{A}$ , and 3rd-order and 4th-order tensors  $\underline{\mathbf{A}}$ .

The Tensor Trains [38], [40], [44], called also Matrix Product States (MPS) in quantum information theory [15], [45]–[48], is the simplest TN model<sup>2</sup>.

For some very high-order data tensors it has been

<sup>2</sup>In fact, the TT was rediscovered several times under different names: MPS, valence bond states and density matrix renormalization group (DMRG). The DMRG usually means not only tensor format but also power-full computational algorithms (see [49] and references therein).

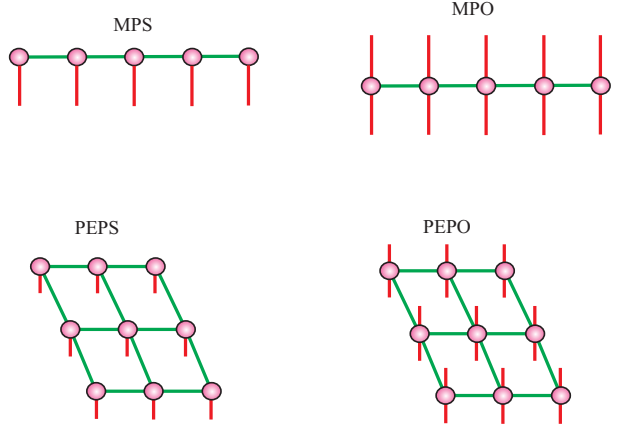


**Figure 12:** Basic tensor networks with open boundary conditions (OBC): The Matrix Product State (MPS) or (vector) Tensor Train (TT), the Matrix Product Operator (MPO) or Matrix TT, the Projected Entangled-Pair States (PEPS) or Tensor Product State (TPS) and the Projected Entangled-Pair Operators (PEPO).

observed that the ranks  $R_n$  of 3rd-order tensors increase rapidly with the order of the tensor, for any choice of tensor network that is a tree (including TT and HT decompositions) [35].

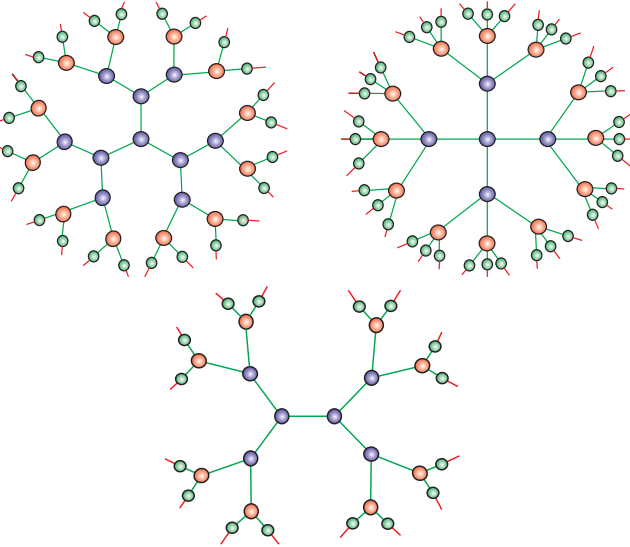
For such cases, PEPS and the Multi-scale Entanglement Renormalization Ansatz (MERA) tensor networks can be used which contain cycles, but have hierarchical structures (see Fig. 13) (c). For the PEPS and MERA TNs the ranks can be kept considerably smaller, at the cost of employing 5th and 4th-order core tensors and consequently a higher computational complexity w.r.t. their ranks [50], [51].

Some interesting connections between tensor networks and graphical models used extensively in machine learning and statistics as shown in Table II [41], [52]–[55]. Despite clear analogy, more research is needed to find more deep and precise relationships [55].

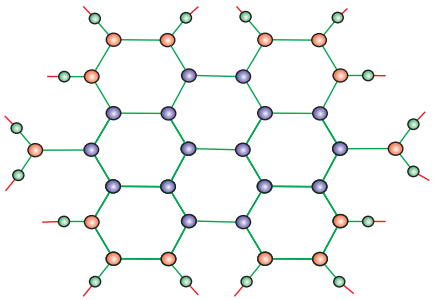
## B. Changing the Structure of Tensor Networks

One advantage of a graphical representation of a tensor network is that it allows us to perform even most complex mathematical operations in intuitive and easy to understand way. Another important advantage is the ability to modify or optimize a TN structure, that is, to change its topology, preserving physical modes unchanged. In fact, in some applications it is quite useful to modify the topology of a tensor network with or without approximation by providing simplified or more convenient graphical representation of the

(a) Hierarchical Tucker (HT) or Tree Tensor Network State (TTNS) with 3rd-order and 4th-order cores



(b) Honey-Comb lattice for a 16th-order data tensor



(c) MERA for 8th-order tensor

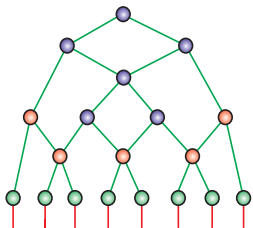


**Figure 13:** Architectures of the fundamental TNs, which can be considered as distributed models of the Tucker- $N$  models. Green nodes denote factor matrices, while blue and red nodes denote cores.

same higher-order data tensor [56]–[58]. For instance, tensor networks may consist of many cycles, those can't be reduced or completely eliminated in order to reduce computational complexity of

**TABLE II:** Similarities and links between tensor networks (TNs) and graphical models used in Machine Learning (ML) and Statistics. The categories are not exactly the same, but they closely correspond.

Tensor Networks	Graphical Models in ML/Statistics
TT/MPS	Hidden Markov Models (HMM)
HT/TTNS	Gaussian Mixture Model (GMM)
TNS/PEPS	Markov Random Field (MRF) and Conditional Random Field (CRF)
MERA	Deep Belief Networks (DBN)
DMRG and MALS Algs.	Forward-Backward Algs., Block Nonlinear Gauss-Seidel Methods

contraction of core tensors and to provide stability of computation. Again, observe a strong link with loop elimination in control theory, in addition tensor networks having many cycles may not admit stable algorithm. By changing the topology to a tree structure (TT/HT models), we can often reduce complexity of computation and improve stability of algorithms.

Performing contraction of core tensors iteratively for tree-structured tensor networks has usually a much smaller complexity than tensor networks containing many cycles. One could transform a specific tensor network with cycles into a tree structure, perform stable computations<sup>3</sup>, with it and re-transform it back to the original structure if necessary. Furthermore, in the cases that we need to compare or analyze a set of blocks of tensor data, it is important that such tensors are represented by the same or very similar structures to analyze link or correlation between them or detect common cores or hidden components. Performing such analysis with differently structured tensor networks is in general difficult or even impossible.

A Tensor network can be relatively easily transformed from one form to another one via tensor contractions, reshaping and basic matrix factorizations, typically using SVD [39], [40]. The basic approach to modify tensor structure is to perform: sequential core contractions, unfolding contracting tensors into matrices, performing matrix factorizations (typically, SVD) and finally reshaping matrices back to new core tensors. These principles are

<sup>3</sup>The TT decomposition is stable in the sense that the best approximation of a data tensor with bounded TT-ranks always exist and a quasi-optimal approximation can be computed by a sequence of truncated SVDs of suitably reshaping matrices of cores [39], [40].

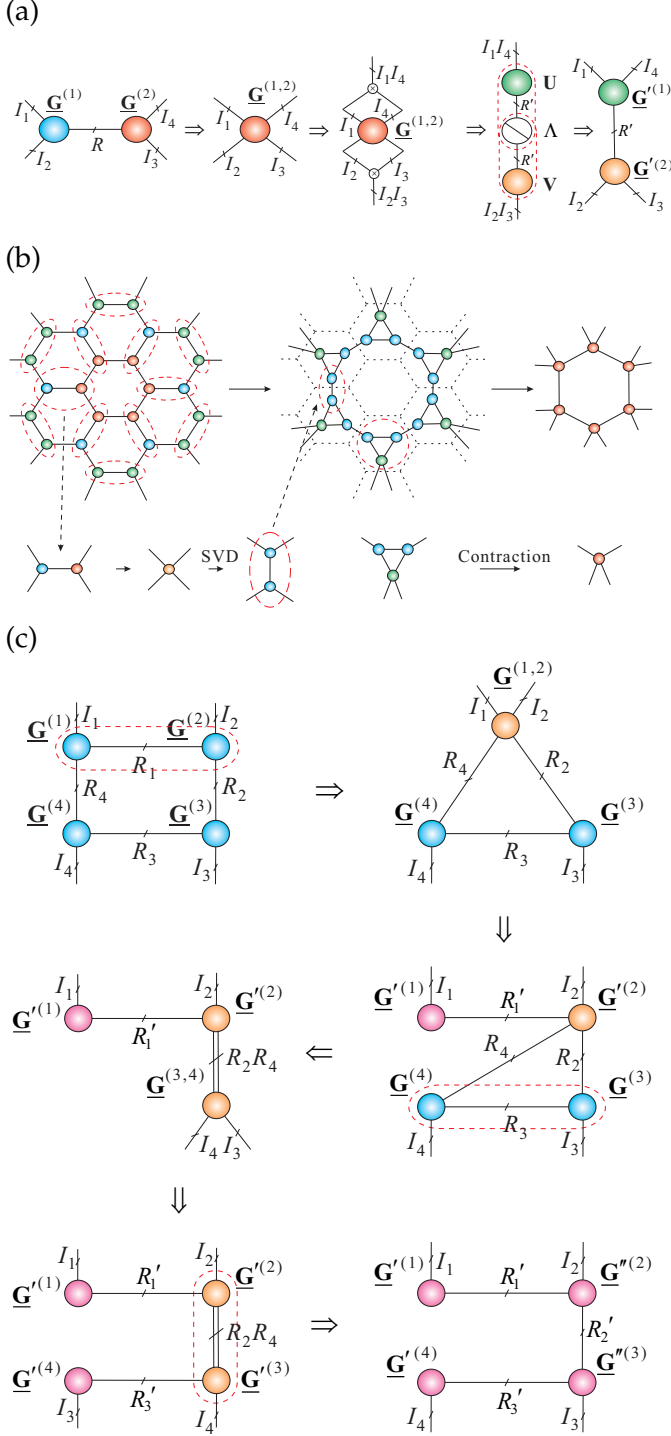


**Figure 14:** Illustration of basic transformation of tensors via: (a) Contraction, unfolding, matrix factorization (SVD) and reshaping of matrices back into tensors. (b) Transformation of Honey-Comb lattice into Tensor Chain (TC) via tensor contractions and the SVD. (c) Transformation of the TC, i.e., a TT/MPS with periodic boundary conditions (PBC) to the standard TT, i.e., the MPS with open boundary conditions (OBC).

illustrated graphically in Figs 14 (a), (b), (c).

For example, in Fig 14 (a) in the first step we perform a contraction of two core tensors  $\underline{\mathbf{G}}^{(1)} \in \mathbb{R}^{I_1 \times I_2 \times R}$  and  $\underline{\mathbf{G}}^{(2)} \in \mathbb{R}^{R \times I_3 \times I_4}$ , as:

$$\underline{\mathbf{G}}^{(1,2)} = \underline{\mathbf{G}}^{(1)} \times_3^1 \underline{\mathbf{G}}^{(2)} \in \mathbb{R}^{I_1 \times I_2 \times I_3 \times I_4}, \quad (6)$$

with entries  $g_{i_1, i_2, i_3, i_4}^{(1,2)} = \sum_{r=1}^R g_{i_1, i_2, r}^{(1)} g_{r, i_3, i_4}^{(2)}$ . In the next step, we transform the tensor  $\underline{\mathbf{G}}^{(1,2)}$  into a matrix via unfolding and low-rank matrix factorization via the SVD

$$\underline{\mathbf{G}}_{i_1, i_4; i_2, i_3}^{(1,2)} \cong \mathbf{U} \Sigma \mathbf{V}^T \in \mathbb{R}^{I_1 I_4 \times I_2 I_3}. \quad (7)$$

In the last step, we reshape factor matrices  $\mathbf{U} \Sigma^{1/2} \in \mathbb{R}^{I_1 I_4 \times R'}$  and  $\mathbf{V} \Sigma^{1/2} \in \mathbb{R}^{R' \times I_2 I_3}$  back to new core tensors:  $\underline{\mathbf{G}}'^{(1)} \in \mathbb{R}^{I_1 \times R' \times I_4}$  and  $\underline{\mathbf{G}}'^{(2)} \in \mathbb{R}^{I_2 \times I_3 \times R'}$ .

The above procedure has been applied in Fig. 14 (b) to transform Honey-Comb lattice into tensor chain (TC) along with tensor contraction of three cores [57].

In Fig. 14 (c) we have illustrated how to convert tensor chain (TC) into TT/MPS with OBC, by contracting sequentially two core tensors, unfolding them, applying SVD and reshaping matrices back into core tensors [56]. More precisely, in the first step, we perform a contraction of two tensors  $\underline{\mathbf{G}}^{(1)} \in \mathbb{R}^{I_1 \times R_4 \times R_1}$  and  $\underline{\mathbf{G}}^{(2)} \in \mathbb{R}^{R_1 \times R_2 \times I_2}$ , as:

$$\underline{\mathbf{G}}^{(1,2)} = \underline{\mathbf{G}}^{(1)} \times_3^1 \underline{\mathbf{G}}^{(2)} \in \mathbb{R}^{I_1 \times R_4 \times R_2 \times I_2}, \quad (8)$$

with entries  $g_{i_1, r_4, r_2, i_2}^{(1,2)} = \sum_{r_1=1}^{R_1} g_{i_1, r_4, r_1}^{(1)} g_{r_1, r_2, i_2}^{(2)}$ . In the next step, we can transform this tensor  $\underline{\mathbf{G}}^{(1,2)}$  into a matrix in order to perform the truncated SVD:

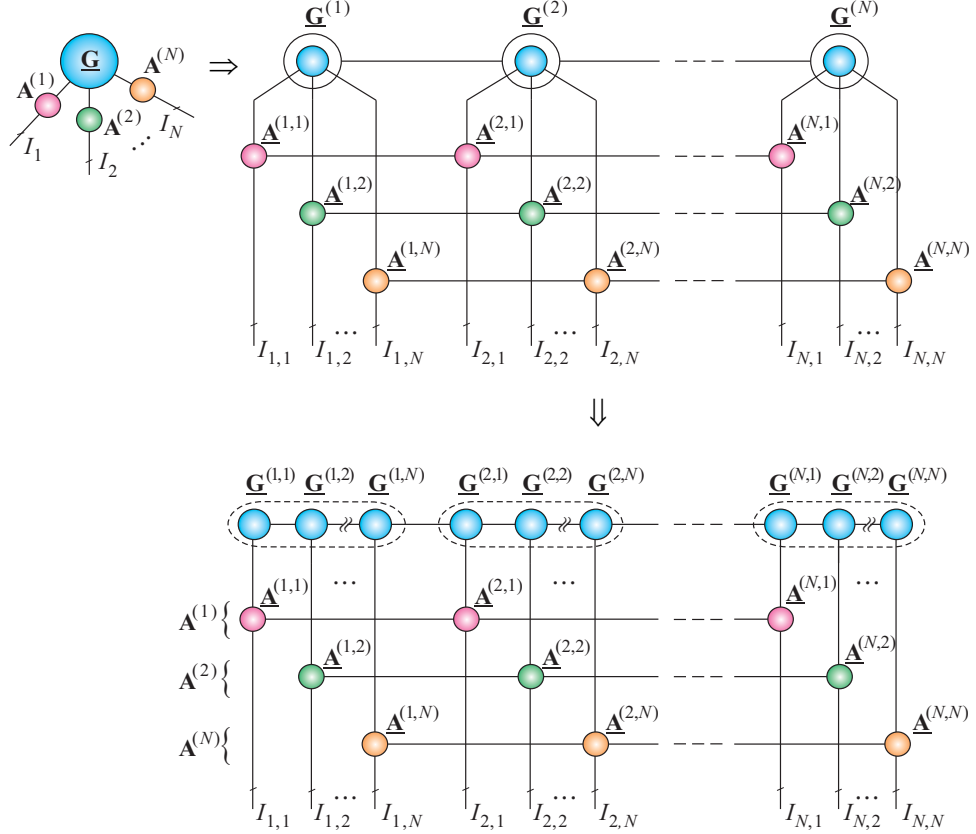
$$\underline{\mathbf{G}}_{i_1; r_4, r_2, i_2}^{(1,2)} \cong \mathbf{U} \Sigma \mathbf{V}^T \in \mathbb{R}^{I_1 \times R_4 R_2 I_2}. \quad (9)$$

In the next step, we reshape orthogonal matrices  $\mathbf{U} \Sigma^{1/2} \in \mathbb{R}^{I_1 \times R'_1}$  and  $\mathbf{V} \Sigma^{1/2} \in \mathbb{R}^{R'_1 \times R_4 R_2 I_2}$  back to core tensors:  $\underline{\mathbf{G}}'^{(1)} = \mathbf{U} \Sigma^{1/2} \in \mathbb{R}^{1 \times I_1 \times R'_1}$  and  $\underline{\mathbf{G}}'^{(2)} \in \mathbb{R}^{R'_1 \times R_4 \times R_2 \times I_2}$ . The procedure is repeated again and again for different pair of cores as illustrated in the Fig. 14 (c).

### C. Distributed (Concatenated) Representation of Tensors

A simple approach to reduce the size or rank of core tensors is to apply distributed tensor networks (DTNs), which consists of two kind of cores (nodes): internal nodes which has no free edges and external nodes which have free edges representing natural (physical) indices of a data tensor as illustrated in Figs. 13 and 15. A simple idea is

(a) Tensor Train (TT) model – MPS/MPO with the Open Boundary Conditions (OBC)



(b) Tensor Chain (TC) model – MPS/MPO with the Periodic Boundary Conditions (PBC)

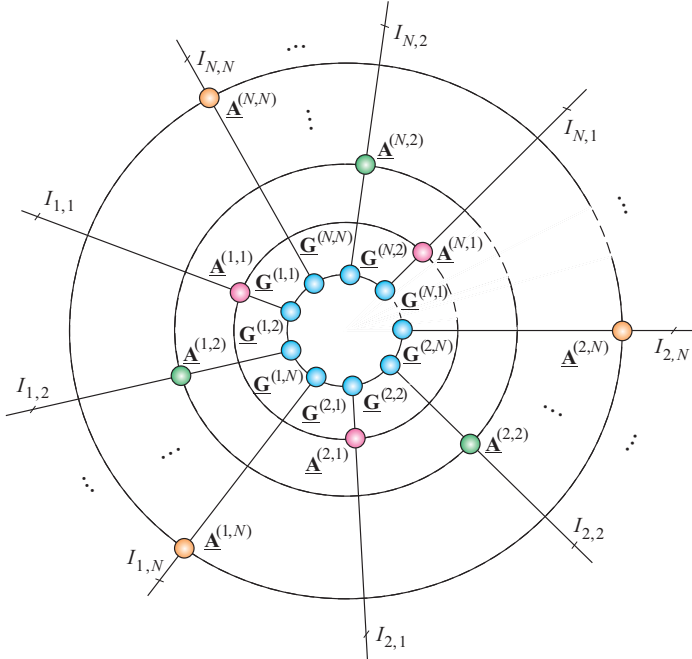


**Figure 15:** New distributed models of the Tucker- $N$  decomposition  $\mathbf{X} = \mathbf{G} \times_1 \mathbf{A}^{(1)} \times_2 \mathbf{A}^{(2)} \cdots \times_N \mathbf{A}^{(N)} \in \mathbb{R}^{I_1 \times I_2 \times \cdots \times I_N}$ , with  $I_n = I_{1,n} I_{2,n} \cdots I_{N,n}$ ,  $(n = 1, 2, \dots, N)$ .

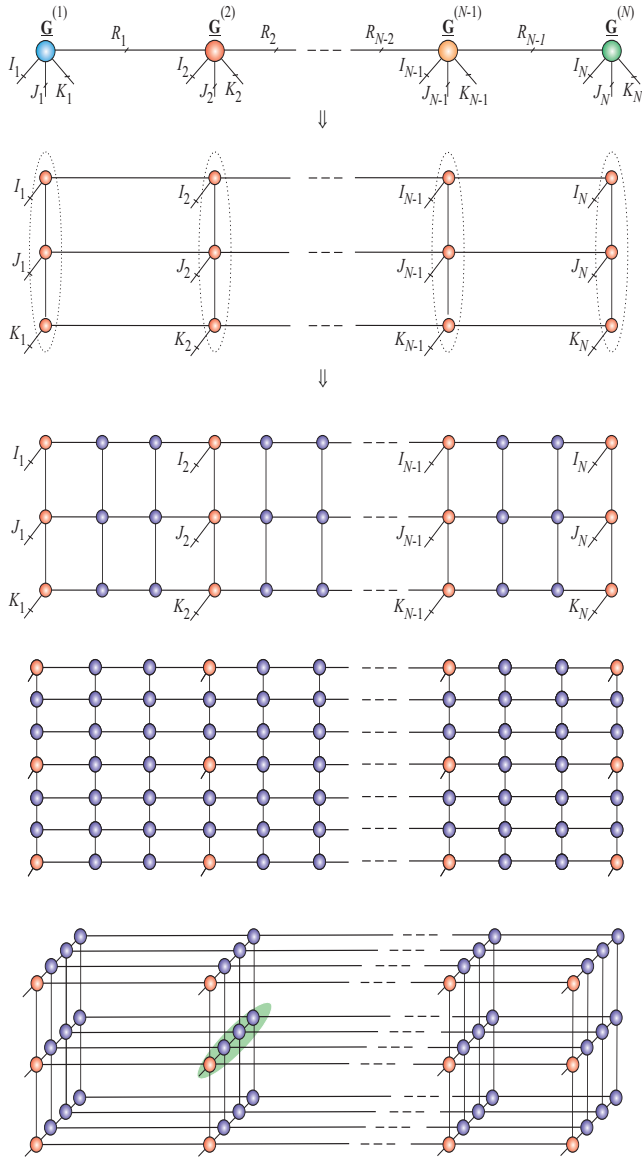


**Figure 16:** Graphical representation of TT via Tensor Product State (TPS) or equivalently PEPS for a large-scale data tensor and its transformation to distributed 2D and 3D PEPS [58].

that each of the core tensor in an original TN is itself repeatedly replaced by another TN (see Fig. 16), resulting in another TN in which only some core tensors are associated with physical (natural) modes of the original data tensor [58].

The main advantage of DTNs is that the size of each of the core tensors in the internal tensor network structure is usually much smaller than the initial core tensor so consequently the total number of parameters can be reduced [58]. However, it should be noted that the contraction of the resulting tensor network becomes more difficult when

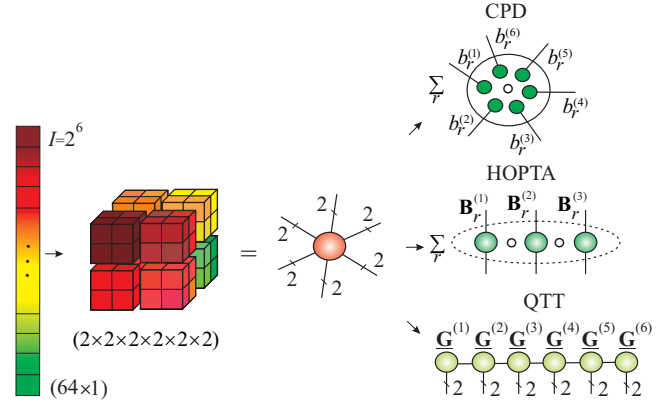


**Figure 17:** The conceptual illustration of tensorization of a large-scale vector into a higher-order quantized tensor. In order to achieve super-compression we need to apply a suitable tensor decomposition: e.g., CPD decomposition into rank-1 tensors  $\underline{X} \cong \sum_{r=1}^R b_r^{(1)} \circ b_r^{(2)} \circ \dots \circ b_r^{(6)}$ , Hierarchical Outer Product Tensor Approximation (HOPTA) using rank- $q$  terms:  $\underline{X} \cong \sum_{r=1}^R \mathbf{B}_r^{(1)} \circ \mathbf{B}_r^{(2)} \circ \mathbf{B}_r^{(3)}$  or quantized TT (QTT) using 3rd-order cores:  $\underline{X} = \underline{G}^{(1)} \times_3^1 \underline{G}^{(2)} \times_3^1 \dots \times_3^1 \underline{G}^{(6)}$ .

compared to the initial tree structure. This is due to the fact that the distributed tensor network contains loops.

Many algorithms applied to tensor networks scale with the size  $R_k$  or  $I_k$  of the core tensors of the network. In spite of the usually polynomial scaling of these algorithms, the computations quickly become intractable for increasing  $R_k$ , so that a network containing core tensors with small dimensions are favorable in general. See as examples the distributed Tucker models shown in Fig. 15 (a) and (b).

#### IV. Tensorization – Blessing of Dimensionality

The procedure of creating a higher-order tensor from lower-order original data is referred to as *tensorization*. In other words, lower-order data tensors can be reshaped (reformatted) into high-order tensors. The purpose of a such tensorization or reshaping is to achieve a low-rank approximation with high level of compression. For example, big vectors, matrices even low-order tensors can be easily tensorized to very high-order tensors, then efficiently compressed by applying a suitable tensor network decomposition; this is the underlying principle for big data analysis [1], [2], [16], [59] (see also Figs. 17 - 20).

### A. Curse of Dimensionality

The term curse of dimensionality, in the context of tensors, refers to the fact that the number of elements of an  $N$ th-order ( $I \times I \times \cdots \times I$ ) tensor,  $I^N$ , grows exponentially with the tensor order  $N$ . For example, for the Tucker decomposition the number of entries of an original data tensor but also a core tensor scales exponentially in the tensor order, for instance, the number of entries of an  $N$ th-order ( $R \times R \times \cdots \times R$ ) core tensor is  $R^N$ .

If all computations are performed on a CP tensor format and not on the raw data tensor itself, then instead of the original  $I^N$  raw data entries, the number of parameters in a CP decomposition reduces to  $NRI$ , which scales linearly in  $N$  and  $I$ . This effectively bypasses the curse of dimensionality, however the CP approximation may provide a poor fit to the data and may involve numerical problems, since existing CPD algorithms are not stable for high-order tensors. In this paper we exploit TT decompositions which are stable and robust with ability to control an approximation error i.e., to achieve any desired accuracy of TT approximation [40], [60]. The main idea of using low-rank tensor-structured approximations is to reduce the complexity of computation and relax or avoid the curse of dimensionality.

### B. Quantized Tensor Networks

The curse of dimensionality can be overcome relatively easily through quantized tensor networks, which represent a tensor of possibly very high-order as a set of sparsely interconnected of low dimensions (typically, 3rd-order) cores [59], [60]. The concept of quantized tensor networks was first proposed by Oseledets [59] and Khoromskij [16].

For example, the quantization and tensorization of a huge vector  $\mathbf{x} \in \mathbb{R}^I$ ,  $I = 2^K$  can be achieved through reshaping to give an  $(2 \times 2 \times \cdots \times 2)$  tensor  $\underline{\mathbf{X}}$  of order  $K$ , as illustrated in Fig. 17. Such a quantized tensor  $\underline{\mathbf{X}}$  often admits low-rank matrix/tensor approximations, so that a good compression of a huge vector  $\mathbf{x}$  can be achieved by enforcing a maximum possible low-rank structure on the tensor  $\underline{\mathbf{X}}$ , thus admitting highly compressed representation via a tensor network.

Even more generally, an  $N$ th-order tensor  $\underline{\mathbf{X}} \in \mathbb{R}^{I_1 \times \cdots \times I_N}$ , with  $I_n = q^{K_n}$ , can be quantized in all modes simultaneously to yield a  $(q \times q \times \cdots \times q)$  quantized tensor  $\underline{\mathbf{Y}}$  of higher-order, with small  $q$ .

In practice, a fine ( $q = 2, 3, 4$ ) quantization is desirable to create as many virtual modes as possible, thus allowing us to implement an efficient low-rank tensor approximations. For example, the binary encoding ( $q = 2$ ) reshapes an  $N$ th-order tensor with  $(2^{K_1} \times 2^{K_2} \times \cdots \times 2^{K_N})$  elements into a tensor of order  $(K_1 + K_2 + \cdots + K_N)$ , with the same number of elements. In other words, the idea of the quantized tensor is quantization of the each  $n$ -th “physical” mode (dimension) by replacing it with  $K_n$  “virtual” modes, provided that the corresponding mode size  $I_n$  are factorized as  $I_n = I_{n,1} I_{n,2} \cdots I_{n,K_n}$ . This corresponds to reshaping the  $n$ -th mode of size  $I_n$  into  $K_n$  modes of sizes  $I_{n,1}, I_{n,2}, \dots, I_{n,K_n}$ .

In example shown in Fig. 18, the Tensor Train of huge 3rd-order tensor is expressed by the strong Kronecker products of block tensors with relatively small 3rd-order tensor blocks. Since large-scale tensors cannot be loaded explicitly in main memory, they usually reside in distributed storage by splitting tensors to smaller blocks. Our approach is to apply tensor networks and represent big data by high-order tensors not explicitly but in compressed TT formats.

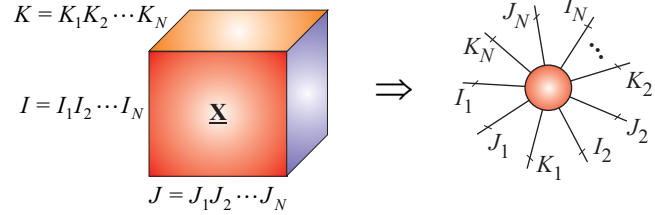
The TT decomposition applied to quantized tensors is referred to as the QTT; it was first introduced as a compression scheme for large-scale structured matrices, which admit low-rank TT approximation [59], and also developed for more general settings [16], [61], [62]. The attractive property of QTT is that not only its rank is typically small (below 10) but it is almost independent or at least uniformly bounded by data size, providing a logarithmic (sub-linear) reduction of storage requirements:  $\mathcal{O}(I^N) \rightarrow \mathcal{O}(N \log_q(I))$  – so-called super-compression [16].

Note also that, unlike in Tucker or CPD, the TT decomposition relies on a certain ordering of the modes so that reordering modes may affect the numerical values of TT ranks significantly.

Quantization is quite important for reducing the computational complexity further, since it allows the TT decomposition to resolve and represent more structure in the data by splitting the “virtual” dimensions introduced by the quantization, as well as the “physical” ones. In practice it appears the most efficient to use as fine a quantization as possible (typically, with  $q = 2$ ) and to generate as many virtual modes as possible.

A TT decomposition of the quantized vector is referred to as QTT decomposition of the original vector; the ranks of this TT decomposition are

(a)



(b)

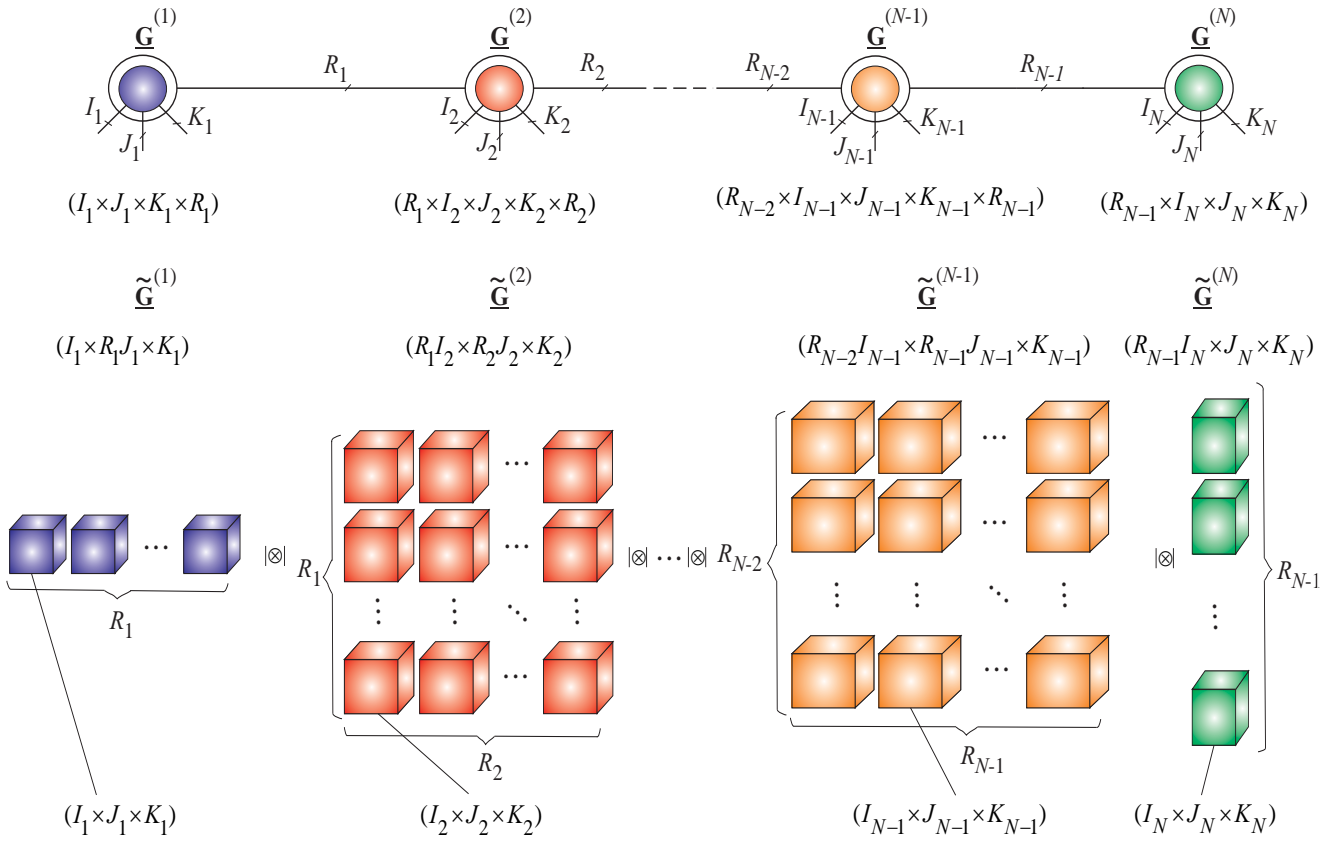


**Figure 18:** (a) Example 1 of tensorization and decomposition of a large-scale 3rd-order tensor  $\underline{\mathbf{X}} \in \mathbb{R}^{I \times J \times K}$  into  $3N$ th-order tensor, assuming that  $I = I_1 I_2 \cdots I_N$ ,  $J = J_1 J_2 \cdots J_N$  and  $K = K_1 K_2 \cdots K_N$ . (b) Decomposition of the tensor via generalized Tensor Train referred to as the Tensor Product State (TPS). The data tensor can be expressed by the strong Kronecker product of block tensors as  $\underline{\mathbf{X}} \cong \underline{\mathbf{G}}^{(1)} | \otimes | \underline{\mathbf{G}}^{(2)} | \otimes | \cdots \otimes \underline{\mathbf{G}}^{(N)} \in \mathbb{R}^{I_1 \cdots I_N \times J_1 \cdots J_N \times K_1 \cdots K_N}$ , where each block of the core  $\underline{\mathbf{G}}^{(n)} \in \mathbb{R}^{R_{n-1} I_n \times R_n J_n \times K_n}$  is a 3rd-order tensor of size  $(I_n \times J_n \times K_n)$ , with  $R_0 = R_N = 1$ . The strong Kronecker product of two block cores  $\underline{\mathbf{G}}^{(n)} \in \mathbb{R}^{R_{n-1} I_n \times R_n J_n \times K_n}$  and  $\underline{\mathbf{G}}^{(n+1)} \in \mathbb{R}^{R_n I_{n+1} \times R_{n+1} J_{n+1} \times K_{n+1}}$  is defined as the block tensor  $\underline{\mathbf{C}} = \underline{\mathbf{G}}^{(n)} | \otimes | \underline{\mathbf{G}}^{(n+1)} \in \mathbb{R}^{R_{n-1} I_n I_{n+1} \times R_{n+1} J_n J_{n+1} \times K_n K_{n+1}}$ , with 3rd-order tensor blocks  $\underline{\mathbf{C}}_{r_{n-1}, r_{n+1}} = \sum_{r_n=1}^{R_n} \underline{\mathbf{G}}_{r_{n-1}, r_n}^{(n)} \otimes \underline{\mathbf{G}}_{r_n, r_{n+1}}^{(n+1)} \in \mathbb{R}^{I_n I_{n+1} \times J_n J_{n+1} \times K_n K_{n+1}}$ , where  $\underline{\mathbf{G}}_{r_{n-1}, r_n}^{(n)} \in \mathbb{R}^{I_n \times J_n \times K_n}$  and  $\underline{\mathbf{G}}_{r_n, r_{n+1}}^{(n+1)} \in \mathbb{R}^{I_{n+1} \times J_{n+1} \times K_{n+1}}$  are block tensors of  $\underline{\mathbf{G}}^{(n)}$  and  $\underline{\mathbf{G}}^{(n+1)}$ , respectively. In the special cases:  $J = K = 1$  and  $K = 1$  the model simplifies to standard tensor train models shown in Fig. 20 (a) and (b).

called ranks of the QTT decomposition of the original vector.

## V. Mathematical and Graphical Representation of Tensor Trains

In order to perform efficiently various mathematical operations in the TT formats we need to represent TT decompositions in compact and easily understandable mathematical and graphical representations [2], [13].

### A. Vector TT/MPS Decomposition

The (vector) tensor train (TT/MPS) for  $N$ th-order data tensor  $\underline{\mathbf{X}} \in \mathbb{R}^{I_1 \times I_2 \times \dots \times I_N}$  can be described in the standard (tedious and rather complicated) scalar form as [40], [63]:

$$\underline{x}_{i_1, i_2, \dots, i_N} \cong \sum_{r_1, r_2, \dots, r_{N-1}=1}^{R_1, R_2, \dots, R_{N-1}} g_{i_1, r_1}^{(1)} g_{r_1, i_2, r_2}^{(2)} \cdots g_{r_{N-1}, i_N}^{(N)} \quad (10)$$

or equivalently by using slice representations (see Fig. 19 (a)):

$$\underline{x}_{i_1, i_2, \dots, i_N} \cong \mathbf{G}^{(1)}(i_1) \mathbf{G}^{(2)}(i_2) \cdots \mathbf{G}^{(N)}(i_N), \quad (11)$$

where slice matrices are defined as

$$\mathbf{G}^{(n)}(i_n) = \mathbf{G}^{(n)}(:, i_n, :) \in \mathbb{R}^{R_{n-1} \times R_n},$$

i.e.,  $\mathbf{G}^{(n)}(i_n)$  is an  $i_n$ th lateral slice of the core  $\underline{\mathbf{G}}^{(n)} \in \mathbb{R}^{R_{n-1} \times I_n \times R_n}$  for  $n = 1, 2, \dots, N$ , with  $R_0 = R_N = 1$ .

However we can use several more convenient compact mathematical forms as follows (see Figs. 19 and 20(a) and Table III):

- 1) In a tensor form using multilinear products of cores:

$$\underline{\mathbf{X}} \cong \underline{\mathbf{G}}^{(1)} \times_3^1 \underline{\mathbf{G}}^{(2)} \times_3^1 \cdots \times_3^1 \underline{\mathbf{G}}^{(N-1)} \times_3^1 \underline{\mathbf{G}}^{(N)} = [\underline{\mathbf{G}}^{(1)}, \underline{\mathbf{G}}^{(2)}, \dots, \underline{\mathbf{G}}^{(N-1)}, \underline{\mathbf{G}}^{(N)}], \quad (12)$$

where 3rd-order cores<sup>4</sup> are defined as  $\underline{\mathbf{G}}^{(n)} \in \mathbb{R}^{R_{n-1} \times I_n \times R_n}$  for  $n = 1, 2, \dots, N$  with  $R_0 = R_N = 1$  (see Fig. 20(a)).

- 2) In tensor/vector form expressed as summation of rank-1 tensors, by using outer products of fibers (see Fig. 19 (b)):

$$\underline{\mathbf{X}} \cong \sum_{r_1, r_2, \dots, r_{N-1}=1}^{R_1, R_2, \dots, R_{N-1}} \mathbf{g}_{i_1, r_1}^{(1)} \circ \mathbf{g}_{r_1, i_2, r_2}^{(2)} \circ \cdots \circ \mathbf{g}_{r_{N-1}, i_N}^{(N)} \quad (13)$$

<sup>4</sup>Note that the cores  $\underline{\mathbf{G}}^{(1)}$  and  $\underline{\mathbf{G}}^{(N)}$  are now two-dimensional arrays (matrices), but to apply uniform representation, we assume that 2nd-order cores are represented also as 3rd-order cores of mode sizes  $1 \times I_1 \times R_1$  and  $R_{N-1} \times I_N \times 1$ , respectively.

where  $\mathbf{g}_{r_{n-1}, r_n}^{(n)} = \mathbf{G}^{(n)}(r_{n-1}, :, r_n) \in \mathbb{R}^{I_n}$  are mode-2 fibers, i.e., column vectors of matrices  $\mathbf{G}^{(n)} = [\mathbf{g}_{1,1}^{(n)}, \mathbf{g}_{2,1}^{(n)}, \dots, \mathbf{g}_{R_{n-1}, 1}^{(n)}, \mathbf{g}_{1,2}^{(n)}, \dots, \mathbf{g}_{R_{n-1}, R_n}^{(n)}] \in \mathbb{R}^{I_n \times R_{n-1} R_n}$  ( $n = 1, 2, \dots, N$ ), with  $R_0 = R_N = 1$  or equivalently in the vector form using the Kronecker products

$$\mathbf{x} \cong \sum_{r_1, r_2, \dots, r_{N-1}=1}^{R_1, R_2, \dots, R_{N-1}} \mathbf{g}_{i_1, r_1}^{(1)} \otimes \mathbf{g}_{r_1, r_2}^{(2)} \otimes \cdots \otimes \mathbf{g}_{r_{N-1}, 1}^{(N)}, \quad (14)$$

where the vector is defined as  $\mathbf{x} = \underline{\mathbf{x}}_{i_1, i_2, \dots, i_N} = \text{vec}(\underline{\mathbf{X}}) \in \mathbb{R}^{I_1 I_2 \cdots I_N}$ .

- 3) In the vector form expressed by the strong Kronecker products of block matrices [2], [64] (see Fig. 20(a)):

$$\underline{\mathbf{x}}_{i_1, i_2, \dots, i_N} \cong \underline{\mathbf{G}}^{(1)} | \otimes | \underline{\mathbf{G}}^{(2)} | \otimes | \cdots | \otimes | \underline{\mathbf{G}}^{(N)}, \quad (15)$$

where the cores  $\underline{\mathbf{G}}^{(n)} \in \mathbb{R}^{R_{n-1} \times I_n \times R_n}$  are represented by block matrices  $\underline{\mathbf{G}}^{(n)} = (\mathbf{G}_{(3)}^{(n)})^T \in \mathbb{R}^{R_{n-1} I_n \times R_n}$  for  $n = 1, 2, \dots, N$ , with blocks  $\mathbf{g}_{r_{n-1}, r_n}^{(n)} \in \mathbb{R}^{I_n \times 1}$ ,  $R_0 = R_N = 1$ , and the symbol  $|\otimes|$  denotes the strong Kronecker product.

In general, the strong Kronecker product of two block matrices (e.g., unfolding cores) [2], [65], [66]:

$$\mathbf{A} = \begin{bmatrix} \mathbf{A}_{1,1} & \cdots & \mathbf{A}_{1,R_2} \\ \vdots & \ddots & \vdots \\ \mathbf{A}_{R_1,1} & \cdots & \mathbf{A}_{R_1,R_2} \end{bmatrix} \in \mathbb{R}^{R_1 I \times R_2 J}$$

and

$$\mathbf{B} = \begin{bmatrix} \mathbf{B}_{1,1} & \cdots & \mathbf{B}_{1,R_3} \\ \vdots & \ddots & \vdots \\ \mathbf{B}_{R_2,1} & \cdots & \mathbf{B}_{R_2,R_3} \end{bmatrix} \in \mathbb{R}^{R_2 K \times R_3 L},$$

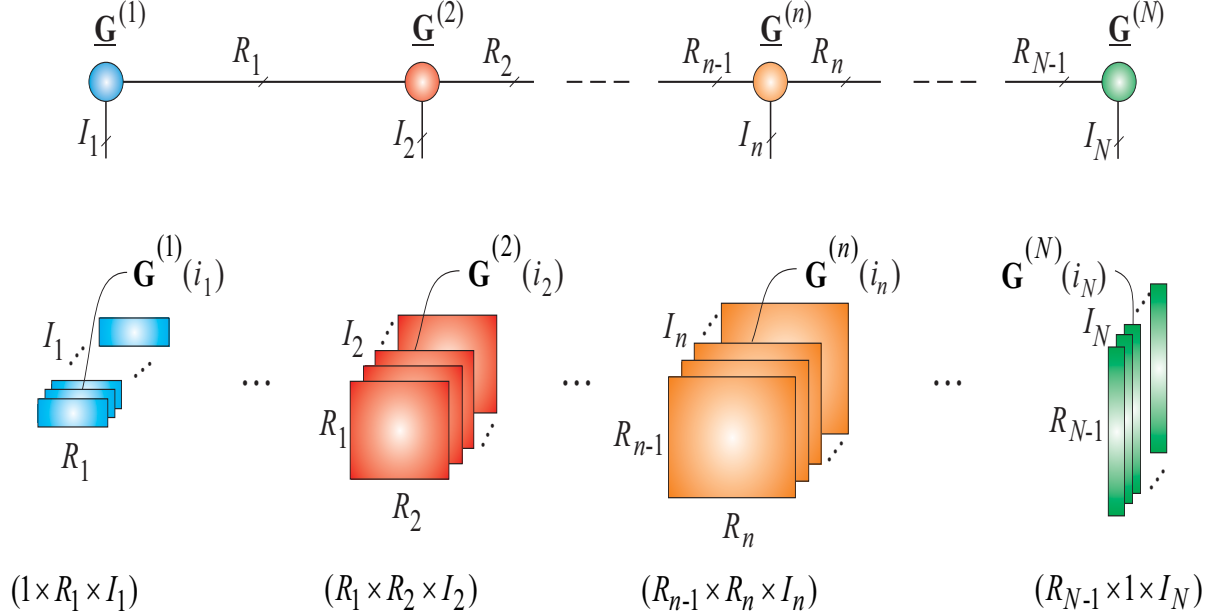
is defined as a block matrix

$$\mathbf{C} = \mathbf{A} | \otimes | \mathbf{B} \in \mathbb{R}^{R_1 I K \times R_3 J L}, \quad (16)$$

with blocks  $\mathbf{C}_{r_1, r_3} = \sum_{r_2=1}^{R_2} \mathbf{A}_{r_1, r_2} \otimes \mathbf{B}_{r_2, r_3} \in \mathbb{R}^{I K \times K L}$ , where  $\mathbf{A}_{r_1, r_2} \in \mathbb{R}^{I \times J}$  and  $\mathbf{B}_{r_2, r_3} \in \mathbb{R}^{K \times L}$  are block matrices of  $\mathbf{A}$  and  $\mathbf{B}$ , respectively.

- 13) The strong Kronecker product representation of a TT is probably the most comprehensive and useful form for displaying a tensor train since it allows us to perform all operations by using compact block matrices.

(a)



(b)

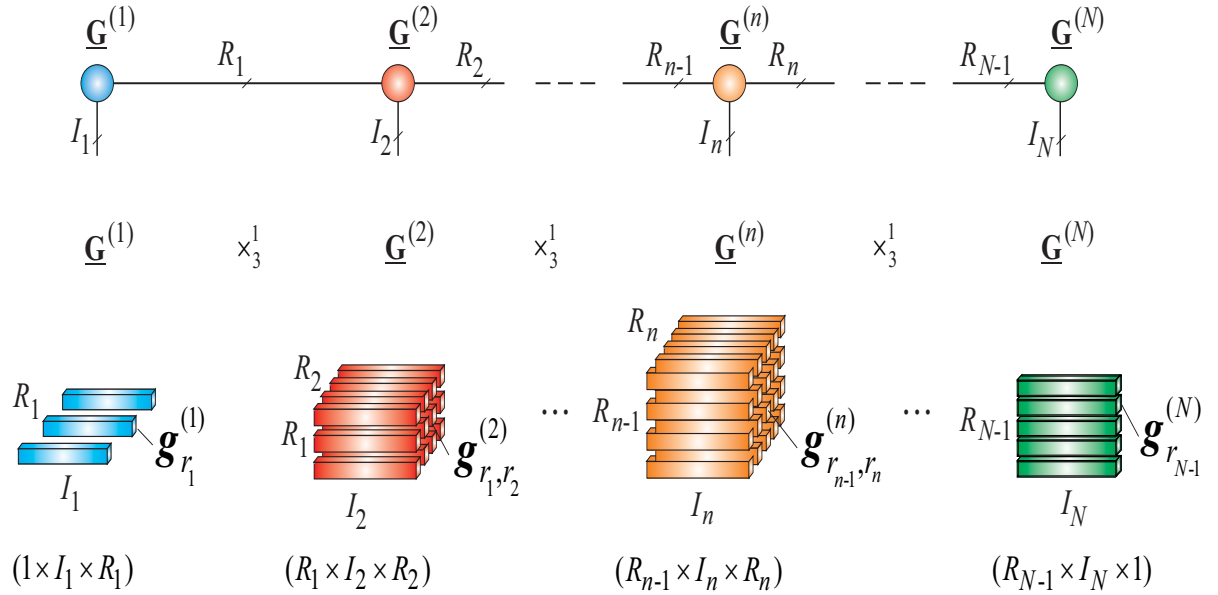


**Figure 19:** Alternative representations of the tensor train decomposition (TT/MPS) for an  $N$ th-order tensor  $\underline{\mathbf{X}} \in \mathbb{R}^{I_1 \times I_2 \times I_3 \times \dots \times I_N}$ ; (a) Representation of the TT/MPS in a scalar form via slice matrices as:  $x_{i_1, i_2, \dots, i_N} \cong \mathbf{G}^{(1)}(i_1) \mathbf{G}^{(2)}(i_2) \dots \mathbf{G}^{(N)}(i_N) = \sum_{r_1=1}^{R_1} \sum_{r_2=1}^{R_2} \dots \sum_{r_{N-1}=1}^{R_{N-1}} g_{1, i_1, r_1}^{(1)} g_{r_1, i_2, r_2}^{(2)} g_{r_2, i_3, r_3}^{(3)} \dots g_{r_{N-1}, i_N, 1}^{(N)}$ ; (b) expressed by the outer product of vectors (sum of rank-1 tensors) as:  $\underline{\mathbf{X}} \cong \sum_{r_1=1}^{R_1} \sum_{r_2=1}^{R_2} \dots \sum_{r_{N-1}=1}^{R_{N-1}} (\mathbf{g}_{1, r_1}^{(1)} \circ \mathbf{g}_{r_1, r_2}^{(2)} \circ \dots \circ \mathbf{g}_{r_{N-2}, r_{N-1}}^{(N-1)} \circ \mathbf{g}_{r_{N-1}, 1}^{(N)})$ . All vectors  $\mathbf{g}_{r_{N-1}, 1}^{(N)} \in \mathbb{R}^{I_N}$  are considered to be the column vectors.

**TABLE III:** Equivalent forms of the Tensor Trains (TT): MPS and MPO (with open boundary conditions) representation of an  $N$ th-order tensor  $\underline{\mathbf{X}} \in \mathbb{R}^{I_1 \times I_1 \times \cdots \times I_N}$  and a  $2N$ th-order tensor  $\underline{\mathbf{Y}} \in \mathbb{R}^{I_1 \times J_1 \times I_2 \times J_2 \cdots \times I_N \times J_N}$ , respectively. It is assumed that the TT rank is  $\{R_1, R_2, \dots, R_{N-1}\}$ , with  $R_0 = R_N = 1$ .

TT/MPS	TT/MPO
Tensor Representations: Multilinear Products (tensor contractions)	
$\underline{\mathbf{X}} = \underline{\mathbf{G}}^{(1)} \times_3^1 \underline{\mathbf{G}}^{(2)} \times_3^1 \cdots \times_3^1 \underline{\mathbf{G}}^{(N-1)} \times_3^1 \underline{\mathbf{G}}^{(N)}$	$\underline{\mathbf{Y}} = \underline{\mathbf{G}}^{(1)} \times_4^1 \underline{\mathbf{G}}^{(2)} \times_4^1 \cdots \times_4^1 \underline{\mathbf{G}}^{(N-1)} \times_4^1 \underline{\mathbf{G}}^{(N)}$
$\underline{\mathbf{G}}^{(n)} \in \mathbb{R}^{R_{n-1} \times I_n \times R_n}, \quad (n = 1, 2, \dots, N)$	$\underline{\mathbf{G}}^{(n)} \in \mathbb{R}^{R_{n-1} \times I_n \times J_n \times R_n}$
Tensor Representations: Outer Products	
$\underline{\mathbf{X}} = \sum_{r_1, r_2, \dots, r_{N-1}=1}^{R_1, R_2, \dots, R_{N-1}} \mathbf{g}_{1, r_1}^{(1)} \circ \mathbf{g}_{r_1, r_2}^{(2)} \circ \cdots \circ \mathbf{g}_{r_{N-2}, r_{N-1}}^{(N-1)} \circ \mathbf{g}_{r_{N-1}, 1}^{(N)}$	$\underline{\mathbf{Y}} = \sum_{r_1, r_2, \dots, r_{N-1}=1}^{R_1, R_2, \dots, R_{N-1}} \mathbf{G}_{1, r_1}^{(1)} \circ \mathbf{G}_{r_1, r_2}^{(2)} \circ \cdots \circ \mathbf{G}_{r_{N-2}, r_{N-1}}^{(N-1)} \circ \mathbf{G}_{r_{N-1}, 1}^{(N)}$
$\mathbf{g}_{r_{n-1}, r_n}^{(n)} \in \mathbb{R}^{I_n}$ blocks of a matrix $\tilde{\mathbf{G}}^{(n)} = (\mathbf{G}_{(3)}^{(n)})^T \in \mathbb{R}^{R_{n-1} I_n \times R_n}$	$\mathbf{G}_{r_{n-1}, r_n}^{(n)} \in \mathbb{R}^{I_n \times J_n}$ blocks of a matrix $\tilde{\mathbf{G}}^{(n)} \in \mathbb{R}^{R_{n-1} I_n \times R_n J_n}$
Vector/Matrix Representations: Strong Kronecker Products	
$\underline{\mathbf{x}}_{i_1 \cdots i_N} = \tilde{\mathbf{G}}^{(1)} \mid \otimes \mid \tilde{\mathbf{G}}^{(2)} \mid \otimes \mid \cdots \mid \otimes \mid \tilde{\mathbf{G}}^{(N)} \in \mathbb{R}^{I_1 I_2 \cdots I_N}$	$\underline{\mathbf{Y}}_{\overline{i_1 \cdots i_N}; \overline{j_1 \cdots j_N}} = \tilde{\mathbf{G}}^{(1)} \mid \otimes \mid \tilde{\mathbf{G}}^{(2)} \mid \otimes \mid \cdots \mid \otimes \mid \tilde{\mathbf{G}}^{(N)} \in \mathbb{R}^{I_1 \cdots I_N \times J_1 \cdots J_N}$
$\tilde{\mathbf{G}}^{(n)} \in \mathbb{R}^{R_{n-1} I_n \times R_n}$ a block matrix with blocks $\mathbf{g}_{r_{n-1}, r_n}^{(n)} \in \mathbb{R}^{I_n}$	$\tilde{\mathbf{G}}^{(n)} \in \mathbb{R}^{R_{n-1} I_n \times R_n J_n}$ a block matrix with blocks $\mathbf{G}_{r_{n-1}, r_n}^{(n)} \in \mathbb{R}^{I_n \times J_n}$
Scalar (standard) Representations	
$x_{i_1, i_2, \dots, i_N} = \sum_{r_1, r_2, \dots, r_{N-1}=1}^{R_1, R_2, \dots, R_{N-1}} g_{1, i_1, r_1}^{(1)} g_{r_1, i_2, r_2}^{(2)} g_{r_2, i_3, r_3}^{(3)} \cdots g_{r_{N-1}, i_N, 1}^{(N)}$	$y_{i_1, j_1, i_2, j_2, \dots, i_N, j_N} = \sum_{r_1, r_2, \dots, r_{N-1}=1}^{R_1, R_2, \dots, R_{N-1}} g_{1, i_1, j_1, r_1}^{(1)} g_{r_1, i_2, j_2, r_2}^{(2)} \cdots g_{r_{N-1}, i_N, j_N, 1}^{(N)}$
$g_{r_{n-1}, i_n, r_n}^{(n)}$ entries of a 3rd-order core $\underline{\mathbf{G}}^{(n)} \in \mathbb{R}^{R_{n-1} \times I_n \times R_n}$	$g_{r_{n-1}, i_n, j_n, r_n}^{(n)}$ entries of a 4th-order core $\underline{\mathbf{G}}^{(n)} \in \mathbb{R}^{R_{n-1} \times I_n \times J_n \times R_n}$
Slice Representations	
$x_{i_1, i_2, \dots, i_N} = \mathbf{G}^{(1)}(i_1) \mathbf{G}^{(2)}(i_2) \cdots \mathbf{G}^{(N-1)}(i_{N-1}) \mathbf{G}^{(N)}(i_N)$	$y_{i_1, j_1, i_2, j_2, \dots, i_N, j_N} = \mathbf{G}^{(1)}(i_1, j_1) \mathbf{G}^{(2)}(i_2, j_2) \cdots \mathbf{G}^{(N)}(i_N, j_N)$
$\mathbf{G}^{(n)}(i_n) \in \mathbb{R}^{R_{n-1} \times R_n}$ lateral slices of cores $\underline{\mathbf{G}}^{(n)} \in \mathbb{R}^{R_{n-1} \times I_n \times R_n}$	$\mathbf{G}^{(n)}(i_n, j_n) \in \mathbb{R}^{R_{n-1} \times R_n}$ slices of cores $\underline{\mathbf{G}}^{(n)} \in \mathbb{R}^{R_{n-1} \times I_n \times J_n \times R_n}$

## B. Matrix TT (MPO) Decomposition

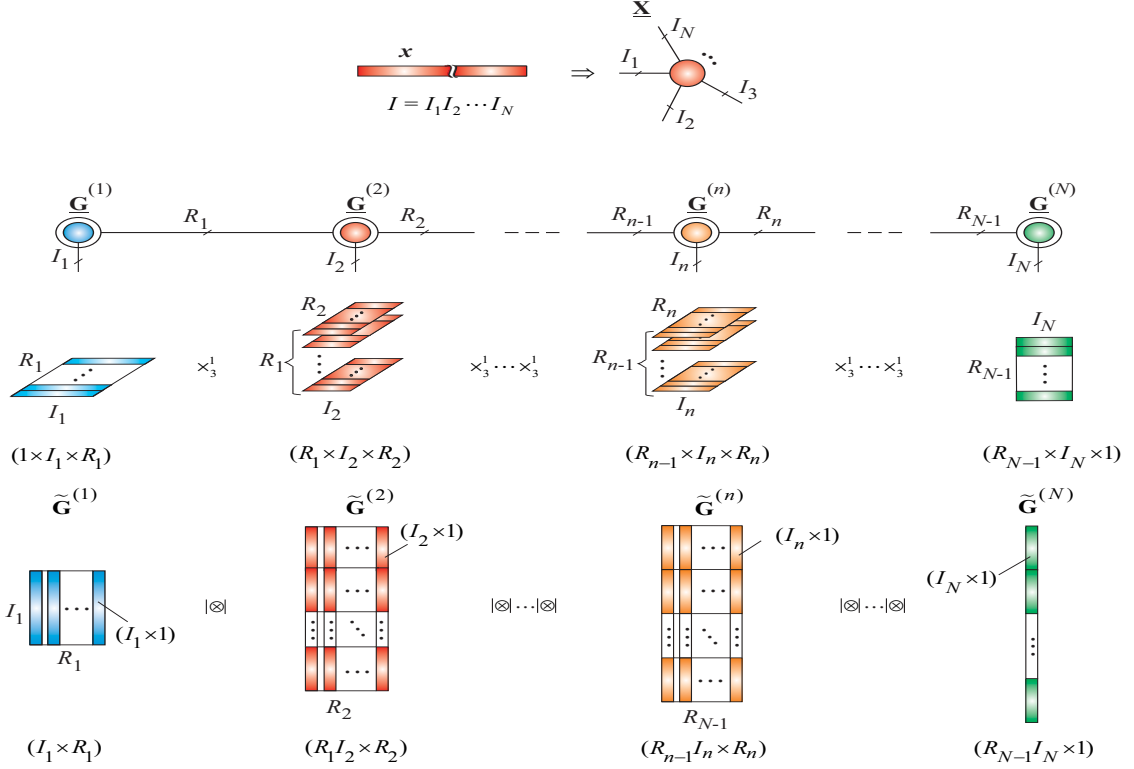
In a similar way, we can represent a large scale matrix  $\mathbf{X} \in \mathbb{R}^{I \times J}$ , as a  $2N$ th-order tensor  $\underline{\mathbf{X}} \in \mathbb{R}^{I_1 \times J_1 \times I_2 \times J_2 \cdots I_N \times J_N}$  with  $I = I_1 I_2 \cdots I_N$  and  $J = J_1 J_2 \cdots J_N$  (see Fig. 20 (b)). This leads to an important model: the matrix TT, called also MPO (Matrix Product Operator with open boundary conditions) that consists of chain (train) of 3rd-order and 4th-

order cores<sup>5</sup> as illustrated in Fig. 20 (b). Note that the 3rd-order core tensors can be represented as a block row and column vectors in which each element (block) is a matrix (a lateral slice) of the cores, while 4th-order core tensor can be interpreted equivalently as a block matrix as illustrated in Fig. 20 (b).

Since  $\mathbf{X}$  is usually a full rank matrix the straight-

<sup>5</sup>Note that the cores  $\underline{\mathbf{G}}^{(1)}$  and  $\underline{\mathbf{G}}^{(N)}$  are now three-dimensional arrays, however to apply uniform representation, we assume that 3rd-order cores are considered also as 4th-order cores of mode sizes:  $1 \times I_1 \times J_1 \times R_1$  and  $R_{N-1} \times I_N \times J_N \times 1$ , respectively.

(a)



(b)

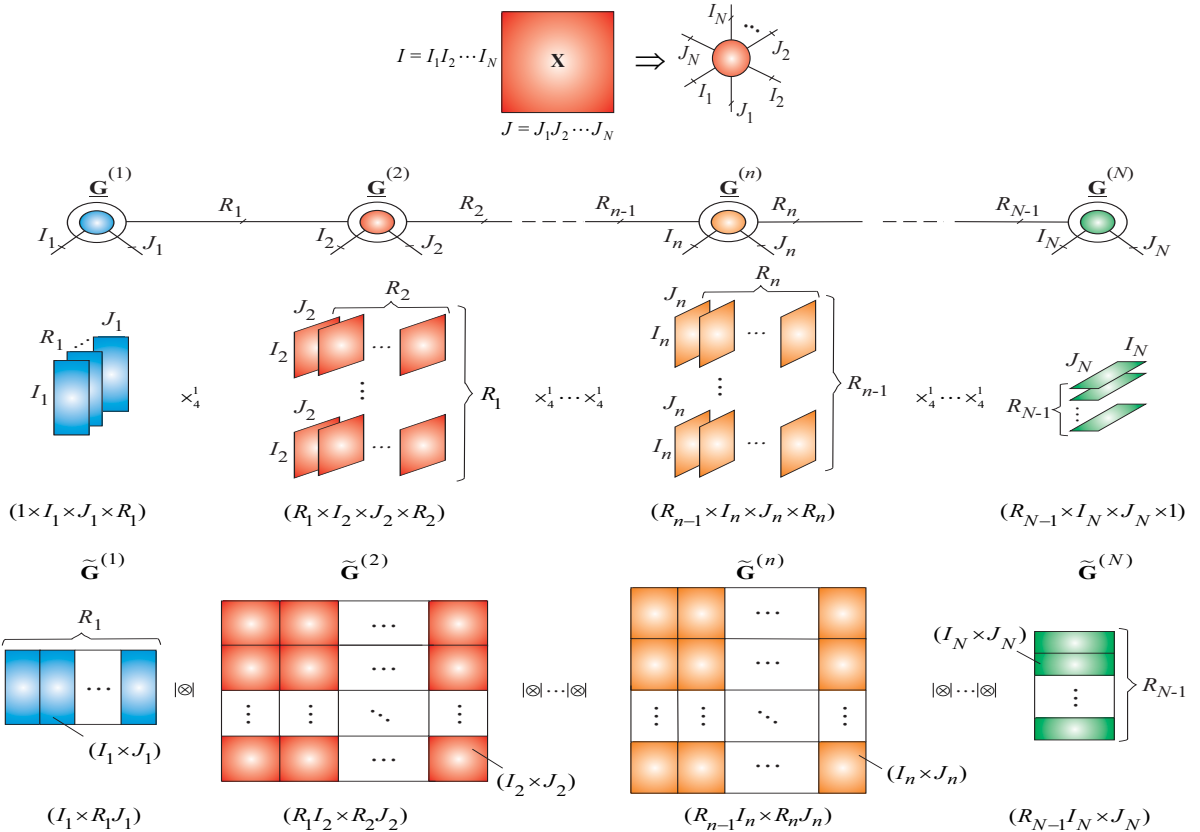


**Figure 20:** Example 2 of tensorization and TT decompositions of a huge vector (a) and a matrix (b). TT networks are represented via strong Kronecker products of block matrices.

forward  $2N$  dimensional exact TT decomposition is inefficient, as it has the rank  $R_n = I^N$  in the middle of a chain. Therefore, the matrix TT/MPO decompositions employ the index permutation as illustrated in Fig. 20 (b), and can be described in a scalar form as:

$$x_{i_1, j_1, \dots, i_N, j_N} \cong \sum_{r_1=1}^{R_1} \sum_{r_2=1}^{R_2} \dots \sum_{r_{N-1}=1}^{R_{N-1}} g_{1, i_1, j_1, r_1}^{(1)} g_{r_1, i_2, j_2, r_2}^{(2)} \dots g_{r_{N-2}, i_{N-1}, j_{N-1}, r_{N-1}}^{(N-1)} g_{r_{N-1}, i_N, j_N, 1}^{(N)}. \quad (17)$$

or equivalently using slice representation

$$x_{i_1, j_1, \dots, i_N, j_N} \cong \mathbf{G}^{(1)}(i_1, j_1) \mathbf{G}^{(2)}(i_2, j_2) \dots \mathbf{G}^{(N)}(i_N, j_N), \quad (18)$$

where  $\mathbf{G}^{(n)}(i_n, j_n) \cong \underline{\mathbf{G}}^{(n)}(:, i_n, j_n, :)$  are slices of the cores  $\underline{\mathbf{G}}^{(n)} \in \mathbb{R}^{R_{n-1} \times I_n \times J_n \times R_n}$

However, the TT/MPO model for an  $2N$ th-order tensor  $\underline{\mathbf{X}} \in \mathbb{R}^{I_1 \times J_1 \times \dots \times I_N \times J_N}$  can be described mathematically and graphically, in more elegant global and compact forms<sup>6</sup> (see also Table III for detailed and comparative descriptions):

A) In the tensor compact form using multilinear products

$$\underline{\mathbf{X}} \cong \underline{\mathbf{G}}^{(1)} \times_4^1 \underline{\mathbf{G}}^{(2)} \times_4^1 \dots \times_4^1 \underline{\mathbf{G}}^{(N)} = [\underline{\mathbf{G}}^{(1)}, \underline{\mathbf{G}}^{(2)}, \dots, \underline{\mathbf{G}}^{(N)}], \quad (19)$$

where the cores are defined as  $\underline{\mathbf{G}}^{(n)} \in \mathbb{R}^{R_{n-1} \times I_n \times J_n \times R_n}$ , with  $R_0 = R_N = 1$ ,  $(n = 1, 2, \dots, N)$ .

B) In the block matrix form using the strong Kronecker products:

$$\mathbf{x} \cong \tilde{\mathbf{G}}^{(1)} | \otimes | \tilde{\mathbf{G}}^{(2)} | \otimes | \dots | \otimes | \tilde{\mathbf{G}}^{(N)}, \quad (20)$$

where  $\mathbf{X} = \mathbf{X}_{(\overline{i_1, i_2, \dots, i_N}; \overline{j_1, j_2, \dots, j_N})} \in \mathbb{R}^{I_1 I_2 \dots I_N \times J_1 J_2 \dots J_N}$  is unfolding matrix of  $\underline{\mathbf{X}}$  and  $\tilde{\mathbf{G}}^{(n)} \in \mathbb{R}^{R_{n-1} I_n \times R_n J_n}$  are block matrices with blocks  $\mathbf{G}_{r_{n-1}, r_n}^{(n)} \in \mathbb{R}^{I_n \times J_n}$  and the number of blocks  $R_{n-1} \times R_n$ . In the special case, when ranks of the TT/MPO  $R_n = 1$ ,  $\forall n$  the strong Kronecker products simplify to the standard Kronecker products.

## VI. Basic Operations in TT Formats

Using the compact representations of the TT/MPS and TT/MPO decompositions described in the previous section, we can perform easily basic mathematical operations (e.g., matrix by vector and matrix by matrix multiplications) using

<sup>6</sup>i.e., not for each individual entry of a tensor.

block matrices. For example, the large-scale matrix equation

$$\mathbf{Ax} = \mathbf{y}, \quad (21)$$

where  $\mathbf{A} \in \mathbb{R}^{I \times J}$ ,  $\mathbf{x} \in \mathbb{R}^J$  and  $\mathbf{y} \in \mathbb{R}^I$  can be represented in TT format (after performing suitable tensorization of the matrix and vectors), as shown in Fig 21 (a), with  $I = I_1 I_2 \dots I_N$  and  $J = J_1 J_2 \dots J_N$ , and the cores defined as

$$\begin{aligned} \underline{\mathbf{A}}^{(n)} &\in \mathbb{R}^{P_{n-1} \times I_n \times J_n \times P_n} \\ \underline{\mathbf{X}}^{(n)} &\in \mathbb{R}^{R_{n-1} \times J_n \times R_n} \\ \underline{\mathbf{Y}}^{(n)} &\in \mathbb{R}^{Q_{n-1} \times I_n \times Q_n}. \end{aligned}$$

By representing the entries of the matrix  $\mathbf{A}$  and vectors  $\mathbf{x}$  and  $\mathbf{y}$  by outer products as

$$\begin{aligned} \underline{\mathbf{A}} &= \sum_{p_1, p_2, \dots, p_{N-1}=1}^{P_1, P_2, \dots, P_{N-1}} \mathbf{A}_{1, p_1}^{(1)} \circ \mathbf{A}_{p_1, p_2}^{(2)} \circ \dots \circ \mathbf{A}_{p_{N-1}, 1}^{(N)} \\ \underline{\mathbf{X}} &= \sum_{r_1, r_2, \dots, r_{N-1}=1}^{R_1, R_2, \dots, R_{N-1}} \mathbf{x}_{r_1}^{(1)} \circ \mathbf{x}_{r_1, r_2}^{(2)} \circ \dots \circ \mathbf{x}_{r_{N-1}}^{(N)} \\ \underline{\mathbf{Y}} &= \sum_{q_1, q_2, \dots, q_{N-1}=1}^{Q_1, Q_2, \dots, Q_{N-1}} \mathbf{y}_{q_1}^{(1)} \circ \mathbf{y}_{q_1, q_2}^{(2)} \circ \dots \circ \mathbf{y}_{q_{N-1}}^{(N)} \end{aligned} \quad (22)$$

we can establish the following formulas:

$$\begin{aligned} \mathbf{y}_{q_{n-1}, q_n}^{(n)} &= \mathbf{y}_{r_{n-1} \overline{p_{n-1}}, \overline{r_n p_n}}^{(n)} \\ &= \mathbf{A}_{p_{n-1}, p_n}^{(n)} \mathbf{x}_{r_{n-1}, r_n}^{(n)} \in \mathbb{R}^{I_n}, \end{aligned} \quad (23)$$

with  $Q_n = P_n R_n$  for  $n = 1, 2, \dots, N$ .

On the other hand, by representing the matrix  $\mathbf{A}$  and vectors  $\mathbf{x}$ ,  $\mathbf{y}$  via the strong Kronecker products:

$$\begin{aligned} \mathbf{A} &= \tilde{\mathbf{A}}^{(1)} | \otimes | \tilde{\mathbf{A}}^{(2)} | \otimes | \dots | \otimes | \tilde{\mathbf{A}}^{(N)} \\ \mathbf{x} &= \tilde{\mathbf{X}}^{(1)} | \otimes | \tilde{\mathbf{X}}^{(2)} | \otimes | \dots | \otimes | \tilde{\mathbf{X}}^{(N)} \\ \mathbf{y} &= \tilde{\mathbf{Y}}^{(1)} | \otimes | \tilde{\mathbf{Y}}^{(2)} | \otimes | \dots | \otimes | \tilde{\mathbf{Y}}^{(N)}, \end{aligned} \quad (24)$$

with  $\tilde{\mathbf{A}}^{(n)} \in \mathbb{R}^{P_{n-1} I_n \times J_n P_n}$ ,  $\tilde{\mathbf{X}}^{(n)} \in \mathbb{R}^{R_{n-1} J_n \times R_n}$  and  $\tilde{\mathbf{Y}}^{(n)} \in \mathbb{R}^{Q_{n-1} I_n \times Q_n}$ , we can easily establish a simple relationship

$$\begin{aligned} \tilde{\mathbf{Y}}^{(n)} &= \tilde{\mathbf{A}}^{(n)} | \cdot | \tilde{\mathbf{X}}^{(n)} \in \mathbb{R}^{R_{n-1} P_{n-1} I_n \times R_n P_n}, \\ &n = 1, 2, \dots, N, \end{aligned} \quad (25)$$

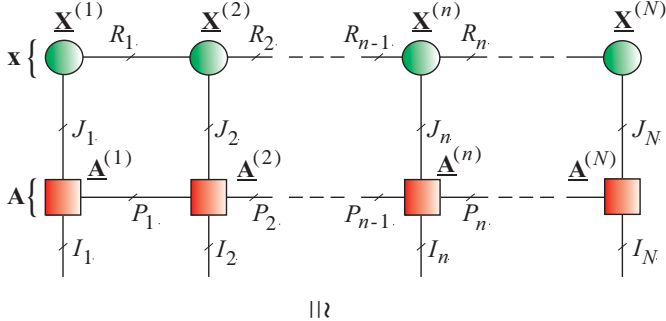
where operator  $|\cdot|$  means the AC product of two block matrices.

In general, the AC product of a block matrix  $\mathbf{A}^{(n)} \in \mathbb{R}^{P_{n-1} I_n \times P_n J_n}$  (with blocks  $\mathbf{A}_{p_{n-1}, p_n}^{(n)} \in \mathbb{R}^{I_n \times J_n}$ ) and a block matrix  $\mathbf{B}^{(n)} \in \mathbb{R}^{R_{n-1} J_n \times R_n K_n}$  (with blocks  $\mathbf{B}_{r_{n-1}, r_n}^{(n)} \in \mathbb{R}^{J_n \times K_n}$ ) is defined as a block matrix  $\mathbf{C}^{(n)} = \mathbf{A}^{(n)} | \cdot | \mathbf{B}^{(n)} \in \mathbb{R}^{Q_{n-1} I_n \times Q_n K_n}$  (with blocks

$\mathbf{C}_{q_{n-1}, q_n}^{(n)} = \mathbf{A}_{p_{n-1}, p_n}^{(n)} \mathbf{B}_{r_{n-1}, r_n}^{(n)} \in \mathbb{R}^{I_n \times K_n}$  as illustrated in Fig. 22.

The AC product of two block matrices is similar to the Tracy-Singh product but the Kronecker product for block matrices is replaced by the ordinary products matrix-by-matrix.

(a)



(b)

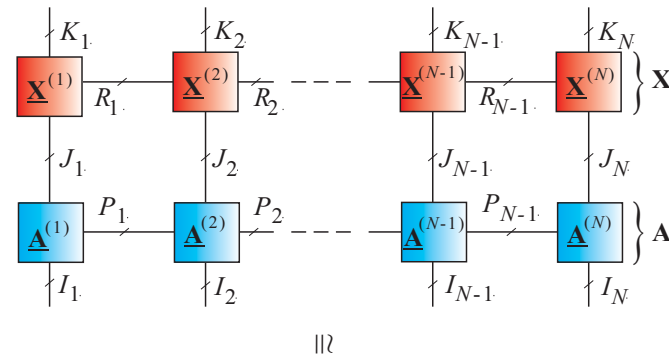


Figure 21: Distributed representation of matrix equations (a)  $\mathbf{Ax} = \mathbf{y}$  and (b)  $\mathbf{AX} = \mathbf{Y}$  in TT formats.

In a similar way, we can represent in TT format a matrix equation

$$\mathbf{Y} \cong \mathbf{AX} = \mathbf{AB}^T, \quad (26)$$

where  $\mathbf{A} \in \mathbb{R}^{I \times J}$ ,  $\mathbf{X} = \mathbf{B}^T \in \mathbb{R}^{J \times K}$  and  $\mathbf{Y} \in \mathbb{R}^{I \times K}$  as shown in Fig 21 (b), with  $I = I_1 I_2 \cdots I_N$ ,  $J = J_1 J_2 \cdots J_N$  and  $K = K_1 K_2 \cdots K_N$  with the cores

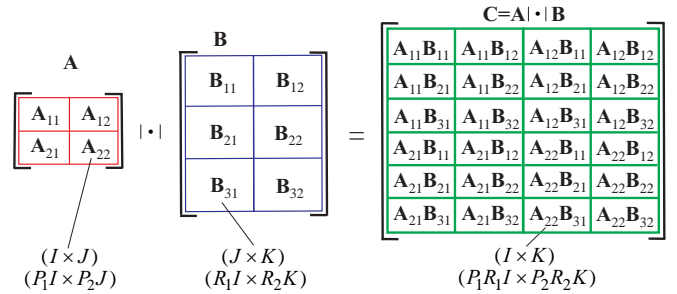


Figure 22: Graphical illustration of the AC product for two block matrices.

defined as

$$\begin{aligned} \mathbf{A}^{(n)} &\in \mathbb{R}^{P_{n-1} \times I_n \times P_n \times J_n} \\ \underline{\mathbf{X}}^{(n)} &\in \mathbb{R}^{R_{n-1} \times J_n \times R_n \times K_n} \\ \underline{\mathbf{Y}}^{(n)} &\in \mathbb{R}^{Q_{n-1} \times I_n \times Q_n \times K_n}. \end{aligned}$$

It can be proved that by assuming that matrices:  $\mathbf{A} \in \mathbb{R}^{I \times J}$  and  $\mathbf{X} \in \mathbb{R}^{J \times K}$  are represented in TT formats and expressed via the strong Kronecker product of block matrices as:  $\mathbf{A} = \tilde{\mathbf{A}}^{(1)} \otimes |\tilde{\mathbf{A}}^{(2)}| \otimes \dots \otimes |\tilde{\mathbf{A}}^{(N)}$  and  $\mathbf{X} = \tilde{\mathbf{X}}^{(1)} \otimes |\tilde{\mathbf{X}}^{(2)}| \otimes \dots \otimes |\tilde{\mathbf{X}}^{(N)}$ , with  $\tilde{\mathbf{A}}^{(n)} \in \mathbb{R}^{P_{n-1} I_n \times J_n P_n}$  and  $\tilde{\mathbf{X}}^{(n)} \in \mathbb{R}^{R_{n-1} J_n \times K_n R_n}$ , respectively, then the matrix  $\mathbf{Y} = \mathbf{AX}$  can be expressed in TT format via the strong Kronecker products:  $\mathbf{Y} = \tilde{\mathbf{Y}}^{(1)} \otimes |\tilde{\mathbf{Y}}^{(2)}| \otimes \dots \otimes |\tilde{\mathbf{Y}}^{(N)}$ , where  $\tilde{\mathbf{Y}}^{(n)} = \tilde{\mathbf{A}}^{(n)} \cdot |\tilde{\mathbf{X}}^{(n)}| \in \mathbb{R}^{Q_{n-1} I_n \times K_n Q_n}$ , ( $n = 1, 2, \dots, N$ ), with blocks  $\tilde{\mathbf{Y}}_{q_{n-1}, q_n}^{(n)} = \tilde{\mathbf{A}}_{p_{n-1}, p_n}^{(n)} \tilde{\mathbf{X}}_{r_{n-1}, r_n}^{(n)}$ , where  $Q_n = R_n P_n$ ,  $\forall n$ .

The above operation assumes precise contraction of cores. However, an exact contraction of core tensors for very large scale data is impossible, and the choice of the approximating procedure determines the efficiency and accuracy of algorithms implemented for specific computational or optimization problems [27]. In other words, contraction operations as matrix-by-vector or matrix-by-matrix products TT ranks grows and the TT ranks could become excessively large and therefore truncation (called also recompression) or low-rank matrix approximations are needed. In the truncation procedure (usually, performed via QR/SVD or CUR) the core tensors  $\underline{\mathbf{G}}^{(n)}$  are approximated by other core tensors with minimal possible TT-ranks with desired prescribed accuracy [40].

## VII. Tensor Train (TT/MPS) Splitting

In practical applications it is very useful and efficient to divide a TT decomposition, representing

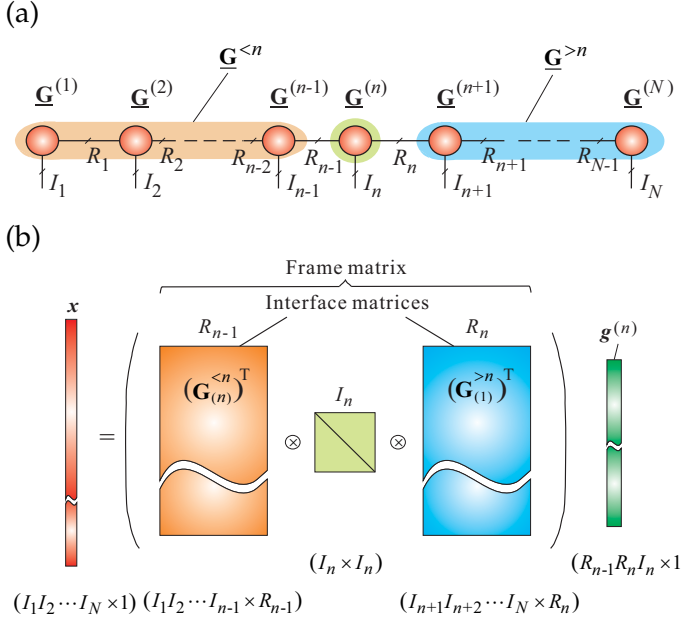


**Figure 23:** Extraction of a single core. (a) Graphical representation and notations of vector tensor train and subtrains. (b) Graphical illustration of the equation expressed via interface matrices or a frame matrix (see Eqs. (31) and (32)).

a tensor  $\underline{\mathbf{X}} = [\underline{\mathbf{G}}^{(1)}, \underline{\mathbf{G}}^{(2)}, \dots, \underline{\mathbf{G}}^{(N)}] \in \mathbb{R}^{I_1 \times I_2 \times \dots \times I_N}$ , into subtrains as illustrated in Fig. 23.

### A. Extraction of a single core

For this purpose, we define subtrains as follows

$$\underline{\mathbf{G}}^{<n} = [\underline{\mathbf{G}}^{(1)}, \underline{\mathbf{G}}^{(2)}, \dots, \underline{\mathbf{G}}^{(n-1)}] \in \mathbb{R}^{I_1 \times I_2 \times \dots \times I_{n-1} \times R_{n-1}} \quad (27)$$

$$\underline{\mathbf{G}}^{>n} = [\underline{\mathbf{G}}^{(n+1)}, \underline{\mathbf{G}}^{(n+2)}, \dots, \underline{\mathbf{G}}^{(N)}] \in \mathbb{R}^{R_n \times I_{n+1} \times \dots \times I_N} \quad (28)$$

with corresponding unfolding matrices called interface matrices:

$$\underline{\mathbf{G}}_{(n)}^{<n} \in \mathbb{R}^{R_{n-1} \times I_1 I_2 \cdots I_{n-1}} \quad (29)$$

$$\underline{\mathbf{G}}_{(1)}^{>n} \in \mathbb{R}^{R_n \times I_{n+1} \cdots I_N} \quad (30)$$

Using basic multilinear algebra, we can construct a set of linear equations referred to as the frame equation:

$$\mathbf{x} = \underline{\mathbf{G}}_{\neq n} \mathbf{g}^{(n)}, \quad n = 1, 2, \dots, N, \quad (31)$$

where  $\mathbf{x} = \text{vec}(\underline{\mathbf{X}}) \in \mathbb{R}^{I_1 I_2 \cdots I_N}$ ,  $\mathbf{g}^{(n)} = \text{vec}(\underline{\mathbf{G}}^{(n)}) \in \mathbb{R}^{R_{n-1} I_n R_n}$  and a tall-and-skinny matrix, called the frame matrix, formulated as

$$\underline{\mathbf{G}}_{\neq n} = (\underline{\mathbf{G}}_{(n)}^{<n})^T \otimes \mathbf{I}_{I_n} \otimes (\underline{\mathbf{G}}_{(1)}^{>n})^T \in \mathbb{R}^{I_1 I_2 \cdots I_N \times R_{n-1} I_n R_n}. \quad (32)$$

The frame and interface matrices help to show a very important property of TT, – TT is linear with respect to each core  $\underline{\mathbf{G}}^{(n)}$  in the vectorized form [40].

### B. Extraction of two cores for two-sided DMRG

In a similar way, we can formulate equations for the 2-sided DMRG, where we extract block of two consecutive cores (see Fig. 24):

$$\mathbf{x} = \underline{\mathbf{G}}_{\neq n, n+1} \mathbf{g}^{(n, n+1)}, \quad n = 1, 2, \dots, N-1, \quad (33)$$

where the frame (tall-and-skinny) matrix is formulated as

$$\begin{aligned} \underline{\mathbf{G}}_{\neq n, n+1} &= (\underline{\mathbf{G}}_{(n)}^{<n})^T \otimes \mathbf{I}_{I_n} \otimes \mathbf{I}_{I_{n+1}} \otimes (\underline{\mathbf{G}}_{(1)}^{>n+1})^T \\ &\in \mathbb{R}^{I_1 I_2 \cdots I_N \times R_{n-1} I_n I_{n+1} R_{n+1}} \end{aligned} \quad (34)$$

and  $\mathbf{g}^{(n, n+1)} = \text{vec}[\underline{\mathbf{G}}_{(3)}^{(n)} \underline{\mathbf{G}}_{(1)}^{(n+1)}] = \text{vec}(\underline{\mathbf{G}}^{(n, n+1)}) \in \mathbb{R}^{R_{n-1} I_n I_{n+1} R_{n+1}}$  for  $n = 1, 2, \dots, N-1$ .

Simple matrix manipulations give the following useful relationships [13]:

$$\mathbf{X}_{(n)} = \underline{\mathbf{G}}_{(n)}^{(n)} (\underline{\mathbf{G}}_{(n)}^{<n} \otimes \underline{\mathbf{G}}_{(1)}^{>n}), \quad (35)$$

$$\underline{\mathbf{G}}_{\neq n+1} = \underline{\mathbf{G}}_{\neq n, n+1} (\mathbf{I}_{R_{n+1} I_{n+1}} \otimes \underline{\mathbf{G}}_{(3)}^{(n) T}). \quad (36)$$

If cores are normalized in a such way that all cores to the left of the currently considered (optimized) core  $\underline{\mathbf{G}}^{(n)}$  are left-orthogonal:

$$\underline{\mathbf{G}}_{(3)}^{(k)} \underline{\mathbf{G}}_{(3)}^{(k) T} = \mathbf{I}_{R_k}, \quad k < n, \quad (37)$$

and all cores to the right of the  $\underline{\mathbf{G}}^{(n)}$  are right-orthogonal, i.e.:

$$\underline{\mathbf{G}}_{(1)}^{(p)} \underline{\mathbf{G}}_{(1)}^{(p) T} = \mathbf{I}_{R_{p-1}}, \quad p > n, \quad (38)$$

then the frames matrices have orthogonal columns [67]–[69]:

$$\underline{\mathbf{G}}_{\neq n}^T \underline{\mathbf{G}}_{\neq n} = \mathbf{I}_{R_{n-1} I_n R_n}, \quad (39)$$

$$\underline{\mathbf{G}}_{\neq n, n+1}^T \underline{\mathbf{G}}_{\neq n, n+1} = \mathbf{I}_{R_{n-1} I_n I_{n+1} R_{n+1}}. \quad (40)$$

Orthogonalization of cores is usually performed by the QR/SVD algorithm [40] (see Section VIII for detail).

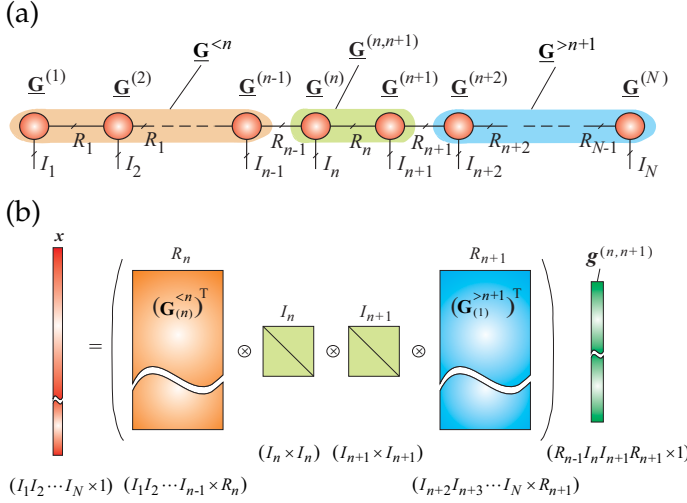


**Figure 24:** Extraction of two cores: (a) Graphical representation of the tensor train and subtrains. (b) Graphical illustration of the frame equation (see Eqs. (33) and (34)).

### VIII. Application of TT Decompositions to Large-Scale Optimization Problems

For extremely large-scale problems, due to curse of dimensionality, most computation and optimization problems (such as solving eigenvalue problems, SVD, sparse PCA, Canonical Correlation Analysis (CCA), system of linear equations) are intractable when using standard numerical methods.

Our goal and objective is to seek for alternative solutions for specific optimization problems in approximative tensor compressed formats. The key idea discussed in this section is to represent huge data in TT formats and to apply some kind of separation of variables [68]–[70]. In other words, we approximate involved vectors and matrices by suitable TT networks and convert a large-scale specific optimization problem into a set of much smaller optimization problems.

We next illustrate this approach by considering several fundamental optimization problems for very large-scale data.

#### A. Computing a Few Extreme Eigenvalues and Eigenvectors for Symmetric EVD in TT Format

In many applications we need to compute extreme (minimum or maximum) eigenvalues and corresponding eigenvectors of a huge structured symmetric matrix. The basic problem we try to solve is the standard symmetric eigenvalue decomposition (EVD), which can be formulated as

$$\mathbf{A} \mathbf{x}_k = \lambda_k \mathbf{x}_k, \quad (k = 1, 2, \dots, K), \quad (41)$$

where  $\mathbf{x}_k \in \mathbb{R}^I$  are the orthonormal eigenvectors,  $\lambda_k$  are the corresponding eigenvalues of a symmetric matrix  $\mathbf{A} \in \mathbb{R}^{I \times I}$  (e.g., a positive-definite covariance matrix of zero-mean signals  $\mathbf{y}(t)$ ). Note that (41) can be written in the matrix form as

$$\mathbf{X}^T \mathbf{A} \mathbf{X} = \Lambda_K, \quad (42)$$

where  $\Lambda_K$  is the diagonal matrix of  $K$  smallest or largest eigenvalues (ranked in ascending or descending order, respectively).

#### 1) Tensor Network for Computing Single Eigenvalue and Corresponding Eigenvector:

Many iterative algorithms for extreme eigenvalue and the corresponding eigenvector exploit the Rayleigh quotient (RQ) of the symmetric matrix as a cost function. The Rayleigh quotient  $R(\mathbf{x})$  is defined for  $\mathbf{x} \neq \mathbf{0}$ , as

$$J(\mathbf{x}) = R(\mathbf{x}, \mathbf{A}) = \frac{\mathbf{x}^T \mathbf{A} \mathbf{x}}{\mathbf{x}^T \mathbf{x}} = \frac{\langle \mathbf{A} \mathbf{x}, \mathbf{x} \rangle}{\langle \mathbf{x}, \mathbf{x} \rangle}, \quad (43)$$

where

$$\lambda_{\max} = \max R(\mathbf{x}, \mathbf{A}), \quad \lambda_{\min} = \min R(\mathbf{x}, \mathbf{A}), \quad (44)$$

where  $\lambda_{\max}$  and  $\lambda_{\min}$  denote respectively largest and smallest eigenvalue of the matrix  $\mathbf{A}$ . More generally, the critical points and critical values of  $R(\mathbf{x}, \mathbf{A})$  are the eigenvectors and eigenvalues of  $\mathbf{A}$ .

If the matrix  $\mathbf{A}$  admits low-rank TT approximation, we can convert large-scale problems into smaller optimization problems by representing the eigenvector  $\mathbf{x}$  and the matrix  $\mathbf{A}$  in TT (MPO/MPS) formats (see also Fig. 25) as:

$$\begin{aligned} \underline{\mathbf{A}} &= [\underline{\mathbf{A}}^{(1)}, \underline{\mathbf{A}}^{(2)}, \dots, \underline{\mathbf{A}}^{(N)}] \\ \underline{\mathbf{X}} &= [\underline{\mathbf{X}}^{(1)}, \underline{\mathbf{X}}^{(2)}, \dots, \underline{\mathbf{X}}^{(N)}] \end{aligned} \quad (45)$$

and by computing iteratively the frame equation  $\mathbf{x} = \underline{\mathbf{X}}_{\neq n} \mathbf{x}^{(n)}$ , ( $n = 1, 2, \dots, N$ ), with the frame matrices:

$$\underline{\mathbf{X}}_{\neq n} = (\underline{\mathbf{X}}_{(n)}^{<n})^T \otimes \mathbf{I}_{I_n} \otimes (\underline{\mathbf{X}}_{(1)}^{>n})^T \in \mathbb{R}^{I_1 I_2 \cdots I_{n-1} I_n R_n}.$$

Assuming that cores  $\underline{\mathbf{X}}^{(n)}$  are constrained to be left and right orthogonal, we can minimize (or maximize) the RQ as follows:

$$\begin{aligned} \min_{\mathbf{x}} J(\mathbf{x}) &= \min_{\mathbf{x}^{(n)}} J(\underline{\mathbf{X}}_{\neq n} \mathbf{x}^{(n)}) \\ &= \min_{\mathbf{x}^{(n)}} \frac{\langle \bar{\mathbf{A}}^{(n)} \mathbf{x}^{(n)}, \mathbf{x}^{(n)} \rangle}{\langle \mathbf{x}^{(n)}, \mathbf{x}^{(n)} \rangle}, \quad n = 1, 2, \dots, N, \end{aligned} \quad (46)$$

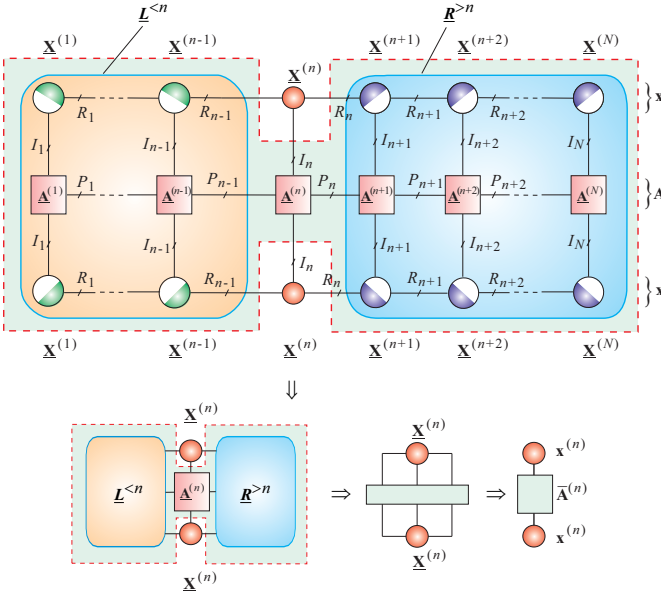


**Figure 25:** Computation of a single extreme eigenvalue and the corresponding eigenvector  $\mathbf{x} \in \mathbb{R}^I$  in the TT format for a symmetric matrix  $\mathbf{A} \in \mathbb{R}^{I \times I}$ . The frame matrix maps a TT core into a large vector. The tensor network corresponds to the Rayleigh quotient, with the matrix  $\mathbf{A}$  and vectors  $\mathbf{x} \in \mathbb{R}^I$  given in the tensor train format with distributed indices  $I = I_1 I_2 \cdots I_N$ . The cores included in the shaded areas form the matrix  $\bar{\mathbf{A}}^{(n)}$  (the effective Hamiltonian), which can be computed by sequential core contractions.

where  $\mathbf{x}^{(n)} = \text{vec}(\underline{\mathbf{X}}^{(n)}) \in \mathbb{R}^{R_{n-1} I_n R_n}$  and the matrix  $\bar{\mathbf{A}}$ , often called the effective Hamiltonian, and can be expressed as

$$\bar{\mathbf{A}}^{(n)} = (\mathbf{X}_{\neq n})^T \mathbf{A} \mathbf{X}_{\neq n} \in \mathbb{R}^{R_{n-1} I_n R_n \times R_{n-1} I_n R_n} \quad (47)$$

for  $n = 1, 2, \dots, N$ .

Note that the matrices  $\bar{\mathbf{A}}^{(n)}$  are usually much smaller than the original matrix  $\mathbf{A}$  if the TT rank is relatively small, then, the large-scale optimization problem can be converted into a much smaller set of EVDs, i.e., by solving the set of equations:

$$\bar{\mathbf{A}}^{(n)} \mathbf{x}^{(n)} = \lambda \mathbf{x}^{(n)}, \quad n = 1, 2, \dots, N. \quad (48)$$

In practice, we never compute the matrices  $\bar{\mathbf{A}}^{(n)}$  directly by Eq. (47), but iteratively via optimized and approximative contraction of cores of the tensor network as shown in Fig. 26.

This is achieved by sweeping through the tensor network in a recursive forward and backward manner and forth through each node. An initial guess for all cores  $\underline{\mathbf{X}}^{(n)}$  is first made, and then we sweep through the set of the cores with the index  $n$ , keeping all other cores fixed and choosing the  $\underline{\mathbf{X}}^{(n)}$ ,

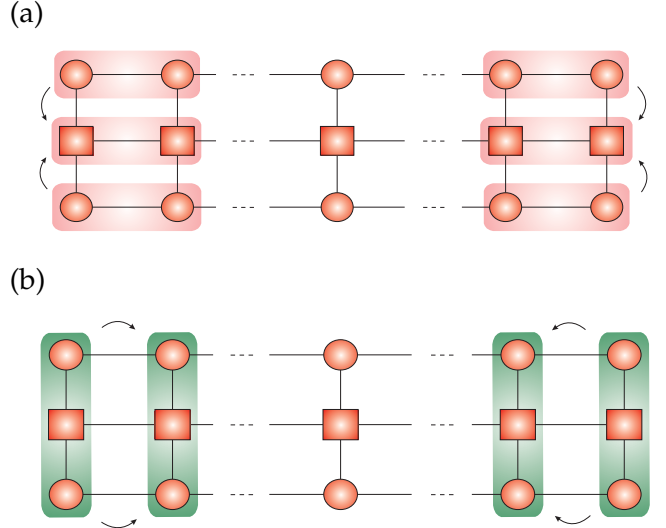


**Figure 26:** (a) Non-optimal (inefficient) and (b) optimal (efficient) contraction of the TT (MPS/MPO) network.

such that the cost function gradually decreases. By repeating such sweeps (from the left to the right and from the right to the left) through the tensor network several times that usually leads to a converged approximation. Note that this sweeping process works in a similar fashion as a self-consistent recursive loops, where we iteratively and gradually improve the solution.

In order to efficiently estimate the matrix  $\bar{\mathbf{A}}^{(n)}$ , we need to compute blocks  $\underline{\mathbf{L}}^{<n}$  and  $\underline{\mathbf{R}}^{>n}$  (see Fig. 25). However,  $\underline{\mathbf{L}}^{<n}$  and  $\underline{\mathbf{R}}^{>n}$  can be built iteratively in order to best reuse available information; this involves an optimal arrangement of a tensor network contraction. In a practical implementation of the algorithm the full network contraction is never carried out globally, but we rather look at blocks  $\underline{\mathbf{L}}^n$  and  $\underline{\mathbf{R}}^{>n}$  that are growing and shrinking in size sweeping along the tensor network [49]. In other words, the construction of blocks  $\underline{\mathbf{L}}^{<n}$  and  $\underline{\mathbf{R}}^{>n}$  is an iterative process in a way that directly matches block growth and shrinkage. If we sweep through the chain from right to left or vice-versa we can build up  $\underline{\mathbf{L}}^{<n}$  and  $\underline{\mathbf{R}}^{>n}$  iteratively from the previous steps, which is the most efficient way [49]. Furthermore, we can exploit left- and right-orthogonalization of the cores in order to simplify the tensor contraction process [13], [68], [69].

As in any iterative optimization based on gradient descent the cost function can only decrease, however we have no guarantee that a global minimum is achieved. Moreover, for some initial conditions the iteration process can be slow.

To alleviate these problems we can exploit double site DMRG, in which we join two neighboring factors (cores), optimize the resulting “supernode” called also “super-core” or “super-block”, and split again the result into separated factors by low-rank matrix factorizations [49], [68], [69], [71].

**2) Tensor Network for Computing Several Extreme Eigenvalues and Corresponding Eigenvectors for Symmetric Eigenvalue Problem:** In a more general case, in order to compute a few, say  $K$  eigenvectors corresponding to  $K$  algebraically smallest eigenvalues for a symmetric matrix  $\mathbf{A} \in \mathbb{R}^{I \times I}$ , we can employ the following trace minimization problem with orthogonality constraints

$$\min_{\mathbf{X}} \text{tr}(\mathbf{X}^T \mathbf{A} \mathbf{X}), \quad \text{s.t. } \mathbf{X}^T \mathbf{X} = \mathbf{I}_K, \quad (49)$$

where  $\mathbf{X} = [\mathbf{x}_1, \mathbf{x}_2, \dots, \mathbf{x}_K] \in \mathbb{R}^{I \times K}$ , which is equivalent to the following unconstrained problem

$$\min_{\mathbf{X}} \{ \text{tr}(\mathbf{X}^T \mathbf{A} \mathbf{X}) + \alpha \|\mathbf{X}^T \mathbf{X} - \mathbf{I}_K\|_F^2 \}, \quad (50)$$

where the penalty parameter  $\alpha > 0$  takes suitable finite value [72].

When computing  $K > 1$  eigenvectors, we need to work with  $K$  vectors  $\mathbf{x}_k$  in parallel. Instead of representing each vector individually in the TT format, we can represent them jointly in a block TT format<sup>7</sup> introduced by Dolgov et al. [68] (see also Pižorn, I. and Verstraete [67] and Kressner et al. [69]). In the block TT all cores are 3rd-order tensors, except one which is 4th-order tensor, where additional physical index  $K$  represents the number of vectors as shown in Fig. 27 (a). It should be noted that the position of such 4th-order core  $\mathbf{G}^{(n)}$ , which carries the index  $K$  is not fixed; we will move it back and forth from position 1 to  $N$  during the sequential optimization [68], [70].

If the block TT model is used to represent  $K$  orthogonal vectors, then the matrix frame equation takes the slightly modified form:

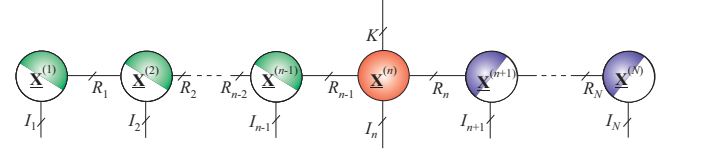
$$\mathbf{X} = \mathbf{X}_{\neq n} \mathbf{X}^{(n)} \in \mathbb{R}^{I \times K}, \quad n = 1, 2, \dots, N, \quad (51)$$

where  $\mathbf{X}^{(n)} \in \mathbb{R}^{R_{n-1} I_n R_n \times K}$ .

Hence, we can express the trace in (49) as follows:

$$\begin{aligned} \text{tr}(\mathbf{X}^T \mathbf{A} \mathbf{X}) &= \text{tr}((\mathbf{X}_{\neq n} \mathbf{X}^{(n)})^T \mathbf{A} \mathbf{X}_{\neq n} \mathbf{X}^{(n)}) \\ &= \text{tr}((\mathbf{X}^{(n)})^T [\mathbf{X}_{\neq n}^T \mathbf{A} \mathbf{X}_{\neq n}] \mathbf{X}^{(n)}) \\ &= \text{tr}(\mathbf{X}^{(n) T} \bar{\mathbf{A}}^{(n)} \mathbf{X}^{(n)}), \end{aligned} \quad (52)$$

(a) Block tensor train with left- and right-orthogonal cores



(b) Tensor network corresponding to the optimization problem (49)

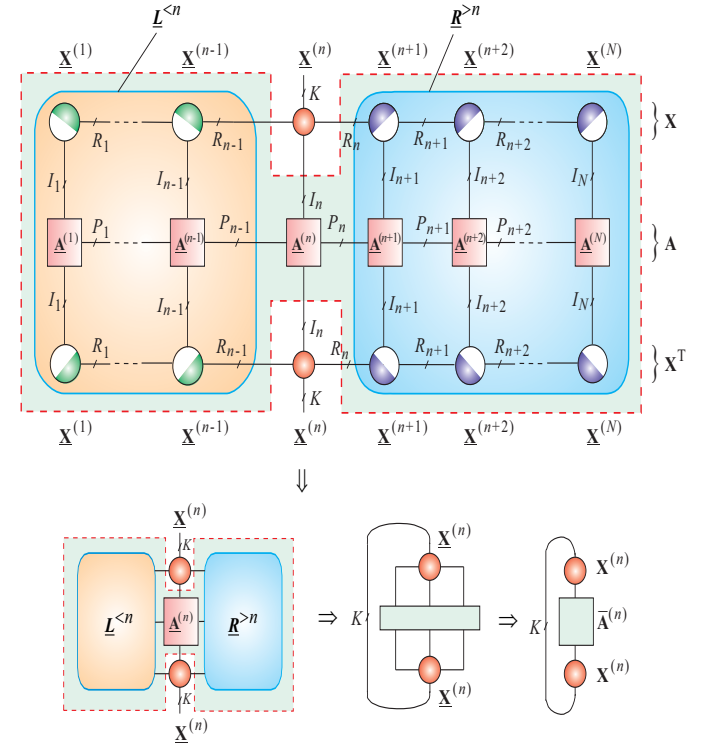


**Figure 27:** Computation of  $K$  eigenvectors corresponding to  $K$  extreme eigenvalues in TT format for the symmetric matrix  $\mathbf{A} \in \mathbb{R}^{I \times I}$  and the orthogonal matrix  $\mathbf{X} \in \mathbb{R}^{I \times K}$  given in the distributed block tensor train formats. The extreme eigenvalues are computed as  $\Lambda = \mathbf{X}^{(n) T} \bar{\mathbf{A}}^{(n)} \mathbf{X}^{(n)}$ .

where  $\bar{\mathbf{A}}^{(n)} = \mathbf{X}_{\neq n}^T \mathbf{A} \mathbf{X}_{\neq n}$ .

Assuming that frame matrices have orthogonal columns, we can convert the optimization problem (49) into a set of linked optimization problems:

$$\min_{\mathbf{X}^{(n)}} \text{tr}(\mathbf{X}^{(n) T} \bar{\mathbf{A}}^{(n)} \mathbf{X}^{(n)}), \quad \text{s.t. } \mathbf{X}^{(n) T} \mathbf{X}^{(n)} = \mathbf{I}_K \quad (53)$$

for  $n = 1, 2, \dots, N$ , where  $\bar{\mathbf{A}}^{(n)}$  is computed iteratively by tensor network contraction shown in Fig. 27 (b). In other words, the above problem is solved iteratively via optimized iterative contraction of the tensor network. This means that an active block

<sup>7</sup>Instead of the block TT format for distributed matrix representations, we can use alternative models, see Fig. 33.

(core) is sequentially selected in an iterative manner for  $n = 1, 2, \dots, N$  by sweeping from left to right and back from right to left and so on until convergence [68], [69].

It should be noted that the global orthogonality constraint  $\mathbf{X}^T \mathbf{X} = \mathbf{I}_K$  is equivalent to the set of local orthogonality constraints  $(\mathbf{X}^{(n)})^T \mathbf{X}^{(n)} = \mathbf{I}_K, \forall n$ , since due to left and right orthogonality of the cores, we can write:

$$\begin{aligned} \mathbf{X}^T \mathbf{X} &= \mathbf{X}^{(n)}{}^T \mathbf{X}_{\neq n}^T \mathbf{X}_{\neq n} \mathbf{X}^{(n)} \\ &= \mathbf{X}^{(n)}{}^T \mathbf{X}^{(n)}, \forall n. \end{aligned} \quad (54)$$

### B. Tensor Networks for Tracking a Few Extreme Singular Values and Vectors for SVD and Sparse PCA

The computation of the largest singular value and the corresponding left- and right eigenvector can be performed via the following optimization problem

$$\max_{\mathbf{u}, \mathbf{v}} \{ \mathbf{u}^T \mathbf{A} \mathbf{v} \}, \text{ s.t. } \|\mathbf{u}\|_2^2 = 1, \|\mathbf{v}\|_2^2 = 1, \quad (55)$$

where  $\mathbf{A} \in \mathbb{R}^{I \times J}$  is arbitrary data matrix that admits low-rank TT decomposition. Using TT decomposition of vectors  $\mathbf{u} \in \mathbb{R}^I, \mathbf{v} \in \mathbb{R}^J$  and the data matrix  $\mathbf{A}$  and assuming that cores  $\underline{\mathbf{U}}^{(n)}$  and  $\underline{\mathbf{V}}^{(n)}$  are kept left- and right- orthogonal, the optimization problem (55) can be converted into a set of usually much smaller scale optimization problems as follows (see Fig. 28 (a)):

$$\begin{aligned} \max_{\mathbf{u}^{(n)}, \mathbf{v}^{(n)}} & \{ (\mathbf{u}^{(n)})^T \bar{\mathbf{A}}^{(n)} \mathbf{v}^{(n)} \}, \\ \text{s.t. } & \|\mathbf{u}^{(n)}\|_2^2 = 1, \|\mathbf{v}^{(n)}\|_2^2 = 1, \forall n, \end{aligned} \quad (56)$$

where  $\mathbf{u}^{(n)} = \text{vec}(\underline{\mathbf{U}}^{(n)}) \in \mathbb{R}^{\tilde{R}_{n-1} I_n \tilde{R}_n}$  and  $\mathbf{v}^{(n)} = \text{vec}(\underline{\mathbf{V}}^{(n)}) \in \mathbb{R}^{R_{n-1} J_n \tilde{R}_n}$  and

$$\bar{\mathbf{A}}^{(n)} = (\mathbf{U}_{\neq n})^T \mathbf{A} \mathbf{V}_{\neq n} \in \mathbb{R}^{\tilde{R}_{n-1} I_n \tilde{R}_n \times R_{n-1} J_n R_n} \quad (57)$$

for  $n = 1, 2, \dots, N$ .

Note that taking into account that the frame matrices  $\mathbf{U}_{\neq n} \in \mathbb{R}^{I_1 I_2 \dots I_N \times \tilde{R}_{n-1} I_n \tilde{R}_n}$  and  $\mathbf{V}_{\neq n} \in \mathbb{R}^{J_1 J_2 \dots J_N \times R_{n-1} I_n R_n}$  are orthogonal and

$$\mathbf{u} = \mathbf{U}_{\neq n} \mathbf{u}^{(n)}, \mathbf{v} = \mathbf{V}_{\neq n} \mathbf{v}^{(n)}, \forall n, \quad (58)$$

we can easily check that  $\|\mathbf{u}\|_2 = \|\mathbf{u}^{(n)}\|_2$  and  $\|\mathbf{v}\|_2 = \|\mathbf{v}^{(n)}\|_2, \forall n$ .

An alternative approach to compute SVD for several maximal singular values and the corresponding left- and right- orthogonal eigenvectors, is to convert the SVD to the problem of symmetric

EVD by applying the following basic relationships. It is evident, that from the SVD of the matrix  $\mathbf{A} = \mathbf{U} \Sigma \mathbf{V}^T \in \mathbb{R}^{I \times J}$ , where  $\Sigma_1 = \text{diag}\{\sigma_1, \dots, \sigma_R\}$ , we have

$$\mathbf{A} \mathbf{A}^T = \mathbf{U} \Sigma_1^2 \mathbf{U}^T, \quad (59)$$

$$\mathbf{A}^T \mathbf{A} = \mathbf{V} \Sigma_2^2 \mathbf{V}^T, \quad (60)$$

where  $\Sigma_1 = \text{diag}\{\sigma_1, \dots, \sigma_I\}$  and  $\Sigma_2 = \text{diag}\{\sigma_1, \dots, \sigma_I\}$ . This means that the singular values of  $\mathbf{A} \in \mathbb{R}^{I \times J}$  are the positive square roots of the eigenvalues of  $\mathbf{A}^T \mathbf{A}$  and the eigenvectors  $\mathbf{U}$  of  $\mathbf{A} \mathbf{A}^T$  are the left singular vectors of  $\mathbf{A}$ . Note that if  $R < I$ , the matrix  $\mathbf{A} \mathbf{A}^T$  will contain at least  $I - R$  additional eigenvalues that are not included as singular values of  $\mathbf{A}$ .

Hence, in order to compute approximately  $K$  smallest singular values and the corresponding right-eigenvectors, we can employ formally the following optimization problem:

$$\begin{aligned} \min_{\mathbf{V} \in \mathbb{R}^{I \times K}} & \text{tr}(\mathbf{V}^T \mathbf{A}^T \mathbf{A} \mathbf{V}), \\ \text{s.t. } & \mathbf{V}^T \mathbf{V} = \mathbf{I}_K. \end{aligned} \quad (61)$$

The SVD problem for large-scale structured matrices that admit low-rank TT approximations can be solved iteratively in TT formats by the following set of smaller optimization (symmetric EVD) problems:

$$\max_{\mathbf{V}^{(n)}} \text{tr}((\mathbf{V}^{(n)})^T [\mathbf{V}_{\neq n}^T \mathbf{A}^T \mathbf{A} \mathbf{V}_{\neq n}] \mathbf{V}^{(n)}), \quad (62)$$

$$\text{s.t. } (\mathbf{V}^{(n)})^T \mathbf{V}^{(n)} = \mathbf{I}_K, n = 1, 2, \dots, N,$$

where  $\mathbf{V}^{(n)} \in \mathbb{R}^{R_{n-1} J_n R_n \times K}$  and

$$\bar{\mathbf{A}}^{(n)} = \mathbf{V}_{\neq n}^T \mathbf{A}^T \mathbf{A} \mathbf{V}_{\neq n} \in \mathbb{R}^{R_{n-1} I_n R_n \times R_{n-1} I_n R_n} \quad (63)$$

for  $n = 1, 2, \dots, N$  are computed sequentially via tensor network contractions as illustrated in Fig. 29.

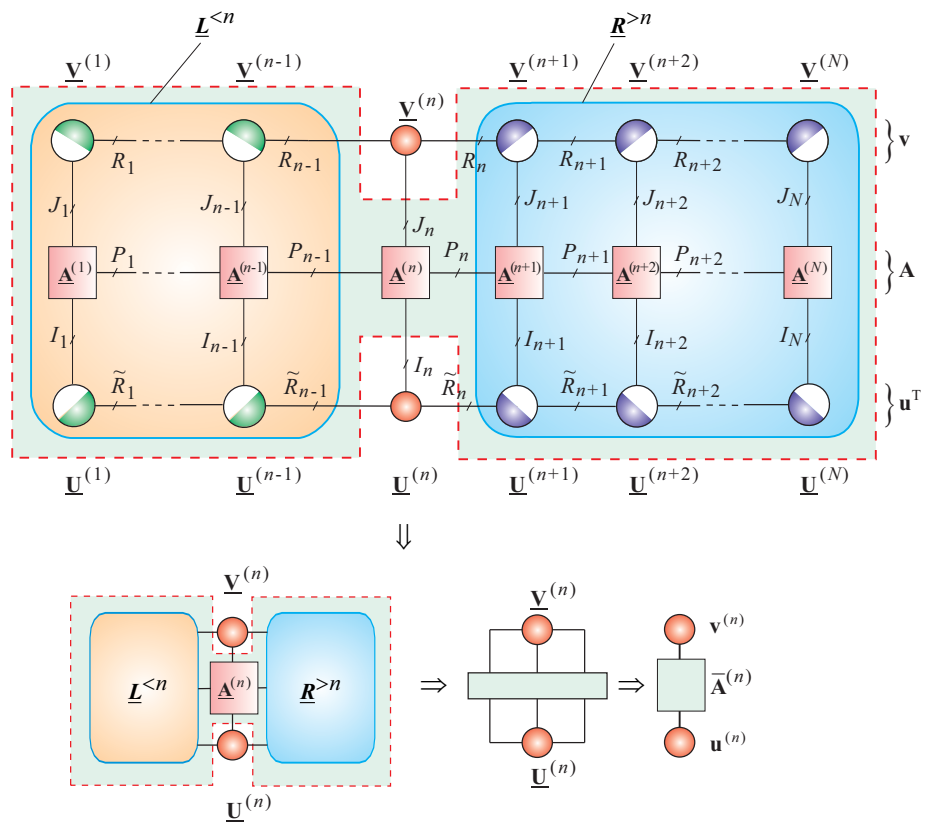
The challenge is how to extend and/or modify the above described approaches to the following large-scale optimization problems for structured matrices, if we need impose additional constraints such as sparsity, nonnegativity, orthogonality or local smoothness:

- Sparse Principal Component Analysis (SPCA) using the Penalized Matrix Decomposition (PMD) [74], [75]

$$\begin{aligned} \max_{\mathbf{u}, \mathbf{v}} & \{ \mathbf{u}^T \mathbf{A} \mathbf{v} \}, \text{ s.t. } \|\mathbf{u}\|_2^2 \leq 1, \|\mathbf{v}\|_2^2 \leq 1, \\ & P(\mathbf{v}) \leq c_1, \end{aligned} \quad (64)$$

where the positive parameter  $c_1$  controls sparsity level and the convex penalty function  $P(\mathbf{v})$

(a)



(b)

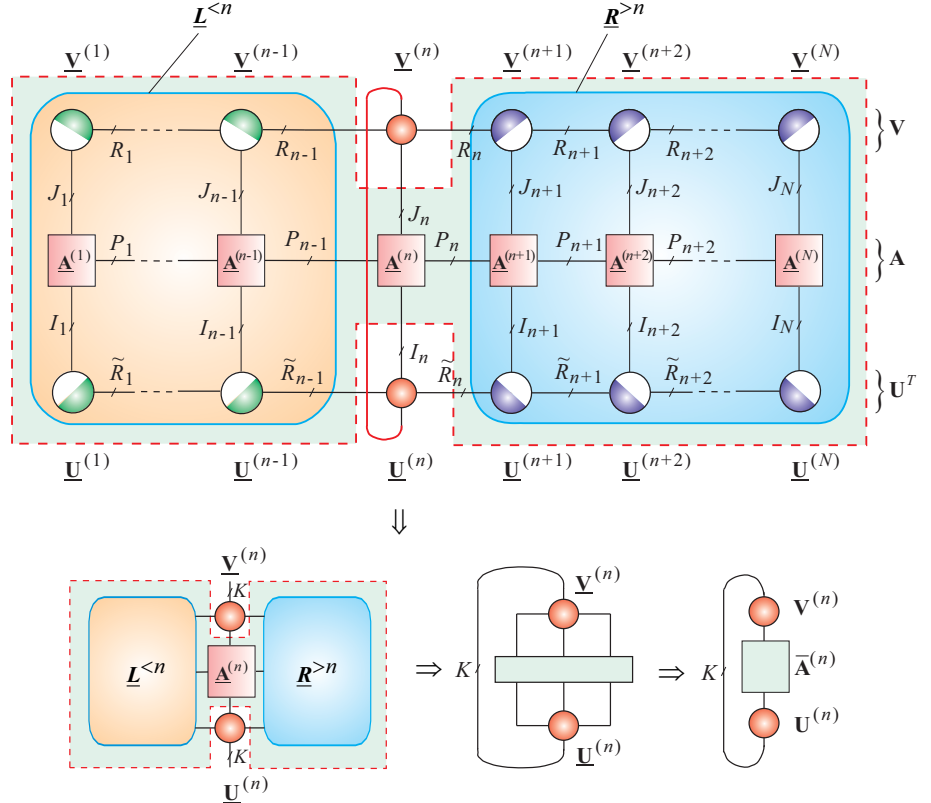
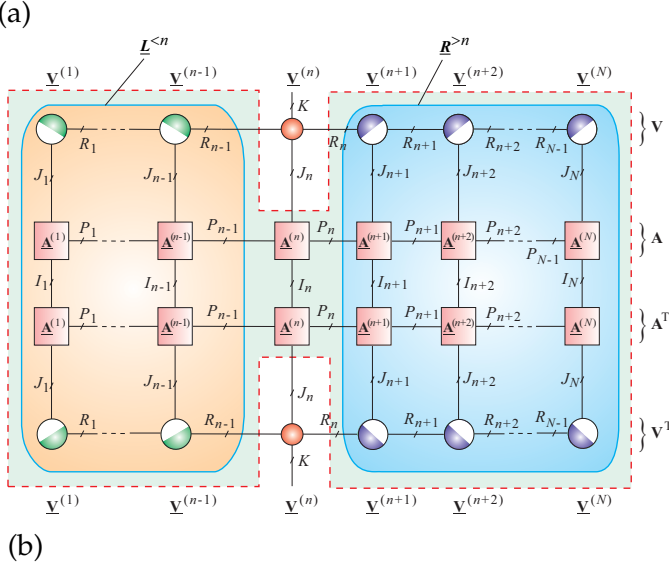


**Figure 28:** (a) Tensor network for computing the SVD singular eigenvectors corresponding to a largest singular value. (b) Tensor network for computing  $K$  left- and right-eigenvectors corresponding to the  $K$  largest singular values via maximization of the trace  $\text{tr}(\mathbf{U}^T \mathbf{A} \mathbf{V})$ , subject to orthogonality constraints  $\mathbf{U}^T \mathbf{U} = \mathbf{I}_k$  and  $\mathbf{V}^T \mathbf{V} = \mathbf{I}_K$  [73]. The singular values are computed as  $\Sigma = \mathbf{U}^{(n)} \mathbf{A}^{(n)} \mathbf{V}^{(n)}$ .



(b)

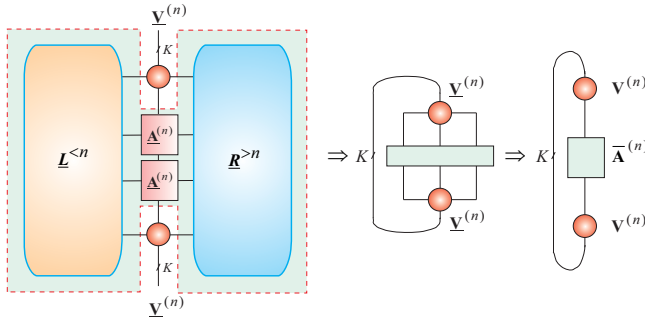


**Figure 29:** Computation of  $K$  right eigenvectors corresponding to  $K$  smallest singular values of the SVD in TT formats.

can take a variety of forms. Useful examples are [75]:

$$\begin{aligned}
 P(\mathbf{v}) &= \|\mathbf{v}\|_1 = \sum_{i=1}^I |v_i| \quad (\text{Lasso}), \\
 P(\mathbf{v}) &= \|\mathbf{v}\|_0 = \sum_{i=1}^I |\text{sign}(v_i)|, \\
 P(\mathbf{v}) &= \sum_{i=1}^I |v_i| + \lambda \sum_{i=2}^I |v_i - v_{i-1}|.
 \end{aligned} \tag{65}$$

- SPCA via regularized SVD (sPCA-rSVD) [76], [77]

$$\begin{aligned}
 &\max_{\mathbf{u}, \mathbf{v}} \{ \mathbf{u}^T \mathbf{A} \mathbf{v} - \alpha P(\mathbf{v}) \} \\
 \text{s.t. } &\|\mathbf{u}\|_2^2 \leq 1, \quad \|\mathbf{v}\|_2^2 \leq 1,
 \end{aligned} \tag{66}$$

- Two-way functional PCA/SVD [78]

$$\begin{aligned}
 &\max_{\mathbf{u}, \mathbf{v}} \{ \mathbf{u}^T \mathbf{A} \mathbf{v} - \frac{\alpha}{2} P_1(\mathbf{u}) P_2(\mathbf{v}) \}, \\
 \text{s.t. } &\|\mathbf{u}\|_2^2 \leq 1, \quad \|\mathbf{v}\|_2^2 \leq 1.
 \end{aligned} \tag{67}$$

- Sparse SVD [79]

$$\max_{\mathbf{u}, \mathbf{v}} \{ \mathbf{u}^T \mathbf{A} \mathbf{v} - \frac{1}{2} \mathbf{u}^T \mathbf{u} \mathbf{v}^T \mathbf{v} - \frac{\alpha_1}{2} P_1(\mathbf{u}) - \frac{\alpha_2}{2} P_2(\mathbf{v}) \}. \tag{68}$$

- Generalized SPCA [80]

$$\begin{aligned}
 &\max_{\mathbf{u}, \mathbf{v}} \{ \mathbf{u}^T \mathbf{Q} \mathbf{A} \mathbf{R} \mathbf{v} - \frac{\alpha_1}{2} P_1(\mathbf{u}) - \frac{\alpha_2}{2} P_2(\mathbf{v}) \}, \\
 \text{s.t. } &\mathbf{u}^T \mathbf{Q} \mathbf{u} \leq 1, \quad \mathbf{v}^T \mathbf{R} \mathbf{v} \leq 1,
 \end{aligned} \tag{69}$$

where  $\mathbf{Q} \in \mathbb{R}^{T \times T}$  and  $\mathbf{R} \in \mathbb{R}^{I \times I}$  are symmetric positive-definite matrices.

- Generalized nonnegative SPCA [81]

$$\begin{aligned}
 &\max_{\mathbf{u}, \mathbf{v}} \{ \mathbf{u}^T \mathbf{A} \mathbf{R} \mathbf{v} - \alpha \|\mathbf{v}\|_1 \}, \\
 \text{s.t. } &\mathbf{u}^T \mathbf{u} \leq 1, \quad \mathbf{v}^T \mathbf{R} \mathbf{v} \leq 1, \quad \mathbf{v} \geq 0.
 \end{aligned} \tag{70}$$

### C. Generalized Eigenvalue Problems in TT formats

In many practical applications, especially in dimension reduction and classification problems (e.g., in PCA/MDS, LPP, ONPP, LDA – see Table IV for more detail), we need to minimize the following trace optimization problem formulated as a generalized eigenvalue problem (GEVD) [82]:

$$\min_{\mathbf{V} \in \mathbb{R}^{I \times K}} \text{tr}(\mathbf{V}^T \mathbf{X} \mathbf{A} \mathbf{X}^T \mathbf{V}), \quad \text{s.t. } \mathbf{V}^T \mathbf{B} \mathbf{V} = \mathbf{I}_K, \tag{71}$$

where it is assumed that the structured data matrices:  $\mathbf{X} \in \mathbb{R}^{I \times J}$ , symmetric matrix  $\mathbf{A} \in \mathbb{R}^{J \times J}$ , and symmetric positive-definite matrix  $\mathbf{B} \in \mathbb{R}^{I \times I}$  are known.

The problem is equivalent to the unconstrained optimization problem

$$\min_{\mathbf{V} \in \mathbb{R}^{I \times K}} \{ \text{tr}(\mathbf{V}^T \mathbf{X} \mathbf{A} \mathbf{X}^T \mathbf{V}) + \alpha \|\mathbf{V}^T \mathbf{B} \mathbf{V} - \mathbf{I}_K\|_F^2 \}. \tag{72}$$

Note that by changing of the variable  $\mathbf{W} = \mathbf{B}^{1/2} \mathbf{V}$  the GEVD can be converted to the standard symmetric EVD problem

$$\min_{\mathbf{W} \in \mathbb{R}^{I \times K}} \text{tr}(\mathbf{W}^T \mathbf{B}^{-1/2} \mathbf{X} \mathbf{A} \mathbf{X}^T \mathbf{B}^{-1/2} \mathbf{W}), \quad \text{s.t. } \mathbf{W}^T \mathbf{W} = \mathbf{I}_K.$$

The objective is to estimate the matrix  $\mathbf{V} \in \mathbb{R}^{I \times K}$  in a TT format, assuming that large-scale matrices  $\mathbf{X}$  and  $\mathbf{A}$  ( $\mathbf{W}, \mathbf{D}, \mathbf{H}$ ) are known and admit low-rank TT approximations. The problem for structured matrices that admit low-rank TT approximations can be solved iteratively:

$$\begin{aligned}
 &\min_{\mathbf{V}^{(n)}} \text{tr}((\mathbf{V}^{(n)})^T [\mathbf{V}_{\neq n}^T \mathbf{X} \mathbf{A} \mathbf{X}^T \mathbf{V}_{\neq n}] \mathbf{V}^{(n)}), \\
 \text{s.t. } &(\mathbf{V}^{(n)})^T [\mathbf{V}_{\neq n}^T \mathbf{B} \mathbf{V}_{\neq n}] \mathbf{V}^{(n)} = \mathbf{I}_K,
 \end{aligned} \tag{73}$$

**TABLE IV:** Cost functions and constraints used in classical feature extraction (dimension reduction) methods that can be formulated as generalized eigenvalue problem (71). The objective is to find an (orthogonal) matrix  $\mathbf{V}$ , assuming that data matrices  $\mathbf{X}, \mathbf{W}, \mathbf{D}, \mathbf{H}$  are known. The symmetric matrix  $\mathbf{A}$  can take different forms:  $\mathbf{A} = \mathbf{I} - \frac{1}{N}\mathbf{1}\mathbf{1}^T$ ,  $\mathbf{A} = \mathbf{D} - \mathbf{W}$ ,  $\mathbf{A} = (\mathbf{I} - \mathbf{W}^T)(\mathbf{I} - \mathbf{W})$ ,  $\mathbf{A} = \mathbf{I} - \mathbf{H}$ , depending on method (for more detail see [82]).

Method	Cost Function (min)	Constraints
Principal Component Analysis/ /Multi-Dimensional Scaling (PCA/MDS)	$\text{tr}[-\mathbf{V}^T \mathbf{X} (\mathbf{I} - \frac{1}{N}\mathbf{1}\mathbf{1}^T) \mathbf{X}^T \mathbf{V}]$	$\mathbf{V}^T \mathbf{V} = \mathbf{I}$
Locally Preserving Projection (LPP)	$\text{tr}[\mathbf{V}^T \mathbf{X} (\mathbf{D} - \mathbf{W}) \mathbf{X}^T \mathbf{V}]$	$\mathbf{V}^T \mathbf{X} \mathbf{D} \mathbf{X}^T \mathbf{V} = \mathbf{I}$
Orthogonal LPP (OLPP)	$\text{tr}[\mathbf{V}^T \mathbf{X} (\mathbf{D} - \mathbf{W}) \mathbf{X}^T \mathbf{V}]$	$\mathbf{V}^T \mathbf{V} = \mathbf{I}$
Neighborhood Preserving Projection (NPP)	$\text{tr}[\mathbf{V}^T \mathbf{X} (\mathbf{I} - \mathbf{W}^T)(\mathbf{I} - \mathbf{W}) \mathbf{X}^T \mathbf{V}]$	$\mathbf{V}^T \mathbf{X} \mathbf{X}^T \mathbf{V} = \mathbf{I}$
Orthogonal NPP (ONPP)	$\text{tr}[\mathbf{V}^T \mathbf{X} (\mathbf{I} - \mathbf{W}^T)(\mathbf{I} - \mathbf{W}) \mathbf{X}^T \mathbf{V}]$	$\mathbf{V}^T \mathbf{V} = \mathbf{I}$
Linear Discriminant Analysis (LDA)	$\text{tr}[\mathbf{V}^T \mathbf{X} (\mathbf{I} - \mathbf{H}) \mathbf{X}^T \mathbf{V}]$	$\mathbf{V}^T \mathbf{X} \mathbf{X}^T \mathbf{V} = \mathbf{I}$
Spectral Clustering (Ratio Cut)	$\text{tr}[\mathbf{V}^T (\mathbf{D} - \mathbf{W}) \mathbf{V}]$	$\mathbf{V}^T \mathbf{V} = \mathbf{I}$
Spectral Clustering (Normalized Cut)	$\text{tr}[\mathbf{V}^T (\mathbf{D} - \mathbf{W}) \mathbf{V}]$	$\mathbf{V}^T \mathbf{D} \mathbf{V} = \mathbf{I}$

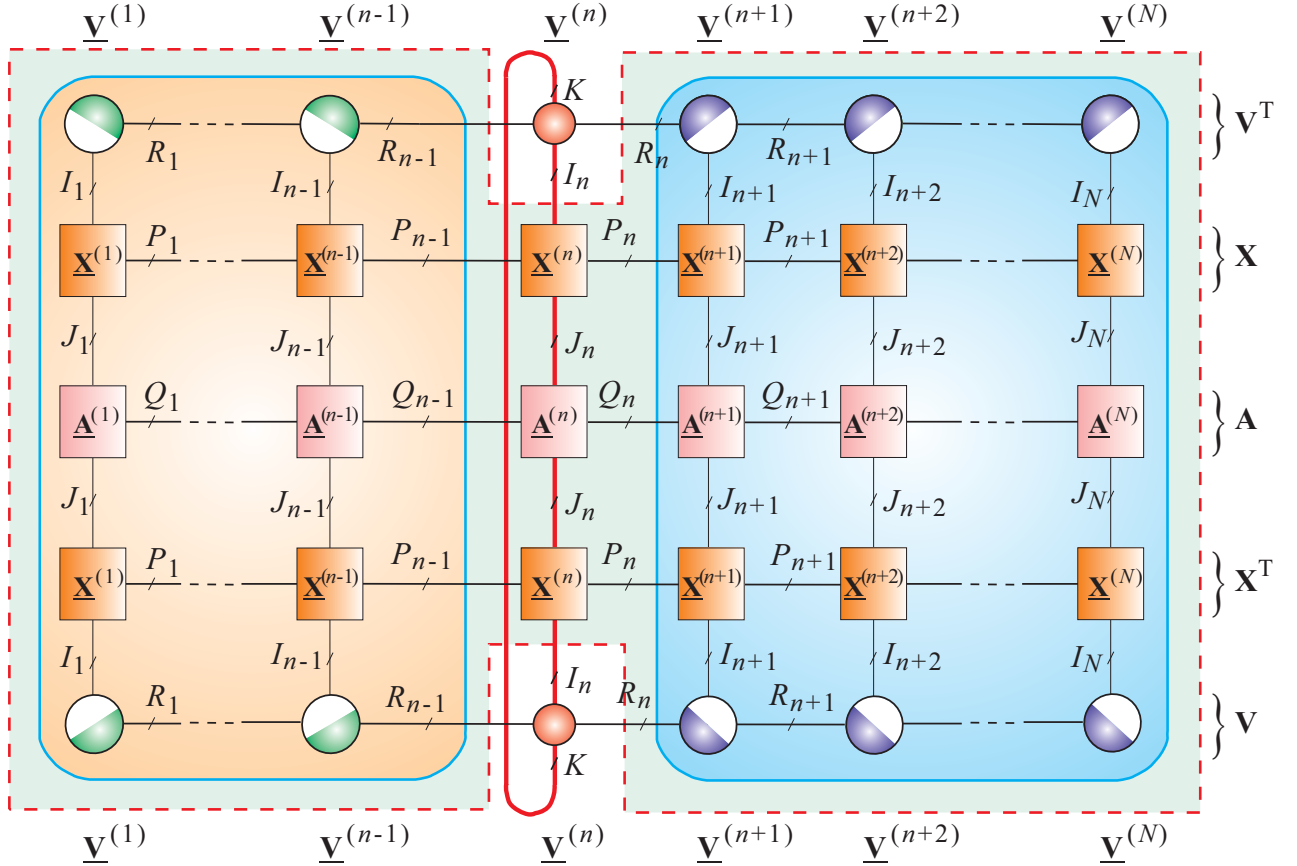


**Figure 30:** Tensor network for computation of  $K$  eigenvectors corresponding to the  $K$  extreme eigenvalues in TT formats for the generalized eigenvalue problem (71).

where the relatively low-dimension matrices:

$$\bar{\mathbf{A}}^{(n)} = [\mathbf{V}_{\neq n}^T \mathbf{X} \mathbf{A} \mathbf{X}^T \mathbf{V}_{\neq n}] \in \mathbb{R}^{R_{n-1} I_n R_n \times R_{n-1} I_n R_n} \quad (74)$$

and

$$\bar{\mathbf{B}}^{(n)} = [\mathbf{V}_{\neq n}^T \mathbf{B} \mathbf{V}_{\neq n}] \in \mathbb{R}^{R_{n-1} I_n R_n \times R_{n-1} I_n R_n} \quad (75)$$

can be computed sequentially for  $n = 1, 2, \dots, N$  via tensor network contractions shown in Fig. 30.

#### D. Canonical Correlation Analysis in TT Format

The Canonical Correlation Analysis (CCA), introduced by Hotelling, can be considered as a generalization of PCA and it is a classical method for determining the relationship between two sets of variables. Given two zero-mean (i.e., centered) data sets  $\mathbf{X} \in \mathbb{R}^{I \times J}$  and  $\mathbf{Y} \in \mathbb{R}^{L \times J}$  on the same set of  $J$  observations, CCA seeks linear combinations of the variables in  $\mathbf{X}$  and the variables in  $\mathbf{Y}$  that are maximally mutually correlated with each other. Formally, the classical CCA computes two projection vectors  $\mathbf{w}_x = \mathbf{w}_x^{(1)} \in \mathbb{R}^I$  and  $\mathbf{w}_y = \mathbf{w}_y^{(1)} \in \mathbb{R}^L$  such that the correlation coefficient

$$\rho = \frac{\mathbf{w}_x^T \mathbf{X} \mathbf{Y}^T \mathbf{w}_y}{\sqrt{(\mathbf{w}_x^T \mathbf{X} \mathbf{X}^T \mathbf{w}_x)(\mathbf{w}_y^T \mathbf{Y} \mathbf{Y}^T \mathbf{w}_y)}} \quad (76)$$

is maximized.

In a similar way, we can formulate kernel CCA by replacing inner product matrices by kernel matrices:

$$\rho = \max_{\alpha_x, \alpha_y} \frac{\alpha_x^T \mathbf{K}_x \mathbf{K}_y \alpha_y}{\sqrt{(\alpha_x^T \mathbf{K}_x \mathbf{K}_x \alpha_x)(\alpha_y^T \mathbf{K}_y \mathbf{K}_y \alpha_y)}}, \quad (77)$$

where  $\mathbf{K}_x \in \mathbb{R}^{J \times J}$  and  $\mathbf{K}_y \in \mathbb{R}^{J \times J}$  are suitably designed kernel matrices. The above optimization problem can be reformulated as a generalized eigenvalue decomposition (GEVD).

Since  $\rho$  is invariant to the scaling of the vectors  $\mathbf{w}_x$  and  $\mathbf{w}_y$ , the standard CCA can be equivalently formulated as the following constrained optimization problem:

$$\max_{\mathbf{w}_x, \mathbf{w}_y} \{ \mathbf{w}_x^T \mathbf{X} \mathbf{Y}^T \mathbf{w}_y \} \quad (78)$$

$$\text{s.t. } \mathbf{w}_x^T \mathbf{X} \mathbf{X}^T \mathbf{w}_x = \mathbf{w}_y^T \mathbf{Y} \mathbf{Y}^T \mathbf{w}_y = 1. \quad (79)$$

We will refer to  $\mathbf{t}_1 = \mathbf{X}^T \mathbf{w}_x$  and  $\mathbf{u}_1 = \mathbf{Y}^T \mathbf{w}_y$  as the canonical variables.

For sparse CCA, we usually assume that the columns of  $\mathbf{X}$  and  $\mathbf{Y}$  have been standardized to have zero mean and standard deviation one. The

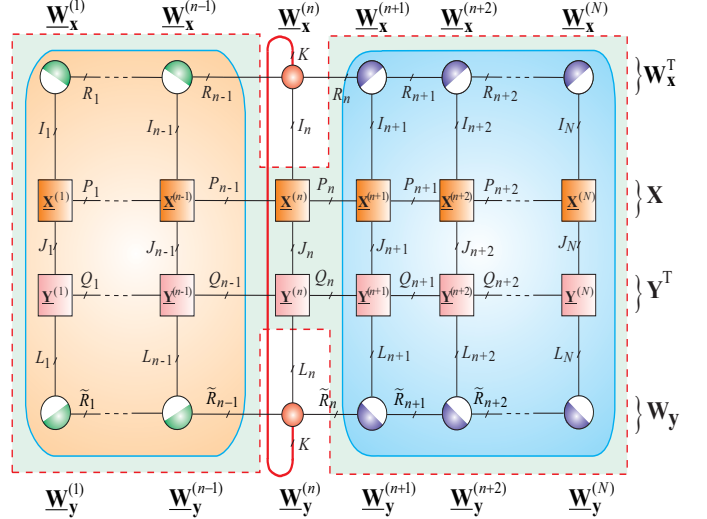


Figure 31: Tensor network for computation of multiple (sparse) CCA.

cross product matrices  $\mathbf{X} \mathbf{X}^T$  and  $\mathbf{Y} \mathbf{Y}^T$  are often approximated by identity matrices, and consequently the constraints  $\mathbf{w}_x^T \mathbf{X} \mathbf{X}^T \mathbf{w}_x \leq 1$  and  $\mathbf{w}_y^T \mathbf{Y} \mathbf{Y}^T \mathbf{w}_y \leq 1$  can be simplified as  $\|\mathbf{w}_x\|_2^2 \leq 1$  and  $\|\mathbf{w}_y\|_2^2 \leq 1$ , respectively under some conditions [75]. Hence, in order to compute sparse CCA we must impose suitable sparsity constraints on the canonical vectors, for example, by applying the PMD approach [74], [75]:

$$\begin{aligned} & \max_{\mathbf{w}_x, \mathbf{w}_y} \{ \mathbf{w}_x^T \mathbf{X} \mathbf{Y}^T \mathbf{w}_y \} \\ & \text{s.t. } \|\mathbf{w}_x\|_2^2 \leq 1, \quad \|\mathbf{w}_y\|_2^2 \leq 1, \\ & \quad P_1(\mathbf{w}_x) \leq c_1, \quad P_2(\mathbf{w}_y) \leq c_2, \end{aligned} \quad (80)$$

where  $P_1$  and  $P_2$  are convex penalty functions and positive parameters  $c_1, c_2$  control sparsity level. Since  $P_1$  and  $P_2$  are generally chosen to yield sparse projection vectors  $\mathbf{w}_x$  and  $\mathbf{w}_y$ , we call this criterion the sparse CCA (see Eqs. (66)).

In order to compute multiple canonical vectors for the standard CCA, we can formulate the following optimization problem:

$$\begin{aligned} & \max_{\mathbf{W}_x, \mathbf{W}_y} \{ \text{tr}(\mathbf{W}_x^T \mathbf{X} \mathbf{Y}^T \mathbf{W}_y) \}, \\ & \text{s.t. } \mathbf{W}_x^T \mathbf{X} \mathbf{X}^T \mathbf{W}_x = \mathbf{I}_K \\ & \quad \mathbf{W}_y^T \mathbf{Y} \mathbf{Y}^T \mathbf{W}_y = \mathbf{I}_K, \end{aligned} \quad (81)$$

where  $\mathbf{W}_x = [\mathbf{w}_x^{(1)}, \mathbf{w}_x^{(2)}, \dots, \mathbf{w}_x^{(K)}] \in \mathbb{R}^{I \times K}$  and  $\mathbf{W}_y = [\mathbf{w}_y^{(1)}, \mathbf{w}_y^{(2)}, \dots, \mathbf{w}_y^{(K)}] \in \mathbb{R}^{L \times K}$ .

This optimization scheme in a TT format is illustrated in Fig. 31 and performs iteratively the

following set of optimization problems:

$$\begin{aligned} & \max_{\mathbf{W}_x^{(n)}, \mathbf{W}_y^{(n)}} \text{tr}((\mathbf{W}_x^{(n)})^T [\mathbf{W}_{x, \neq n}^T \mathbf{X}^T \mathbf{W}_{y, \neq n}] \mathbf{W}_y^{(n)}), \\ \text{s.t. } & (\mathbf{W}_x^{(n)})^T [\mathbf{W}_{x, \neq n}^T \mathbf{X} \mathbf{X}^T \mathbf{W}_{x, \neq n}] \mathbf{W}_x^{(n)} = \mathbf{I}_K \\ & (\mathbf{W}_y^{(n)})^T [\mathbf{W}_{y, \neq n}^T \mathbf{Y} \mathbf{Y}^T \mathbf{W}_{y, \neq n}] \mathbf{W}_y^{(n)} = \mathbf{I}_K, \\ & n = 1, 2, \dots, N. \end{aligned} \quad (82)$$

Note that for large-scale sparse CCA the cross product matrices  $\mathbf{X} \mathbf{X}^T$  and  $\mathbf{Y} \mathbf{Y}^T$  can be approximated by identity matrices, and consequently the above constraints can be simplified [74].

### E. Solving Large-Scale Systems of Linear Equations

Consider a huge system of linear algebraic equations in TT formats:

$$\mathbf{A}\mathbf{x} \cong \mathbf{y} \quad (83)$$

or equivalently (if a matrix  $\mathbf{A}$  is not symmetric positive-definite)

$$\mathbf{A}^T \mathbf{A} \mathbf{x} \cong \mathbf{A}^T \mathbf{y} \quad (84)$$

where  $\mathbf{A} \in \mathbb{R}^{I \times J}$ , (with  $I \geq J$ ),  $\mathbf{y} \in \mathbb{R}^I$  and a matrix  $\mathbf{A}^T \mathbf{A} \in \mathbb{R}^{J \times J}$  is a symmetric positive-definite matrix which does not need to be explicitly computed (see Fig. 32). The objective is to find the vector  $\mathbf{x} \in \mathbb{R}^J$  in a TT format.

To solve this problem in the Least Squares (LS) sense, we minimize the following cost function

$$\begin{aligned} J(\mathbf{x}) &= \|\mathbf{A}\mathbf{x} - \mathbf{y}\|_2^2 = (\mathbf{A}\mathbf{x} - \mathbf{y})^T (\mathbf{A}\mathbf{x} - \mathbf{y}) \\ &= \mathbf{x}^T \mathbf{A}^T \mathbf{A} \mathbf{x} - 2\mathbf{x}^T \mathbf{A}^T \mathbf{y} + \mathbf{y}^T \mathbf{y}, \end{aligned} \quad (85)$$

which can be simplified to

$$J(\mathbf{x}) = \mathbf{x}^T \mathbf{A}^T \mathbf{A} \mathbf{x} - 2\mathbf{x}^T \mathbf{A}^T \mathbf{y}. \quad (86)$$

Using the TT representation of a matrix  $\mathbf{A}$  and vectors  $\mathbf{x}$  and  $\mathbf{y}$  [21], [22], [83], we have:

$$\begin{aligned} \underline{\mathbf{A}} &= [\underline{\mathbf{A}}^{(1)}, \underline{\mathbf{A}}^{(2)}, \dots, \underline{\mathbf{A}}^{(N)}] \\ \underline{\mathbf{X}} &= [\underline{\mathbf{X}}^{(1)}, \underline{\mathbf{X}}^{(2)}, \dots, \underline{\mathbf{X}}^{(N)}] \\ \underline{\mathbf{Y}} &= [\underline{\mathbf{Y}}^{(1)}, \underline{\mathbf{Y}}^{(2)}, \dots, \underline{\mathbf{Y}}^{(N)}] \end{aligned} \quad (87)$$

and upon applying the frame equation  $\mathbf{x} = \underline{\mathbf{X}}_{\neq n} \mathbf{x}^{(n)}$  with frame matrices

$$\underline{\mathbf{X}}_{\neq n} = (\underline{\mathbf{X}}_{(n)}^{<n})^T \otimes \mathbf{I}_{I_n} \otimes (\underline{\mathbf{X}}_{(1)}^{>n})^T \in \mathbb{R}^{J_1 J_2 \cdots J_N \times R_{n-1} J_n R_n},$$

the cost function can be written as

$$\begin{aligned} J(\mathbf{x}) = J(\underline{\mathbf{X}}_{\neq n} \mathbf{x}^{(n)}) &= (\mathbf{x}^{(n)})^T \underline{\mathbf{X}}_{\neq n}^T \mathbf{A}^T \mathbf{A} \underline{\mathbf{X}}_{\neq n} \mathbf{x}^{(n)} \\ &\quad - 2(\mathbf{x}^{(n)})^T \underline{\mathbf{X}}_{\neq n}^T \mathbf{A}^T \mathbf{y}. \end{aligned} \quad (88)$$

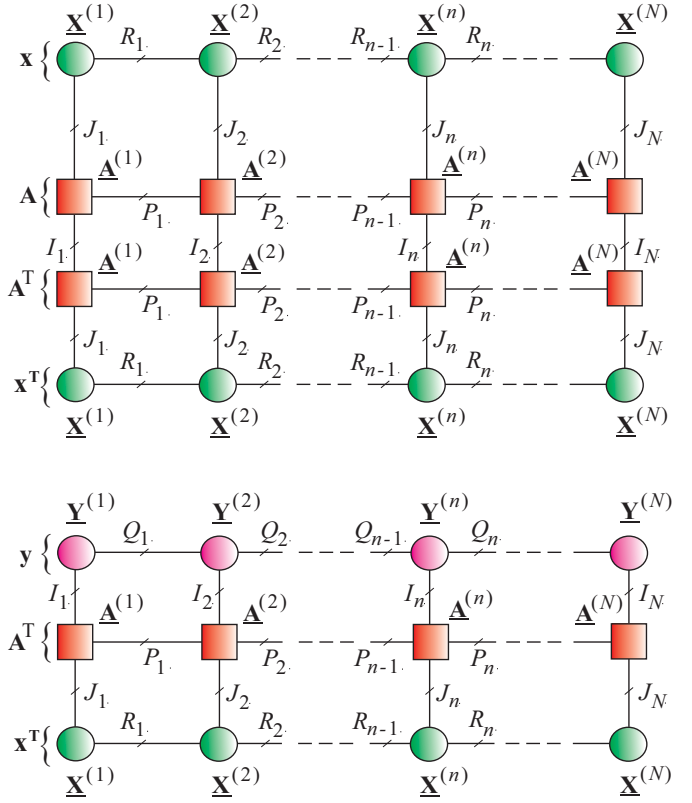


Figure 32: Simplified tensor network scheme for solving systems of linear equations with a huge non-symmetric matrix  $\mathbf{A}$ .

This converts the problem of solving a large-scale system of linear equations into solving smaller systems of algebraic equations iteratively

$$\bar{\mathbf{A}}^{(n)} \mathbf{x}^{(n)} \cong \mathbf{y}^{(n)}, \quad n = 1, 2, \dots, N, \quad (89)$$

where  $\mathbf{x}^{(n)} \in \mathbb{R}^{R_{n-1} J_n R_n}$  and

$$\begin{aligned} \bar{\mathbf{A}}^{(n)} &= \underline{\mathbf{X}}_{\neq n}^T \mathbf{A}^T \mathbf{A} \underline{\mathbf{X}}_{\neq n} \in \mathbb{R}^{R_{n-1} J_n R_n \times R_{n-1} J_n R_n}, \\ \mathbf{y}^{(n)} &= \underline{\mathbf{X}}_{\neq n}^T \mathbf{A}^T \mathbf{y} \in \mathbb{R}^{R_{n-1} J_n R_n}, \end{aligned} \quad (90)$$

under condition that cores are suitably left and right orthonormalized.

Of course, we cannot perform such matrix multiplications explicitly, but in TT formats, i.e., via iterative contraction of cores in the tensor network shown in Fig. 32.

The computations of a huge full vector  $\mathbf{x}$  or  $\mathbf{A}\mathbf{x}$  or a matrix  $\mathbf{A}^T \mathbf{A}$  are not possible due to their extremely large sizes. Via tensorization, by representing them in TT/QTT formats, and iterative contractions of cores, we can avoid the curse of dimensionality.

An assumption that data admits low-rank TT/QTT approximation is a key factor in this approach. However, for data with weak structure the

TT rank could be still large, which makes the calculation difficult or even impossible. The way how TT ranks are chosen and adapted during the algorithm is very important and various approaches to solve large structured linear systems have been proposed [21], [22], [30], [84]–[86].

**Remark.** Some applications admit the use of even more complex TT networks with higher-order cores as illustrated in Fig. 33 (a) and (b), for which we can exploit biorthonormality constraints [87].

## F. Software and Algorithms for Tensor Networks and Tensor Decompositions

Tensor decompositions and tensor networks algorithms require sophisticated software libraries, which are only now being developed.

For standard TDs (CPD, Tucker models) the Tensor Toolbox for MATLAB, originally developed by Kolda and Bader, provides several general-purpose commands and special facilities for handling sparse, dense, and structured standard TDs [88], while the *N*-Way Toolbox for Matlab, by Andersson and Bro, has been developed mostly for Chemometrics [89]. Moreover, we recently developed the TDALAB (<http://bsp.brain.riken.jp/TDALAB>) and TENSORBOX (<http://www.bsp.brain.riken.jp/~phan>), which provides user-friendly interface and advanced algorithms for basic tensor decompositions: Tucker and CPD [90], [91].

The Tensorlab toolbox developed by Sorber, Van Barel and De Lathauwer builds upon a complex optimization framework and offers efficient numerical algorithms for computing the CPD, Block term Decomposition (BTD) or constrained Tucker decompositions. The toolbox includes a library of many constraints (e.g., nonnegativity, orthogonality) and offered the possibility to combine and jointly factorize dense, sparse and incomplete tensors [92].

Similar to the CPD and/or Tucker decompositions, the TT and HT decompositions are often based on generalized unfolding matrices  $X_{[n]}$ , and a good approximation in a decomposition for a given TT/HT-rank can be obtained from the SVDs of the unfolding matrices. In practice, we avoid the explicit construction of these matrices and the SVDs when truncating a tensor via the TT decomposition to lower TT-rank. Such truncation algorithms for TT are described in [40]. HT algorithms that avoid the explicit computation of these SVDs when truncating a tensor that is already in HT decomposition are discussed in [30], [35], [93].

In [94] Oseledets proposed for TT decomposition a new approximative formula in which a *N*th-order data tensor is interpolated using special form of Cross-Approximation, a modification of the CUR algorithm. The total number of entries and the complexity of the interpolation algorithm depend linearly on the order of data tensor *N*, so the developed algorithm does not suffer from the curse of dimensionality. The TT-Cross-Approximation is analog to the SVD/HOSVD like algorithms for TT/MPS, but uses adaptive cross-approximation instead of the computationally more expensive SVD.

The TT Toolbox developed by Oseledets ([http://spring.inm.ras.ru/ose1/?page\\_id=24](http://spring.inm.ras.ru/ose1/?page_id=24)) focusses on TT and QTT structures, which deal with the curse of dimensionality [95]. The Hierarchical Tucker toolbox by Kressner and Tobler [35], [36] ([http://www.sam.math.ethz.ch/NLAgroupt/htucker\\_toolbox.html](http://www.sam.math.ethz.ch/NLAgroupt/htucker_toolbox.html)) and Tensor library by Handschuh, Waehnert and Espig, focus mostly on HT and TT tensor networks, while TensorCalculus by Espig at al. is a C++ library is for more general tensor networks [93].

In quantum physics and chemistry, a number of related software packages have been developed in the context of DMRG techniques for simulating quantum networks; see for example intelligent Tensor (iTensor) by Stoudenmire and White [96]. The iTensor Library is an open source C++ library for rapidly developing and applying tensor network algorithms. The iTensor is competitive with other available codes when performing basic DMRG calculations, but due to its flexibility it is especially well suited for developing next-generation tensor network algorithms such as PEPS.

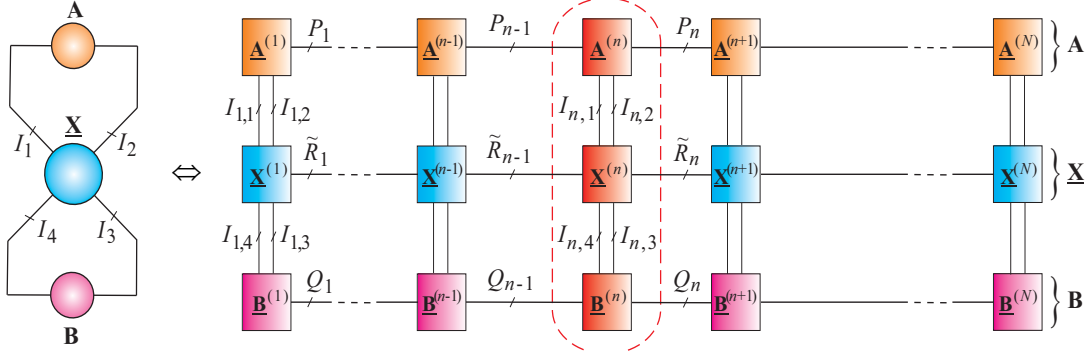
Another promising software is the Universal Tensor Network Library (Uni10) developed in C++ by Yun-Da Hsieh and Ying-Jer Kao (from the National Taiwan University) which provides algorithms for performing contraction of a complicated tensor network with easy to use interface (<http://uni10.org/about.html>). The library is geared toward more complex tensor networks such as PEPS and MERA.

The problems related with optimization and improvements of several existing algorithms for TDs and TNs is an active area of research (see for example [92], [97], [98]).

## IX. Conclusions

Tensor networks, which can be considered as generalization and extension of tensor decompositions, are promising tools for analysis of big data,

(a)



(b)

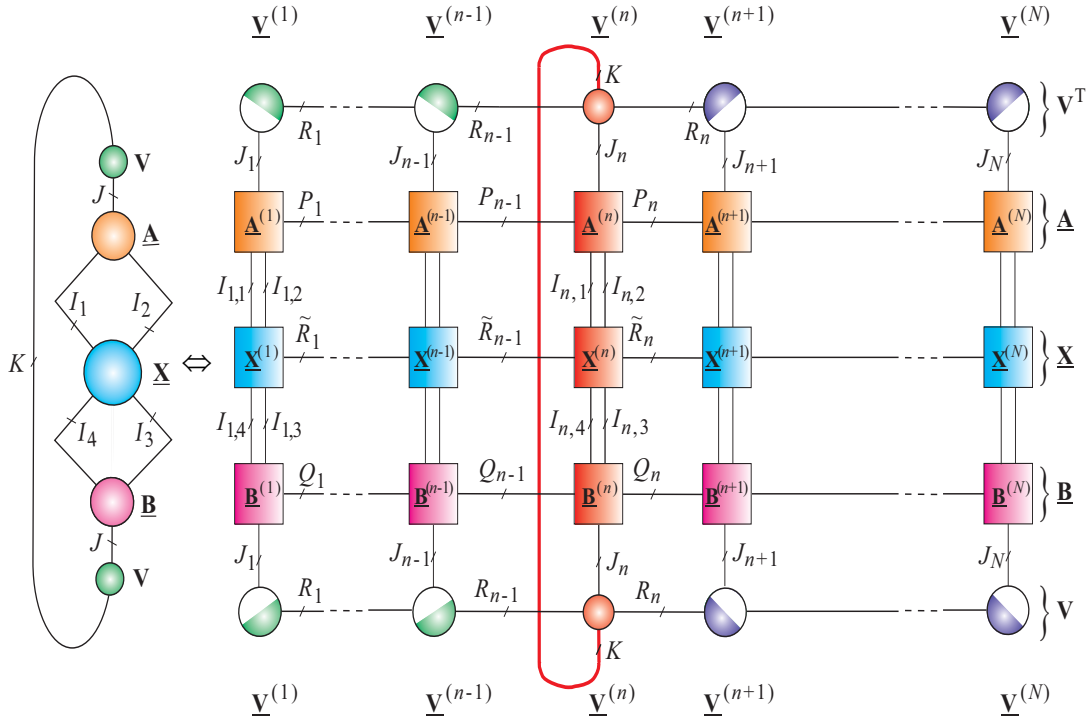


**Figure 33:** Representation of tensor traces in tensor train formats (see also Fig. 9). These models arise in some optimization problems, in which we need to maximize the tensor traces subject to additional constraints imposed on matrices.

especially, for wide family of large-scale optimization problems due to their extremely good compression abilities and distributed processing of data (cloud computing). Moreover, TNs have the ability to address both the strong and the weak coupling between variables, and to deal with incomplete and noisy data. In fact, TDs have already found application in generalized multivariate regression, multi-way blind source separation, sparse representation and coding, feature extraction, classification, clustering and data assimilation [97], [99]–[104].

From a more general perspective, the main con-

cept for big data analytic is to apply a suitable tensorization of the data and to perform an approximate decomposition in TT/QTT formats. By constructing a suitable tensor network we can perform all matrix/vectors operations in tensor network formats. The use of the virtual tensorization or quantization (QTT) allows us to treat more efficiently very large-scale data [61], [62], [66].

In this paper, we have illuminated that tensor networks, especially tensor trains, are very promising tools for big data optimization problems, and have illustrated the natural and distributed repre-

sentations offered by tensor networks for a selected class of optimization problems. This framework can be extended to a broader class of optimization problems, especially for extremely large-scale and untractable numerical problems.

In this approach a large-scale optimization problem is transformed into a set of small-scale linked optimization problems, each over a relative small group of unknown variables, which are grouped via TT decompositions and are represented by low-dimensional cores. In other words, by representing data in TT format we are able to turn a specific class of optimization problem into local tractable subproblems, which have the same structure or type as the original huge optimization problem. This allows us to apply any efficient numerical algorithm to local optimization problems.

The presented approach will work if only two assumptions are satisfied:

- 1) The structured data can be represented in TT formats that admit sufficiently good low-rank approximations.
- 2) Approximate solutions are acceptable [71].

Challenging problems related to low-rank tensor approximations remain that need to be addressed include:

- Current implementations of tensor train decomposition and tensor contractions still require a number of tuning parameters, e.g., approximations accuracy, TT ranks estimation. Improved and semi-automatic TT approximation accuracy criteria, TT rank adaption and control and *a priori* errors bounds need to be developed. Particularly, the unpredictable accumulation of rounding error and TT-rank explosion problem should be better understood and solved [105].
- Convergence analysis tools for TT algorithms should be developed and we need to better understand convergence properties of such algorithms.
- As the complexity of big data increases, this requires more efficient iterative algorithms for their computing, extending beyond the ALS/MALS, DMRG, SVD/QR and CUR/Cross-Approximation class of algorithms.
- Theoretic and methodological approaches are needed to determine what kind of constraints should be imposed on factor matrices/cores in order to extract desired hidden (latent) vari-

ables with meaningful physical interpretation.

- Generalizations of Tensor Train models to more sophisticated tensor networks should be developed to fully integrate complex systems and optimization problems (e.g., a system simulating the biological molecule structure) [105].
- Investigating the uniqueness of various TN models and optimality properties, or lack thereof, are needed and this may lead to faster and/or more reliable algorithms.
- Special techniques are needed to save and process huge ultra large-scale tensors which occupy peta-bytes memory.

In summary, TNs is a fascinating and perspective area of research with many potential applications in optimization problems for massive big data sets.

## REFERENCES

- [1] A. Cichocki, D. Mandic, C. Caiafa, A.-H. Phan, G. Zhou, Q. Zhao, and L. D. Lathauwer, "Multiway component analysis: Tensor decompositions for signal processing applications," *IEEE Signal Processing Magazine*, 2014 (in print).
- [2] A. Cichocki, "Era of big data processing: A new approach via tensor networks and tensor decompositions," *CoRR*, vol. abs/1403.2048, 2014. [Online]. Available: <http://arxiv.org/abs/1403.2048>
- [3] A. Cichocki, R. Zdunek, A.-H. Phan, and S. Amari, *Nonnegative Matrix and Tensor Factorizations: Applications to Exploratory Multi-way Data Analysis and Blind Source Separation*. Chichester: Wiley, 2009.
- [4] T. Kolda and B. Bader, "Tensor decompositions and applications," *SIAM Review*, vol. 51, no. 3, pp. 455–500, September 2009.
- [5] A. Cichocki, "Tensors decompositions: New concepts for brain data analysis?" *Journal of Control, Measurement, and System Integration (SICE)*, vol. 47, no. 7, pp. 507–517, 2011.
- [6] W. Hackbusch, *Tensor Spaces and Numerical Tensor Calculus*, ser. Springer series in computational mathematics. Heidelberg: Springer, 2012, vol. 42.
- [7] A. Smilde, R. Bro, and P. Geladi, *Multi-way Analysis: Applications in the Chemical Sciences*. New York: John Wiley & Sons Ltd, 2004.
- [8] P. Kroonenberg, *Applied Multiway Data Analysis*. New York: John Wiley & Sons Ltd, 2008.
- [9] D. Kressner, M. Steinlechner, and B. Vandereycken, "Low-rank tensor completion by Riemannian optimization," *BIT (in press)*, 2013.
- [10] H. Wang, Q. Wu, L. Shi, Y. Yu, and N. Ahuja, "Out-of-core tensor approximation of multi-dimensional matrices of visual data," *ACM Trans. Graph.*, vol. 24, no. 3, pp. 527–535, 2005.
- [11] S. K. Suter, M. Makhynia, and R. Pajarola, "Tamresh - tensor approximation multiresolution hierarchy for interactive volume visualization," *Comput. Graph. Forum*, vol. 32, no. 3, pp. 151–160, 2013.
- [12] A. H. Phan and A. Cichocki, "PARAFAC algorithms for large-scale problems," *Neurocomputing*, vol. 74, no. 11, pp. 1970–1984, 2011.

[13] N. Lee and A. Cichocki, "Fundamental tensor operations for large-scale data analysis in tensor train formats," *ArXiv e-prints*, May 2014. [Online]. Available: <http://adsabs.harvard.edu/abs/2014arXiv1405.7786L>

[14] R. Orus, "Exploring corner transfer matrices and corner tensors for the classical simulation of quantum lattice systems," *Phys.Rev.*, vol. B85, p. 205117, 2012.

[15] ———, "A Practical introduction to Tensor Networks: Matrix Product States and Projected Entangled Pair States," *The Journal of Chemical Physics*, 2013.

[16] B. Khoromskij, " $O(d \log N)$ -quantics approximation of  $N$ -d tensors in high-dimensional numerical modeling," *Constructive Approximation*, vol. 34, no. 2, pp. 257–280, 2011.

[17] P. Comon, X. Luciani, and A. L. F. de Almeida, "Tensor decompositions, Alternating Least Squares and other Tales," *Jour. Chemometrics*, vol. 23, pp. 393–405, 2009.

[18] H. Lu, K. Plataniotis, and A. Venetsanopoulos, "A survey of multilinear subspace learning for tensor data," *Pattern Recognition*, vol. 44, no. 7, pp. 1540–1551, 2011.

[19] M. Mørup, "Applications of tensor (multiway array) factorizations and decompositions in data mining," *Wiley Interdisc. Rev.: Data Mining and Knowledge Discovery*, vol. 1, no. 1, pp. 24–40, 2011.

[20] N. Sidiropoulos, "Low-rank decomposition of multi-way arrays: A signal processing perspective," in *Proc. of the IEEE SAM 2004, July 18-21, Sitges, Barcelona*, 2004. [Online]. Available: <http://www.sandia.gov/~tgkolda/tdw2004/Nikos04.pdf>

[21] S. V. Dolgov and D. V. Savostyanov, "Alternating minimal energy methods for linear systems in higher dimensions. part ii: Faster algorithm and application to nonsymmetric systems," *arXiv preprint arXiv:1304.1222*, 2013.

[22] ———, "Alternating minimal energy methods for linear systems in higher dimensions. part i: SPD systems," *arXiv preprint arXiv:1301.6068*, 2013.

[23] A. H. Phan, A. Cichocki, P. Tichavsky, D. Mandic, and K. Matsuoka, "On revealing replicating structures in multiway data: A novel tensor decomposition approach," in *Proc. 10th International Conf. LVA/ICA, Tel Aviv, March 12-15*, 2012, pp. 297–305.

[24] R. N. C. Pfeifer, J. Haegeman, and F. Verstraete, "Faster identification of optimal contraction sequences for tensor networks," *ArXiv e-prints*, Apr. 2013. [Online]. Available: <http://adsabs.harvard.edu/abs/2013arXiv1304.6112P>

[25] R. Pfeifer, G. Evenly, S. Singh, and G. Vidal, "NCON: A tensor network contractor for MATLAB," *arXiv preprint arXiv:1402.0939*, 2014.

[26] S. Rajbhandari, A. Nikam, P.-W. Lai, K. Stock, S. Krishnamoorthy, and P. Sadayappan, "Framework for distributed contractions of tensors with symmetry," *Preprint, Ohio State University*, 2013.

[27] M. Lubasch, J. Cirac, and M.-C. Bauls, "Unifying projected entangled pair state contractions," *New Journal of Physics*, vol. 16, no. 3, p. 033014, 2014. [Online]. Available: <http://stacks.iop.org/1367-2630/16/i=3/a=033014>

[28] S. Sachdev, "Tensor networks—a new tool for old problems," *Physics*, vol. 2, p. 90, Oct 2009. [Online]. Available: <http://link.aps.org/doi/10.1103/Physics.2.90>

[29] M. Espig, W. Hackbusch, S. Handschuh, and R. Schneider, "Optimization problems in contracted tensor networks," *Comput. Visual. Sci.*, vol. 14, no. 6, pp. 271–285, 2011.

[30] L. Grasedyck, D. Kressner, and C. Tobler, "A literature survey of low-rank tensor approximation techniques," *CGAMM-Mitteilungen*, vol. 36, pp. 53–78, 2013.

[31] L. Grasedyck and W. Hackbusch, "An introduction to hierarchical (h-) rank and tt-rank of tensors with examples," *Comput. Meth. in Appl. Math.*, vol. 11, no. 3, pp. 291–304, 2011.

[32] W. Hackbusch and S. Kühn, "A new scheme for the tensor representation," *Journal of Fourier Analysis and Applications*, vol. 15, no. 5, pp. 706–722, 2009.

[33] L. Grasedyck, "Hierarchical Singular Value Decomposition of tensors," *SIAM J. Matrix Analysis Applications*, vol. 31, no. 4, pp. 2029–2054, 2010.

[34] A. Uschmajew and B. Vandereycken, "The geometry of algorithms using hierarchical tensors," *Linear Algebra and its Applications*, vol. 439, pp. 133–166, 2013.

[35] D. Kressner and C. Tobler, "htucker—A MATLAB toolbox for tensors in hierarchical Tucker format," *MATHICSE, EPF Lausanne (Preprint 2012)*, available at <http://sma.epfl.ch/~anchpcommon/publications/htucker.pdf>, 2012. [Online]. Available: <http://anchp.epfl.ch/htucker>

[36] ———, "Algorithm 941: htucker—A Matlab toolbox for tensors in Hierarchical Tucker format," *ACM Transactions on Mathematical Software (TOMS)*, vol. 40, no. 3, p. 22, 2014.

[37] C. Lubich, T. Rohwedder, R. Schneider, and B. Vandereycken, "Dynamical approximation of hierarchical Tucker and tensor-train tensors," *SIAM J. Matrix Anal. Appl.*, vol. 34, no. 2, pp. 470–494, 2013.

[38] I. Oseledets and E. E. Tyrtyshnikov, "Breaking the curse of dimensionality, or how to use SVD in many dimensions," *SIAM J. Scientific Computing*, vol. 31, no. 5, pp. 3744–3759, 2009.

[39] G. Vidal, "Efficient classical simulation of slightly entangled quantum computations," *Physical Review Letters*, vol. 91, no. 14, p. 147902, 2003.

[40] I. V. Oseledets, "Tensor-train decomposition," *SIAM J. Scientific Computing*, vol. 33, no. 5, pp. 2295–2317, 2011.

[41] V. Kazeev, M. Khammash, M. Nip, and C. Schwab, "Direct solution of the Chemical Master Equation using Quantized Tensor Trains," *PLOS Computational Biology*, March 2014.

[42] C. Lubich, I. Oseledets, and B. Vandereycken, "Time integration of tensor trains," *ArXiv e-prints*, 2014.

[43] D. Bigoni, A. Engsig-Karup, and Y. Marzouk, "Spectral tensor-train decomposition," *arXiv preprint arXiv:1405.5713*, 2014.

[44] I. Oseledets, E. Tyrtyshnikov, and N. Zamarashkin, "Tensor-train ranks for matrices and their inverses," *Comput. Meth. in Appl. Math.*, vol. 11, no. 3, pp. 394–403, 2011.

[45] D. Perez-Garcia, F. Verstraete, M. M. Wolf, and J. I. Cirac, "Matrix product state representations," *Quantum Info. Comput.*, vol. 7, no. 5, pp. 401–430, Jul. 2007. [Online]. Available: <http://dl.acm.org/citation.cfm?id=2011832.2011833>

[46] F. Verstraete, V. Murg, and J. Cirac, "Matrix product states, projected entangled pair states, and variational renormalization group methods for quantum spin systems," *Advances in Physics*, vol. 57, no. 2, pp. 143–224, 2008.

[47] U. Schollwöck, "Matrix product state algorithms: DMRG, TEBD and relatives," in *Strongly Correlated Systems*. Springer, 2013, pp. 67–98.

[48] T. Huckle, K. Waldherr, and T. Schulte-Herbrüggen, "Computations in quantum tensor networks," *Linear*

*Algebra and its Applications*, vol. 438, no. 2, pp. 750 – 781, 2013.

[49] U. Schollwöck, “The density-matrix renormalization group in the age of matrix product states,” *Annals of Physics*, vol. 326, no. 1, pp. 96–192, 2011.

[50] G. Evenbly and G. Vidal, “Algorithms for entanglement renormalization,” *Physical Review B*, vol. 79, no. 14, p. 144108, 2009.

[51] V. Giovannetti, S. Montangero, and R. Fazio, “Quantum multiscale entanglement renormalization ansatz channels,” *Physical Review Letters*, vol. 101, no. 18, p. 180503, 2008.

[52] J. Morton, “Tensor networks in algebraic geometry and statistics,” *Lecture at Networking Tensor Networks, Centro de Ciencias de Benasque Pedro Pascual, Benasque, Spain*, 2012.

[53] A. Critch and J. Morton, “Algebraic geometry of matrix product states,” *ArXiv e-prints*, Feb. 2014.

[54] A. Novikov and R. Rodomanov, “Putting MRFs on a tensor train,” in *Proceedings of the International Conference on Machine Learning (ICML-14)*, 2014.

[55] A. Critch, “Algebraic Geometry of Hidden Markov and Related Models,” Ph.D. dissertation, University of California, Berkeley, 2013.

[56] S. Handschuh, “Changing the topology of tensor networks,” *ArXiv e-prints*, 2012.

[57] H. Zhao, Z. Xie, Q. Chen, Z. Wei, J. Cai, and T. Xiang, “Renormalization of tensor-network states,” *Physical Review B*, vol. 81, no. 17, p. 174411, 2010.

[58] R. Hübener, V. Nebendahl, and W. Dür, “Concatenated tensor network states,” *New Journal of Physics*, vol. 12, no. 2, p. 025004, 2010.

[59] I. Oseledets, “Approximation of  $2^d \times 2^d$  matrices using tensor decomposition,” *SIAM J. Matrix Analysis Applications*, vol. 31, no. 4, pp. 2130–2145, 2010.

[60] B. Khoromskij, “Tensors-structured numerical methods in scientific computing : Survey on recent advances,” *Chemometrics and Intelligent Laboratory Systems*, vol. 110, no. 1, pp. 1–19, 2011. [Online]. Available: <http://www.mis.mpg.de/de/publications/preprints/2010/prepr2010-21.html>

[61] S. Dolgov and B. Khoromskij, “Two-level QTT-Tucker format for optimized tensor calculus,” *SIAM J. Matrix Analysis Applications*, vol. 34, no. 2, pp. 593–623, 2013.

[62] V. Kazeev and B. Khoromskij, “Low-rank explicit QTT representation of the Laplace operator and its inverse,” *SIAM J. Matrix Analysis Applications*, vol. 33, no. 3, pp. 742–758, 2012.

[63] I. V. Oseledets and E. E. Tyrtyshnikov, “Algebraic wavelet transform via quantics tensor train decomposition,” *SIAM J. Scientific Computing*, vol. 33, no. 3, pp. 1315–1328, 2011.

[64] V. Kazeev, B. Khoromskij, and E. Tyrtyshnikov, “Multilevel Toeplitz matrices generated by tensor-structured vectors and convolution with logarithmic complexity,” *SIAM J. Scientific Computing*, vol. 35, no. 3, 2013.

[65] W. de Launey and J. Seberry, “The strong Kronecker product.” *J. Comb. Theory, Ser. A*, vol. 66, no. 2, pp. 192–213, 1994. [Online]. Available: <http://dblp.uni-trier.de/db/journals/jct/jcta66.html#LauneyS94>

[66] V. Kazeev, O. Reichmann, and C. Schwab, “Low-rank tensor structure of linear diffusion operators in the TT and QTT formats,” *Linear Algebra and its Applications*, vol. 438, no. 11, pp. 4204–4221, 2013.

[67] I. Pižorn and F. Verstraete, “Variational numerical renormalization group: Bridging the gap between NRG and density matrix renormalization group,” *Phys. Rev. Lett.*, vol. 108, p. 067202, Feb 2012. [Online]. Available: <http://link.aps.org/doi/10.1103/PhysRevLett.108.067202>

[68] S. Dolgov, B. Khoromskij, I. Oseledets, and D. Savostyanov, “Computation of extreme eigenvalues in higher dimensions using block tensor train format,” *Computer Physics Communications*, vol. 185, no. 4, pp. 1207–1216, 2014.

[69] D. Kressner, M. Steinlechner, and A. Uschmajew, “Low-rank tensor methods with subspace correction for symmetric eigenvalue problems,” (in print), 2014. [Online]. Available: <http://sma.epfl.ch/~uschmajew/paper/EVAMEN.pdf>

[70] S. Holtz, T. Rohwedder, and R. Schneider, “The alternating linear scheme for tensor optimization in the tensor train format,” *SIAM J. Scientific Computing*, vol. 34, no. 2, 2012.

[71] D. Kressner and A. Uschmajew, “On low-rank approximability of solutions to high-dimensional operator equations and eigenvalue problems,” *arXiv preprint arXiv:1406.7026*, 2014.

[72] Z. Wen, C. Yang, X. Liu, and Y. Zhang, “Trace-penalty minimization for large-scale eigenspace computation,” DTIC Document, Tech. Rep., 2013.

[73] N. Lee and A. Cichocki, “Very large-scale singular value decomposition based on low-rank tensor train networks,” RIKEN BSI, Tech. Rep., 2014 (in preparation).

[74] D. Witten, R. Tibshirani, and T. Hastie, “A penalized matrix decomposition, with applications to sparse principal components and canonical correlation analysis,” *Biostatistics*, vol. 10, no. 3, pp. 515–534, 2009.

[75] D. Witten, “A penalized matrix decomposition, and its applications,” PhD Dissertation, Department of Statistics, Stanford University, 2010.

[76] H. Shen and J. Huang, “Sparse principal component analysis via regularized low rank matrix approximation,” *Journal of Multivariable Analysis*, vol. 99, no. 6, pp. 1015–1034, 2008. [Online]. Available: <http://dx.doi.org/10.1016/j.jmva.2007.06.007>

[77] M. Journee, Y. Nesterov, P. Richtarik, and R. Sepulchre, “Generalized power method for sparse principal component analysis,” *Journal of Machine Learning Research*, vol. 1, pp. 517–553, 2010.

[78] J. Huang, H. Shen, and A. Buja, “The analysis of two-way functional data using two-way regularized singular value decompositions,” *Journal of the American Statistical Association*, vol. 104, no. 488, pp. 1609–1620, 2009. [Online]. Available: <http://EconPapers.repec.org/RePEc:bes:jnlasa:v:104:i:488:y:2009:p:1609-1620>

[79] M. Lee, H. Shen, J. Huang, and J. Marron, “Biclustering via sparse singular value decomposition.” *Biometrics*, vol. 66, no. 4, pp. 1087–1095, 2010. [Online]. Available: <http://www.ncbi.nlm.nih.gov/pubmed/20163403>

[80] G. Allen, “Regularized tensor factorizations and higher-order principal components analysis,” submitted, 2012. [Online]. Available: <http://arxiv.org/pdf/1202.2476.pdf>

[81] G. Allen and M. Maletic-Savatic, “Sparse non-negative generalized PCA with applications to metabolomics,” *Bioinformatics*, vol. 27 (21), pp. 3029–3035, 2011.

[82] E. Kokiopoulou, J. Chen, and Y. Saad, “Trace optimization and eigenproblems in dimension reduction methods,” *Numerical Linear Algebra with Applications*, vol. 18, no. 3, pp. 565–602, 2011.

[83] I. Oseledets and S. Dolgov, “Solution of linear systems

and matrix inversion in the tt-format," *SIAM J. Scientific Computing*, vol. 34, no. 5, 2012.

[84] S. Dolgov and I. Oseledets, "Solution of linear systems and matrix inversion in the tt-format," *SIAM J. Sci. Comput.*, vol. 34, no. 5, pp. A2718–A2739, 2011.

[85] S. Dolgov, "TT-GMRES: Solution to a linear system in the structured tensor format," *Russian Journal of Numerical Analysis and Mathematical Modelling*, vol. 28, no. 2, pp. 149–172, 2013.

[86] I. Oseledets, "Dmrg approach to fast linear algebra in the tt-format," *Comput. Methods Appl. Math.*, vol. 11, no. 3, pp. 382–393, 2011.

[87] Y.-K. Huang, "Biorthonormal transfer-matrix renormalization-group method for non-Hermitian matrices," *Physical Review E*, vol. 83, no. 3, p. 036702, 2011.

[88] B. Bader, T. G. Kolda *et al.*, "MATLAB tensor toolbox version 2.5," Available online, Feb. 2012. [Online]. Available: <http://www.sandia.gov/~tgkolda/TensorToolbox/>

[89] C. Andersson and R. Bro, "The N-way toolbox for MATLAB," *Chemometrics Intell. Lab. Systems*, vol. 52, no. 1, pp. 1–4, 2000. [Online]. Available: <http://www.models.life.ku.dk/source/nwaytoolbox/>

[90] G. Zhou and A. Cichocki, "TDALAB: Tensor Decomposition Laboratory," <http://bsp.brain.riken.jp/TDALAB/>, LABSP, Wako-shi, Japan, 2013. [Online]. Available: <http://bsp.brain.riken.jp/TDALAB/>

[91] A.-H. Phan, P. Tichavský, and A. Cichocki, "Tensorbox: a matlab package for tensor decomposition," <http://www.bsp.brain.riken.jp/~phan/tensorbox.php>, Saitama, Japan, 2012.

[92] L. Sorber, M. Van Barel, and L. De Lathauwer, "Tensorlab v1.0," Feb. 2013. [Online]. Available: <http://esat.kuleuven.be/sista/tensorlab/>

[93] M. Espig, M. Schuster, A. Killatis, N. Waldren, P. Wähnert, S. Handschuh, and H. Auer, "TensorCalculus library," 2012. [Online]. Available: <http://gitorious.org/tensorcalculus>

[94] I. Oseledets and E. Tyrtyshnikov, "TT-cross approximation for multidimensional arrays," *Linear Algebra and its Applications*, vol. 432, no. 1, pp. 70–88, 2010.

[95] I. Oseledets, "TT-toolbox 2.2," 2012. [Online]. Available: [http://spring.inm.ras.ru/ose1/?page\\_id=24](http://spring.inm.ras.ru/ose1/?page_id=24)

[96] E. Stoudenmire and S. White, "TTensor Library Release v0.2.5," Perimeter Institute for Theoretical Physics, Tech. Rep., May 2014. [Online]. Available: <http://dx.doi.org/10.5281/zenodo.10068>

[97] G. Zhou, A. Cichocki, Q. Zhao, and S. Xie, "Efficient nonnegative Tucker decompositions: Algorithms and uniqueness," *CoRR*, vol. abs/1404.4412, 2014. [Online]. Available: <http://arxiv.org/abs/1404.4412>

[98] A. H. Phan, P. Tichavský, and A. Cichocki, "Low complexity Damped Gauss-Newton algorithms for CANDECOMP/PARAFAC," *SIAM Journal on Matrix Analysis and Applications (SIMAX) (in print)*, vol. arXiv/1205.2584, 2013. [Online]. Available: <http://arxiv.org/pdf/1205.2584.pdf>

[99] C. Caiafa and A. Cichocki, "Generalizing the column-row matrix decomposition to multi-way arrays," *Linear Algebra and its Applications*, vol. 433, no. 3, pp. 557–573, 2010.

[100] —, "Computing sparse representations of multidimensional signals using Kronecker bases," *Neural Computation*, vol. 25, no. 1, pp. 186–220, 2013.

[101] Q. Zhao, C. Caiafa, D. Mandic, Z. Chao, Y. Nagasaka, N. Fujii, L. Zhang, and A. Cichocki, "Higher-order partial least squares (HOPLS): A generalized multi-linear regression method, (in print)," *IEEE Trans on Pattern Analysis and Machine Intelligence (PAMI)*, 2013 (in print).

[102] Q. Zhao, C. F. Caiafa, D. Mandic, L. Zhang, T. Ball, A. Schulze-bonhage, and A. S. Cichocki, "Multilinear subspace regression: An orthogonal tensor decomposition approach," in *Advances in Neural Information Processing Systems 24*, J. Shawe-Taylor, R. Zemel, P. Bartlett, F. Pereira, and K. Weinberger, Eds., 2011, pp. 1269–1277.

[103] A. Phan and A. Cichocki, "Extended HALS algorithm for nonnegative Tucker decomposition and its applications for multi-way analysis and classification," *Neurocomputing*, 2011.

[104] —, "Tensor decompositions for feature extraction and classification of high dimensional datasets," *Nonlinear Theory and its Applications, IEICE*, vol. 1, no. 1, pp. 37–68, 2010.

[105] D. Savostyanov, S. Dolgov, J. Werner, and I. Kuprov, "Exact NMR simulation of protein-size spin systems using tensor train formalism," *arXiv preprint arXiv:1402.4516*, 2014.